Regulation of cell fate and meristem maintenance in *Arabidopsis* root development

Colette A. ten Hove

ISBN: 978-90-8559-951-7

Layout and printing: Optima Grafische Communicatie, Rotterdam, The Netherlands

Regulation of cell fate and meristem maintenance in *Arabidopsis* root development

Regulatie van cel identiteit en handhaving van het meristeem gedurende de ontwikkeling van de wortel in *Arabidopsis*
(met een samenvatting in het Nederlands)

Proefschrift

ter verkrijging van de graad van doctor aan de Universiteit Utrecht
op gezag van de rector magnificus, prof.dr. J.C. Stoof,
ingevolge het besluit van het college voor promoties
in het openbaar te verdedigen op
woensdag 24 maart 2010 des ochtends te 10.30 uur

door

Colette Alexandra ten Hove

geboren op 20 maart 1979,
te Zeist

Promotor: Prof.dr. B.J.G. Scheres

Co-promotor: Dr. R. Heidstra

Printing of this thesis was financially supported by the J.E. Jurriaanse Stichting.

From the moment I picked your book up until I laid it down, I was convulsed with laughter. Someday I intend reading it.

Groucho Marx

Contents

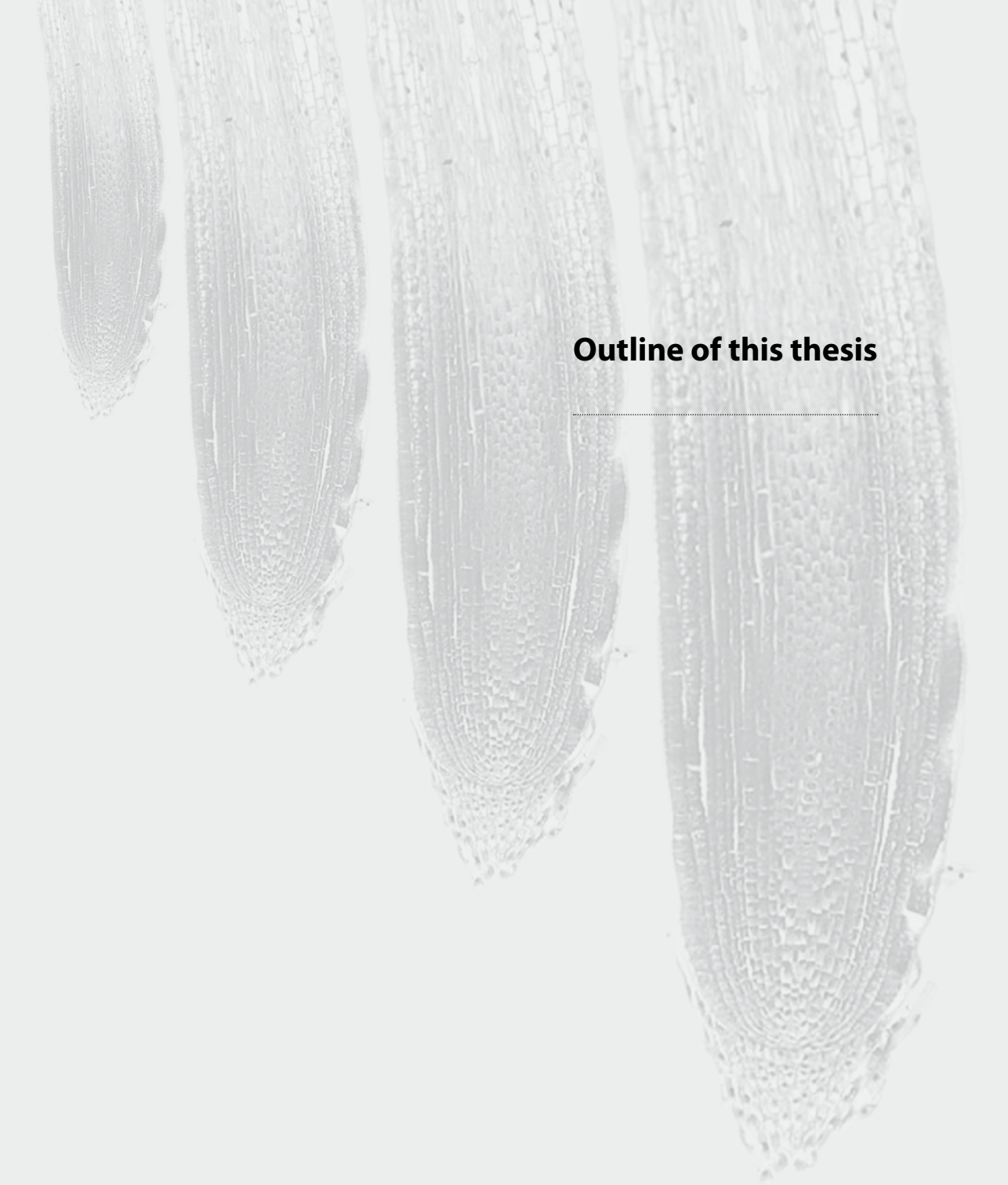

Outline of this thesis

The aim of this study was to gain a broader understanding of the mechanisms controlling root patterning and meristem maintenance by using forward and reverse genetics approaches.

Asymmetric cell division is an essential and universal mechanism for generating diversity and pattern in multicellular organisms. Divisions generating daughter cells different in size, shape, identity and function are fundamental to many developmental processes including fate specification, tissue patterning and self-renewal. **Chapters 1, 2** and **3** of this thesis focus on asymmetric cell division in the *Arabidopsis* root.

It is hypothesized that the angiosperm root meristem has evolved from the shoot apical meristem. Presumably, this is the outcome of the plants adaptation to changing environmental conditions, for example nutrient and water uptake and anchorage. Accordingly, key gene network motifs present in the shoot are expected and have been found to be important in the development and regulation of the root meristem, such as phytohormones, transcription factors as well as peptide ligands and their receptors. **Chapters 4, 5** and **6** of this thesis deal with the conservation of shoot and root meristem maintenance pathways.

Chapter 1 summarizes recent advances in understanding of the mechanisms of cell fate determination by asymmetric cell division in *Arabidopsis thaliana* by focusing on specific examples, including stem cell division, root ground tissue formation and stomatal patterning.

Chapter 2 describes the identification and analysis of *SCHIZORIZA* (*SCZ*). *SCZ* encodes a nuclear factor with homology to heat shock transcription factors that is necessary for the separation of multiple cell fates during asymmetric cell division in the stem cell niche of the *Arabidopsis* root. SCZ acts from the cortex, exerting both autonomous and non-autonomous effects to specify cortex identity and control the separation of cell fates in surrounding layers. The results unveil SCZ as a member of a novel pathway for asymmetric cell division in plants.

SCZ function is further investigated in **Chapter 3** and its interactions with the well characterized root patterning transcription factor genes *SHORT-ROOT* (*SHR*), *SCARECROW* (*SCR*), *PLETHORA1* (*PLT1*) and *PLT2* are described. The results show that *SCZ* functions together with *SHR-SCR* to establish the root stem cell niche during embryogenesis.

Overexpression of CLE family peptides restricts the size of the shoot and root meristem suggesting that conserved signaling pathways are involved in meristem maintenance in both shoots and roots. **Chapter 4** describes an activation tagging screen performed on transgenic plants ectopically expressing the small peptide ligand CLE19 in the root meristem, aimed to identify new components of a root CLE signaling pathway. A recessive mutant, *sol3*, was isolated in which the CLE19

overexpression phenotype is suppressed. Our data show that *SOL3* has a dual role in the root controlling growth and formative cell divisions.

Chapter 5 describes a reverse genetics approach to isolate and characterize leucine-rich repeat receptor-like kinases (LRR RLKs) that are expressed in the root meristem. A collection of homozygous T-DNA insertion lines for 69 LRR RLKs was established and subsequently analyzed for developmental and conditional phenotypes. Possibly due to genetic redundancy the functional loss-of-function studies revealed developmental phenotypes for only one mutant line, *rlk902*, which is further described in Chapter 6. T-DNA insertion mutants were further assayed for their response after exposure to environmental, hormonal/chemical and abiotic stress revealing several novel conditional functions for a number of LRR RLK genes.

Chapter 6 describes the characterization of *rlk902*, a LRR RLK mutant identified from the screen described in Chapter 5. *rlk902* mutants show both reduced root growth and resistance to the oomycete pathogen *Hyaloperonospora arabidopsidis*. Surprisingly, these phenotypes are not caused by *RLK902* inactivation but are linked to the T-DNA insertion. Microarray analysis revealed downregulated gene expression over an 84 kb region upstream of and including *RLK902* in the insertion mutant putatively encompassing the causal gene(s).

At the end of this thesis a summary of the preceding chapters is provided with perspectives for future research.

Chapter 1

Who begets whom? Plant cell fate determination by asymmetric cell division

Colette A. ten Hove and Renze Heidstra

Faculty of Science, Department of Biology, section Molecular Genetics, Utrecht University, Padualaan 8, 3584 CH Utrecht, the Netherlands.

Curr Opin Plant Biol (2008) 11, 34-41.

Summary

Asymmetric cell division generates cell types with different fates. Recent studies have improved our understanding of the molecular mechanisms involved in asymmetric cell division in *Arabidopsis thaliana*. Genetic approaches have identified candidate intrinsic factors and signaling components that mediate extrinsic cues. *WOX* genes appear to be putative intrinsic determinants acting in early embryonic asymmetric divisions. A non-canonical mechanism involving specific SHORT-ROOT/SCARECROW nuclear complexes is implicated in ground tissue asymmetric divisions. Asymmetric stem cell division requires extrinsic organizer signaling, whereas the involvement of intrinsic stem cell segregants is unknown. Finally, new studies on stomatal development have identified several intrinsic acting factors that specify cell fate and an extrinsic signaling cascade that controls the number and plane of asymmetric divisions.

Introduction

Plants and animals are made up of a large number of distinct cell types. Asymmetric cell division is the primary mechanism that leads to a diversity of cell types by creating two cell types from one. Cells can divide asymmetrically to produce two novel daughter cells at the expense of mother cell fate or, in the case of stem cells, one novel cell in addition to a copy of the mother cell. Two principal mechanisms exist by which distinct fates can be conferred on the daughters of the dividing cell: (1) segregation of intrinsic determinants during division and; (2) extrinsic cues that determine fate post-division (Figure 1) (Horvitz and Herskowitz, 1992). Actual development often involves a combination of these two mechanisms. For example, polarization of the mother cell before intrinsic asymmetric division may be under the influence of external spatial information.

In plants, cell movement is limited by the cell wall. Therefore, the orientation and asymmetry of divisions is important in generating the overall cellular pattern during development. In this update, we focus on asymmetric cell divisions involved in embryonic apical–basal patterning, radial ground tissue patterning, stem cell maintenance and the formation of the stomatal complex in light of recent progress; we concentrate on gene networks in *Arabidopsis thaliana*. For a general overview

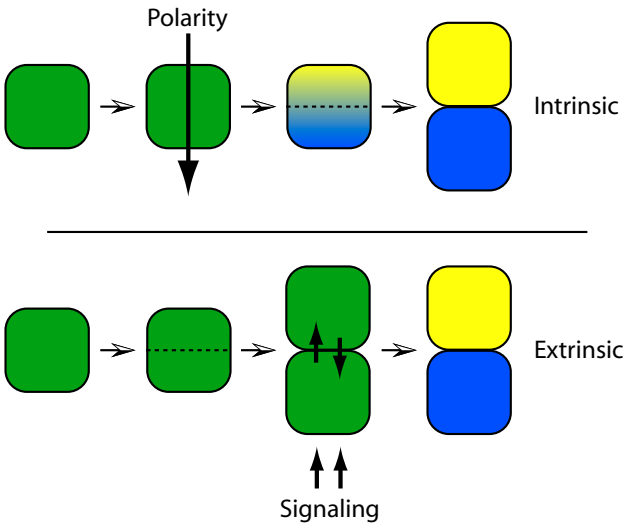

Figure 1. Asymmetric cell divisions. Before intrinsic asymmetric cell division, the mother cell (green) is polarized (i.e. asymmetric in cell shape, or distribution of molecular components; arrow). The intrinsic factors (yellow and/or blue) segregate to daughter cells during division and determine cell fate. During extrinsic asymmetric cell division, daughter cells have equal developmental potential at first (green), but their fates (yellow and blue) diverge later on through interactions with each other or neighboring cells (arrows).

of asymmetric divisions in plant development and a detailed description of cell polarity, cytokinesis and embryonic patterning, the reader is referred elsewhere (Heidstra, 2007; Fischer et al., 2004; Boutte et al., 2007; Jurgens, 2005; Lloyd and Chan, 2006; Jenik et al., 2007).

WOX genes as putative intrinsic factors

The first asymmetric division in diploid plant life is the zygotic division that generates a smaller apical and a larger basal cell, each with different fates. Asymmetry is already evident prior to fertilization, because the nucleus and the vacuole in the egg cell show polar localization (Mansfield and Briarty, 1991). A well-studied later asymmetric division occurs in globular stage embryos, when the hypophysis generates an apical lens-shaped cell that is the progenitor of the root-organizing quiescent center (QC) cells. WOX proteins, members of the homeodomain transcription factor family, of which WUSCHEL (WUS) is the founding member, are candidate intrinsic factors in embryonic asymmetric division with expression dynamics marking changes in cell fate (Figure 2).

WOX2 and *WOX8* mRNAs are initially expressed in both the egg cell and zygote, and segregate together with apical and basal cell fates, respectively (Haecker et al., 2004). The reported dynamic expression pattern of *WOX9*, with mRNA accumulating in the basal cell together with *WOX8* after zygotic division (Haecker et al., 2004), was not observed by Wu et al. (2007), but the authors did identify redundancy in *WOX* gene function. Whereas *wox2* mutant embryos exhibit a transient apical embryonic phenotype *wox8 wox2* double mutants display enhanced apical defects resulting in abnormal cotyledon separation. In addition, removal of *wox8* enhances *wox9*,

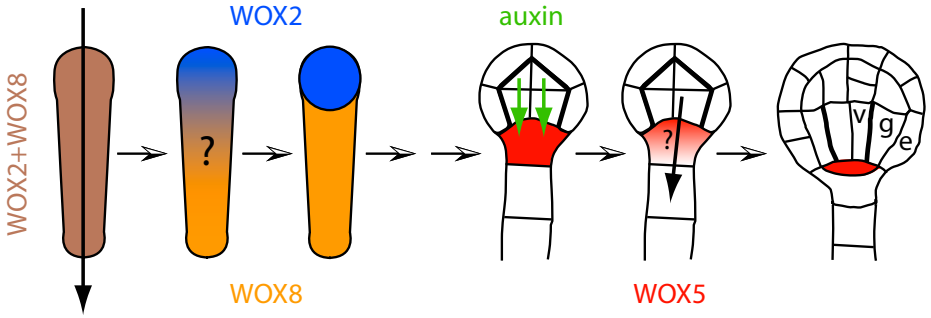

Figure 2. Embryonic asymmetric cell divisions. The zygote is polar (arrow) and expresses WOX2 and WOX8 (brown) that putatively segregate during zygotic division to the apical (blue) and basal cell (orange), respectively. Auxin and/or auxin-induced signals (green arrows) act as extrinsic factors to specify the hypophysis resulting in *WOX5* expression (red). During hypophysis division, putatively involving a polarity cue (arrow), intrinsic WOX5 may segregate to the lens-shaped cell, the precursor of the QC. The thick black lines indicate radial asymmetric divisions giving rise to the three main tissues: vascular (v), ground tissue (g) and epidermis (e).

resulting in embryos showing defects as early as the first cell division (Wu et al., 2007). Interestingly, the MAPKK kinase *YODA* (*YDA*) influences zygotic division and subsequent basal cell fates, indicating a role for extrinsic receptor-mediated signaling in this process (Lukowitz et al., 2004).

Around the 32-cell stage, auxin and/or auxin-induced signals act as extrinsic factors to specify the uppermost suspensor cell as the hypophysis (Friml et al., 2004; Weijers et al., 2006; Friml et al., 2003). With hypophysis specification, expression of another putative intrinsic determinant, the *WOX* family member *WOX5*, initiates and segregates to the lens-shaped QC progenitor cell to be maintained in its descendants (Haecker et al., 2004; Sarkar et al., 2007). Similar expression dynamics is observed for *SCARECROW* (*SCR*) (Wysocka-Diller et al., 2000), but in this case segregation appears to be regulated via a different mechanism, as discussed later. In line with a role for these transcription factors as intrinsic fate determinants, in *wox5* and *scr* mutants the QC is not properly specified (Sarkar et al., 2007; Sabatini et al., 2003). It is not known whether auxin acts to polarize the hypophysis before its asymmetric division.

Thus, zygote and hypophysis asymmetric divisions both segregate WOX proteins as candidate intrinsic determinants. Whereas zygotic division seems to require a maternal input that polarizes the egg cell prior to fertilization and external factors to stabilize post-division fates, hypophysis division possibly requires extrinsic factors for both processes.

Novel mechanism regulating asymmetric ground tissue division

Embryonic radial asymmetric divisions give rise to the three main tissues, epidermis, ground tissue and vascular tissue (Mansfield and Briarty, 1991). The *Arabidopsis* root endodermis and cortex originate from periclinal asymmetric divisions of ground tissue stem cell daughters involving GRAS family transcription factors SHORT-ROOT (SHR) and SCR (Figure 3) (Benfey et al., 1993; Scheres et al., 1995; Di Laurenzio et al., 1996; Helariutta et al., 2000).

SHR is transcribed in the stele, but the SHR protein moves outward to the adjacent QC, ground tissue stem cell and endodermis. There it acts as an endodermal fate determinant, and activates *SCR* that cell-autonomously induces the asymmetric periclinal ground tissue division (Di Laurenzio et al., 1996; Helariutta et al., 2000; Nakajima et al., 2001; Gallagher et al., 2004; Heidstra et al., 2004). Only the ground tissue stem cell daughter undergoes radial asymmetric division, likely due to QC signaling that prevents this division in the stem cell (Sabatini et al., 2003; Di Laurenzio et al., 1996; Heidstra et al., 2004; van den Berg et al., 1997). Following asymmetric division, SHR protein transiently persists in both sister cells before accumulating in the inner endodermal progenitor cells. This indicates that SHR is not an intrinsically

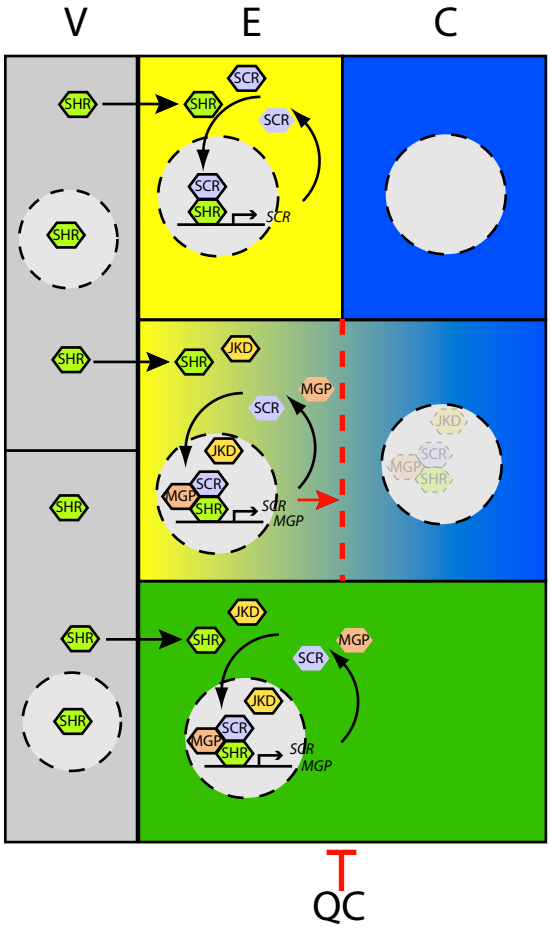

Figure 3. Model of ground tissue patterning. *SHR* is transcribed in the vascular bundle (V; gray) and the SHR protein moves outward to the adjacent ground tissue stem cell (green), its daughter and the endodermis (E; yellow). JKD and SCR expression is set up independent of SHR in the immature ground tissue and endodermis, respectively. There they bind and trap SHR to the nucleus, initiating the feed-forward loop to restrict its movement beyond a single layer. In the stem cell and its daughter, SHR activates expression of *SCR* and *MGP*, resulting in asymmetric division and determination of endodermis and cortex (C; blue) fate. MGP binding to the SHR/SCR complex promotes and JKD binding inhibits asymmetric cell divisions. QC signaling prevents asymmetric division in the ground tissue stem cell (red T-line).

segregated fate determinant and that an active mechanism limits SHR movement to essentially one cell layer (Benfey et al., 1993; Nakajima et al., 2001).

Movement of SHR beyond a single layer in the absence of *SCR* implicates a role for *SCR* in this mechanism (Heidstra et al., 2004; Sena et al., 2004). Not surprisingly, *SCR* is one of six direct SHR targets confirmed by chromatin immunoprecipitation experiments (Cui et al., 2007; Levesque et al., 2006). Some direct SHR targets also

appear to be direct SCR targets. For example, *SCR* binds its own promoter, demonstrating that SCR is controlled by a SHR/SCR-dependent feed-forward loop (Cui et al., 2007). Importantly, in the absence of SCR, SHR binding to other target promoters tested is abolished. The suggested physical interaction between SHR and SCR was confirmed by reciprocal pull-down experiments and yeast two-hybrid analyses (Cui et al., 2007). Binding of SHR to SCR, combined with positive feedback on *SCR* transcription, clarifies previous observations of rapid fate separation and SCR autoactivation upon clonal activation and deletion of *SCR*, respectively (Heidstra et al., 2004). More importantly, it provides an active mechanism to limit SHR to the endodermis and explains additional endodermis layers in *SCR* knockdown plants in which residual SCR cannot sequester all incoming SHR protein to endodermal nuclei (Cui et al., 2007). Nevertheless, endodermis characteristics present in *scr* but lacking in *shr* mutant ground tissue demonstrate that endodermis specification is controlled through SHR targets independent of the SHR–SCR transcription factor complex.

The SHR targets *MAGPIE* (*MGP*), *NUTCRACKER* (*NUC*) (Levesque et al., 2006) and another C2H2 zinc finger transcription factor family member, *JACKDAW* (*JKD*), were independently isolated in a screen for ground tissue expressed genes (Welch et al., 2007). Unlike *MGP* and *NUC*, initiation of *JKD* expression in the embryo is independent of *SHR* and *SCR* activity. *jdk* mutants display ectopic asymmetric divisions in the cortex, generating an additional layer. Prior to these ectopic divisions, *SCR* expression is lowered in endodermal cells, which, according to the model above, allows SHR to expand to the cortex. Indeed, upon ectopic cortex division, inner *jkd* cells start to express *SCR* and nuclear-localized SHR and transit to endodermal fate. *mgp* and *nuc* single and double mutants exhibit a wild type phenotype, but *mgp* RNAi suppresses the *jkd* ground tissue phenotype, suggesting that MGP promotes and JKD inhibits asymmetric cell divisions. Studies in plants and yeast indicate that JKD and MGP form complexes with SHR and SCR in the nucleus (Welch et al., 2007).

Taken together, these studies suggest that asymmetric division and fate specification in the ground tissue are controlled by nuclear factors and their reciprocal interactions.

Conserved mechanisms in asymmetric stem cell division

Stem cells typically depend on extrinsic signals for their maintenance that are provided by organizer cells in a so-called niche (Spradling et al., 2001). In turn, intrinsic stem cell factors are involved in the decision to preserve the stem cell state (Xie et al., 2005).

During embryogenesis, *WUS* transcription is initiated by unknown cues in the progenitors of the shoot-organizing center (OC) and specifies it. Maintenance of

intrinsically acting *WUS* transcripts within the OC itself involves asymmetric divisions eliminating *WUS* expression in the daughters of divided basal OC cells, the mechanism of which is unknown (Mayer et al., 1998; Laux et al., 1996). WUS in the OC induces extrinsic signaling to maintain the overlying stem cells, which in turn emit the signal peptide CLV3 that acts through the CLV1 receptor kinase to restrict the size of the *WUS* expression domain, thereby preventing the accumulation of excess stem cells (reviewed in Sablowski, 2007).

In the root, the auxin–*PLETHORA* (*PLT*) pathway provides positional information to set up the stem cell niche. In parallel, the *SHR–SCR* pathway specifies the organizer, or QC (reviewed in Scheres, 2007). *JKD*, also implicated in radial patterning, is required to maintain QC expression of *SCR* from early embryogenesis onwards (Welch et al., 2007). Laser ablation studies have identified the QC as the source of short-range signals that inhibit differentiation of the contacting stem cells (van den Berg et al., 1997). Ethylene regulates organizer cell numbers through symmetric divisions showing that mitotic quiescence is not a prerequisite for QC function (Ortega-Martinez et al., 2007). In addition, occasional asymmetric self-renewing QC divisions generate daughters that replace stem cells displaced from their position (Kidner et al., 2000).

Downstream of the *SHR*/*SCR* pathway the putative intrinsic organizer factor *WOX5*, which is specifically expressed in the QC, is required to maintain columella stem cells (Sarkar et al., 2007). Mutant combinations with *shr*, *scr* and *plt1 plt2* show that *WOX5* is also, albeit redundantly, required to maintain proximal stem cells. Importantly, *WUS* and *WOX5* are interchangeable between the shoot and root for stem cell maintenance and do not change the fate of differentiating daughters, suggesting an evolutionarily conserved mechanism for stem cell maintenance. Furthermore, ectopic *WOX5* expression similar to shoot ectopic expression of *WUS* results in the accumulation of dividing cells, which in the case of ectopic *WOX5* were shown to maintain a stem cell-like state independent of the QC (Sarkar et al., 2007; Schoof et al., 2000). If the *WUS-WOX5* analogy is further extended with regard to protein movement (Sarkar et al., 2007), which has not been tested for WOX5, then WOX5, like WUS, would induce extrinsic signaling from the organizer to maintain surrounding stem cells.

Stem cells appear very sensitive to RETINOBLASTOMA-RELATED (RBR) levels and clonal analysis suggested that non-autonomous RBR activity from the QC influences stem cell maintenance (Wildwater et al., 2005). This suggests that extrinsic QC signaling is controlled by the *RBR* gene, which also acts downstream of *SCR*. The relation between *WOX5* and *RBR*-dependent extrinsic QC signaling remains to be established. Recently, the *PLT* expression gradient was found to determine cellular activity and function in the root, with high expression levels promoting stem cell

fate in an *RBR*-dependent manner (Galinha et al., 2007). These results indicate that more intrinsic factors may be involved in specifying stem cells and their organizers.

Taken together, these findings indicate that intrinsic shoot and root organizer factors are, at least in part, homologous and may both induce unknown extrinsic signals to maintain stem cells. Such extrinsic factors, e.g. those inducing CLV3 expression in shoot stem cells, remain to be discovered.

Stomata formation by de novo asymmetric divisions

Stomatal development initiates with the specification of meristemoid mother cells (MMCs) within a field of initially equivalent cells through as yet unidentified cues. MMCs undergo asymmetric division to generate a smaller triangular meristemoid. The larger sister cell may enlarge and become a pavement cell or adopt MMC fate. Meristemoids undergo up to three asymmetric divisions before differentiating into small, round guard mother cells (GMCs) that divide symmetrically once more to generate a pair of guard cells around a pore. During specification of stomatal lineages, cells follow a one-cell spacing rule by specifically oriented asymmetric divisions, implying regulation by position-dependent extrinsic signaling cues (Figure 4) (reviewed in Bergmann and Sack, 2007).

Three closely related bHLH proteins, SPEECHLESS (SPCH), MUTE and FAMA, have been identified as intrinsic factors required for cell fate transitions in the stomatal

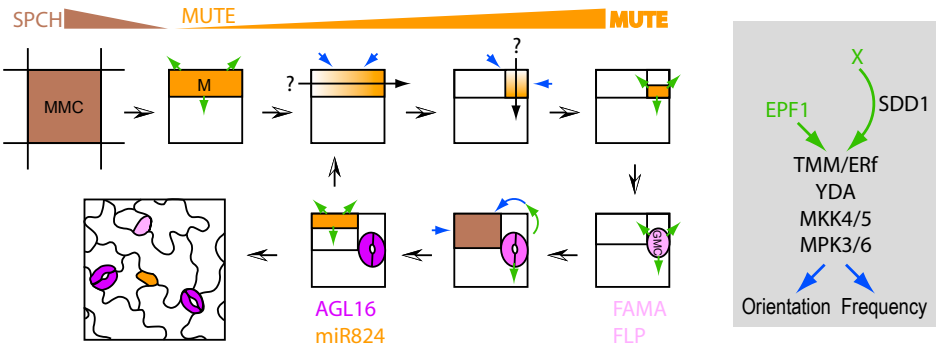

Figure 4. Asymmetric cell divisions in stomatal development. SPCH is expressed in MMCs (brown) and initiates the asymmetric division generating a meristemoid (M, orange), upon which SPCH protein is down-regulated. MUTE as an intrinsic meristemoid factor may be segregated following meristemoid polarization (arrow) and limits asymmetric divisions and induces GMC fate (pink) in a concentration-dependent manner. FAMA and FLP (together with MYB88) are independently required to limit mitotic GMC divisions, and FAMA promotes differentiation into guard cells (purple). *AGL16* and *miR824*, expressed in mature guard cells (dark purple) and nearby satellite meristemoids (orange), respectively, control the formation of higher-order stomatal complexes. Meristemoids, GMCs and young guard cells produce signals (green arrows: EPF1, and X via SDD1). Signaling is relayed (blue arrows) through the TMM/ERf–YDA–MKK4/5–MPK3/6 cascade and directs the orientation and frequency of division to receptive stomatal lineage cells.

lineage (MacAlister et al., 2007; Pillitteri et al., 2007; Ohashi-Ito and Bergmann, 2006). *SPCH* is expressed in a subset of protodermal cells and is necessary and sufficient for asymmetric MMC division (MacAlister et al., 2007; Pillitteri et al., 2007). *MUTE* is mainly expressed in meristemoids and protein levels appear to increase with consecutive rounds of asymmetric meristemoid division. Mutations in *MUTE* result in meristemoids that undergo additional rounds of inward-spiraling asymmetric divisions, terminating with an arrested meristemoid at the center that fails to differentiate into a GMC (MacAlister et al., 2007; Pillitteri et al., 2007). These observations indicate that MUTE is a candidate asymmetrically segregated intrinsic meristemoid factor that limits asymmetric divisions and induces GMC fate in a concentration-dependent manner, although unequal distribution of MUTE has not been observed at the resolution used to examine GFP-fusion protein expression. Expression of *FAMA* and the R2R3-type MYB transcription factor *FOUR LIPS* (*FLP*) with its partly redundant homolog *MYB88* is independently required to limit mitotic GMC divisions. *fama* resembles *flp myb88* double mutants in producing caterpillar-like cells, but only in the latter can cells terminate as guard cells, indicating that FAMA promotes differentiation into guard cells (Ohashi-Ito and Bergmann, 2006; Lai et al., 2005; Yang and Sack, 1995).

A candidate extrinsic 'spacing' signal is encoded by the *EPIDERMAL PATTERNING FACTOR1* (*EPF1*) gene that was identified from a screen in which putative secreted peptides were overexpressed (Hara et al., 2007). *epf1* mutants display increased numbers of stomata with meristemoids adjacent to guard cells or precursors. *EPF1* is expressed in meristemoids, GMCs and young guard cells, and thus appears to act downstream of *SPCH*, consistent with the apparent absence of signaling between MMCs (Geisler et al., 2000). The putative interacting TOO MANY MOUTHS (TMM) and ERECTA family (ERf: ER, ERL1, ERL2) receptors are implicated in the regulation of asymmetric entry and spacing division (Shpak et al., 2005). EPF1 may serve as their ligand, on the basis of observation that *epf1 tmm* double mutants resemble *tmm* (Hara et al., 2007). Genetic interactions did not confirm whether TMM/ERf signaling cues initiate and/or depend on MMC fate and *SPCH* expression for asymmetric entry division. *YDA* acts downstream of the TMM/ERf receptors (Bergmann et al., 2004) and recently this pathway was extended with the identification of the downstream-acting MAPK kinases 4 and 5 (MKK4/5) and MAP kinases 3 and 6 (MPK3/6), which are also involved in relaying environmental inputs (Wang et al., 2007; Bush and Krysan, 2007).

Three levels of signaling limit stomata numbers by influencing asymmetric divisions. First, environmental signals are known to influence stomatal density and may act through the TMM/ERf–YDA–MKK4/5–MPK3/6 pathway (Pedley and Martin, 2005). Second, a signal also acting through the TMM/ERf receptors was proposed

that involves processing mediated by STOMATAL DENSITY AND DISTRIBUTION1 (SDD1, a putative subtilisin-like extra cytoplasmic serine protease) (Nadeau and Sack, 2003; von Groll et al., 2002). Although *SDD1* and *EPF1* expression overlaps in meristemoids and GMCs, the *EPF1* overexpression phenotype does not depend on *SDD1*, indicating that EPF1 is not the substrate (Hara et al., 2007). Third, the MIKC-type MADS box gene *AGAMOUS-LIKE16* (*AGL16*) and its regulating microRNA *miR824* control the formation of higher-order stomatal complexes derived from satellite meristemoids (Kutter et al., 2007). More higher-order stomatal complexes form in plants expressing *miR824*-resistant *AGL16* mRNA and fewer in *agl16-1* mutant or *miR824* overexpressing plants, suggesting that AGL16 promotes the expression of genes necessary for continued asymmetric divisions and/or satellite meristemoid identity. Surprisingly, *AGL16* mRNA is present in guard cells, whereas *miR824* is detected in the satellite meristemoids positioned close by, which led the authors to hypothesize that *AGL16* mRNA moves to neighboring meristemoids. The relation of this pathway to the TMM/ERf receptor signaling cascade is not yet known.

In summary, intrinsic factors, of which MUTE may be a candidate segregated determinant, specify cell fate, and the numbers and planes of asymmetric divisions are under the control of extrinsic signals that represent developmental and environmental cues.

Concluding remarks and future prospects

Recent studies have implicated several intrinsic and extrinsic factors in plant asymmetric cell division. The *WOX* and *bHLH* genes encode putative intrinsic factors involved in asymmetric embryonic and stomatal lineage divisions, respectively. Future studies should disclose whether subcellular localization of RNAs and/or protein occurs for these intrinsic factors to polarize cells and whether unequal inheritance of these factors directs daughter cell fate analogous to animal asymmetric cell divisions. Kinematic analyses that greatly helped to visualize division dynamics in both shoot and root meristems may be a valuable tool for studying asymmetric division dynamics (Wildwater et al., 2005; Campilho et al., 2006; Reddy and Meyerowitz, 2005).

In the ground tissue, the moving SHR transcription factor determines endodermis fate, whereas other nuclear factors restrict its movement and stabilize boundary formation, representing a novel mechanism to regulate asymmetric division.

Plant stem cell biology still suffers from a lack of knowledge on intrinsic stem cell factors and extrinsic signaling. Target analysis of shoot *WUS* and root *PLT* and *SHR/SCR/RBR/WOX5* pathways can help to identify relevant genes. In contrast, an elaborate extrinsic signaling cascade has been identified that directs the number and orientation of asymmetric division planes during stomatal development. De-

termining how this signaling cascade translates into control of cell division plane represents a major challenge for the future.

Acknowledgements

We apologize to those whose publications could not be cited because of space limitations. We are indebted to Ben Scheres for valuable asymmetry discussions and Viola Willemsen and Marijn Luijten for critical reading of the manuscript. CAtH was funded by the Centre for BioSystems Genomics (CBSG), which is part of the Netherlands Genomics Initiative/Netherlands Organization for Scientific Research (NGI/NWO).

References

Benfey, P.N., Linstead, P.J., Roberts, K., Schiefelbein, J.W., Hauser, M.T., and Aeschbacher, R.A. (1993). Root development in *Arabidopsis*: four mutants with dramatically altered root morphogenesis. Development *119*, 57-70.

Bergmann, D.C., Lukowitz, W., and Somerville, C.R. (2004). Stomatal development and pattern controlled by a MAPKK kinase. Science *304*, 1494-1497.

Bergmann, D.C. and Sack, F.D. (2007). Stomatal Development. Annual Review of Plant Biology *58*, 163-181.

Boutte, Y., Ikeda, Y., and Grebe, M. (2007). Mechanisms of auxin-dependent cell and tissue polarity. Current Opinion in Plant Biology 10.1016/j.pbi.2007.07.008.

Bush, S.M. and Krysan, P.J. (2007). Mutational evidence that the *Arabidopsis* MAP kinase MPK6 is involved in anther, inflorescence, and embryo development. J. Exp. Bot. *58*, 2181-2191.

Campilho, A., Garcia, B., Toorn, H., Wijk, H., Campilho, A., and Scheres, B. (2006). Time-lapse analysis of stem-cell divisions in the *Arabidopsis thaliana* root meristem. The Plant Journal *48*, 619-627.

Cui, H., Levesque, M.P., Vernoux, T., Jung, J.W., Paquette, A.J., Gallagher, K.L., Wang, J.Y., Blilou, I., Scheres, B., and Benfey, P.N. (2007). An evolutionarily conserved mechanism delimiting SHR movement defines a single layer of endodermis in plants. Science *316*, 421-425.

Di Laurenzio, L., Wysocka-Diller, J., Malamy, J.E., Pysh, L., Helariutta, Y., Freshour, G., Hahn, M.G., Feldmann, K.A., and Benfey, P.N. (1996). The SCARECROW gene regulates an asymmetric cell division that is essential for generating the radial organization of the *Arabidopsis* root. Cell *86*, 423-433.

Fischer, U., Men, S., and Grebe, M. (2004). Lipid function in plant cell polarity. Current Opinion in Plant Biology *7*, 670-676.

Friml, J., Vieten, A., Sauer, M., Weijers, D., Schwarz, H., Hamann, T., Offringa, R., and Jurgens, G. (2003). Efflux-dependent auxin gradients establish the apical-basal axis of *Arabidopsis*. Nature *426*, 147-153.

Friml, J., Yang, X., Michniewicz, M., Weijers, D., Quint, A., Tietz, O., Benjamins, R., Ouwerkerk, P.B., Ljung, K., Sandberg, G., Hooykaas, P.J., Palme, K., and Offringa, R. (2004). A PINOID-dependent binary switch in apical-basal PIN polar targeting directs auxin efflux. Science *306*, 862-865.

Galinha, C., Hofhuis, H.F., Luijten, M., Willemsen, V., Blilou, I., Heidstra, R., and Scheres, B. (2007). PLETHORA proteins as dose-dependent master regulators of *Arabidopsis* root development. Nature doi:10.1038/nature06206.

Gallagher, K.L., Paquette, A.J., Nakajima, K., and Benfey, P.N. (2004). Mechanisms regulating SHORTROOT intercellular movement. Current Biology *14*, 1847-1851.

Geisler, M., Nadeau, J., and Sack, F.D. (2000). Oriented asymmetric divisions that generate the stomatal spacing pattern in *Arabidopsis* are disrupted by the *too many mouths* mutation. Plant Cell *12*, 2075-2086.

Haecker, A., Gross-Hardt, R., Geiges, B., Sarkar, A., Breuninger, H., Herrmann, M., and Laux, T. (2004). Expression dynamics of WOX genes mark cell fate decisions during early embryonic patterning in *Arabidopsis thaliana*. Development *131*, 657-668.

Hara, K., Kajita, R., Torii, K.U., Bergmann, D.C., and Kakimoto, T. (2007). The secretory peptide gene EPF1 enforces the stomatal one-cell-spacing rule. Genes Dev. *21*, 1720-1725.

Heidstra, R. (2007). Asymmetric cell division in plant development. Prog. Mol Subcell. Biol *45*, 1-37.

Heidstra, R., Welch, D., and Scheres, B. (2004). Mosaic analyses using marked activation and deletion clones dissect *Arabidopsis* SCARECROW action in asymmetric cell division. Genes Dev. *18*, 1964-1969.

Helariutta, Y., Fukaki, H., Wysocka-Diller, J., Nakajima, K., Jung, J., Sena, G., Hauser, M.T., and Benfey, P.N. (2000). The SHORT-ROOT gene controls radial patterning of the *Arabidopsis* root through radial signaling. Cell *101*, 555-567.

Horvitz, H.R. and Herskowitz, I. (1992). Mechanisms of asymmetric cell division: Two Bs or not two Bs, that is the question. Cell *68*, 237-255.

Jenik, P.D., Gillmor, C.S., and Lukowitz, W. (2007). Embryonic patterning in *Arabidopsis thaliana*. Annual Review of Cell and Developmental Biology *23*, doi:10.1146/annurev.cellbio.22.011105.102609.

Jurgens, G. (2005). Cytokinesis in higher plants. Annu. Rev. Plant Biol. *56*, 281-299.

Kidner, C., Sundaresan, V., Roberts, K., and Dolan, L. (2000). Clonal analysis of the *Arabidopsis* root confirms that position, not lineage, determines cell fate. Planta *211*, 191-199.

Kutter, C., Schob, H., Stadler, M., Meins, F., Jr., and Si-Ammour, A. (2007). MicroRNA-mediated regulation of stomatal development in *Arabidopsis*. Plant Cell doi: 10.1105/tpc.107.050377.

Lai, L.B., Nadeau, J.A., Lucas, J., Lee, E.K., Nakagawa, T., Zhao, L., Geisler, M., and Sack, F.D. (2005). The *Arabidopsis* R2R3 MYB proteins FOUR LIPS and MYB88 restrict divisions late in the stomatal cell lineage. Plant Cell *17*, 2754-2767.

Laux, T., Mayer, K.F., Berger, J., and Jurgens, G. (1996). The WUSCHEL gene is required for shoot and floral meristem integrity in *Arabidopsis*. Development *122*, 87-96.

Levesque, M.P., Vernoux, T., Busch, W., Cui, H., Wang, J.Y., Blilou, I., Hassan, H., Nakajima, K., Matsumoto, N., Lohmann, J.U., Scheres, B., and Benfey, P.N. (2006). Whole-genome analysis of the SHORT-ROOT developmental pathway in *Arabidopsis*. PLoS. Biol *4*, e143.

Lloyd, C. and Chan, J. (2006). Not so divided: the common basis of plant and animal cell division. Nat Rev Mol Cell Biol *7*, 147-152.

Lukowitz, W., Roeder, A., Parmenter, D., and Somerville, C. (2004). A MAPKK kinase gene regulates extra-embryonic cell fate in *Arabidopsis*. Cell *116*, 109-119.

MacAlister, C.A., Ohashi-Ito, K., and Bergmann, D.C. (2007). Transcription factor control of asymmetric cell divisions that establish the stomatal lineage. Nature *445*, 537-540.

Mansfield, S.G. and Briarty, L.G. (1991). Early embryogenesis in *Arabidopsis thaliana*. II. The developing embryo. Can. J. Bot. *69*, 461-476.

Mayer, K.F., Schoof, H., Haecker, A., Lenhard, M., Jurgens, G., and Laux, T. (1998). Role of WUSCHEL in regulating stem cell fate in the *Arabidopsis* shoot meristem. Cell *95*, 805-815.

Nadeau, J.A. and Sack, F.D. (2003). Stomatal development: cross talk puts mouths in place. Trends in Plant Science *8*, 294-299.

Nakajima, K., Sena, G., Nawy, T., and Benfey, P.N. (2001). Intercellular movement of the putative transcription factor SHR in root patterning. Nature *413*, 307-311.

Ohashi-Ito, K. and Bergmann, D.C. (2006). *Arabidopsis* FAMA controls the final proliferation/differentiation switch during stomatal development. Plant Cell *18*, 2493-2505.

Ortega-Martinez, O., Pernas, M., Carol, R.J., and Dolan, L. (2007). Ethylene modulates stem cell division in the *Arabidopsis thaliana* root. Science *317*, 507-510.

Pedley, K.F. and Martin, G.B. (2005). Role of mitogen-activated protein kinases in plant immunity. Current Opinion in Plant Biology *8*, 547.

Pillitteri, L.J., Sloan, D.B., Bogenschutz, N.L., and Torii, K.U. (2007). Termination of asymmetric cell division and differentiation of stomata. Nature *445*, 501-505.

Reddy, G.V. and Meyerowitz, E.M. (2005). Stem-Cell Homeostasis and Growth Dynamics Can Be Uncoupled in the *Arabidopsis* Shoot Apex. Science *310*, 663-667.

Sabatini, S., Heidstra, R., Wildwater, M., and Scheres, B. (2003). SCARECROW is involved in positioning the stem cell niche in the *Arabidopsis* root meristem. Genes Dev. *17*, 354-358.

Sablowski, R. (2007). Flowering and determinacy in *Arabidopsis*. J. Exp. Bot. *58*, 899-907.

Sarkar, A.K., Luijten, M., Miyashima, S., Lenhard, M., Hashimoto, T., Nakajima, K., Scheres, B., Heidstra, R., and Laux, T. (2007). Conserved factors regulate signalling in *Arabidopsis thaliana* shoot and root stem cell organizers. Nature *446*, 811-814.

Scheres, B., Di Laurenzio, L., Willemsen, V., Hauser, M.T., Janmaat, K., Weisbeek, P., and Benfey, P.N. (1995). Mutations affecting the radial organisation of the *Arabidopsis* root display specific defects throughout the embryonic axis. Development *121*, 53-62.

Scheres, B. (2007). Stem-cell niches: nursery rhymes across kingdoms. Nat Rev Mol Cell Biol *8*, 345-354.

Schoof, H., Lenhard, M., Haecker, A., Mayer, K.F., Jurgens, G., and Laux, T. (2000). The stem cell population of *Arabidopsis* shoot meristems in maintained by a regulatory loop between the CLAVATA and WUSCHEL genes. Cell *100*, 635-644.

Sena, G., Jung, J.W., and Benfey, P.N. (2004). A broad competence to respond to SHORT ROOT revealed by tissue-specific ectopic expression. Development *131*, 2817-2826.

Shpak, E.D., McAbee, J.M., Pillitteri, L.J., and Torii, K.U. (2005). Stomatal Patterning and Differentiation by Synergistic Interactions of Receptor Kinases. Science *309*, 290-293.

Spradling, A., Drummond-Barbosa, D., and Kai, T. (2001). Stem cells find their niche. Nature *414*, 98-104.

van den Berg, C., Willemsen, V., Hendriks, G., Weisbeek, P., and Scheres, B. (1997). Short-range control of cell differentiation in the *Arabidopsis* root meristem. Nature *390*, 287-289.

von Groll, U., Berger, D., and Altmann, T. (2002). The subtilisin-like serine protease SDD1 mediates cell-to-cell signaling during *Arabidopsis* stomatal development. Plant Cell *14*, 1527-1539.

Wang, H., Ngwenyama, N., Liu, Y., Walker, J.C., and Zhang, S. (2007). Stomatal development and patterning are regulated by environmentally responsive Mitogen-Activated Protein Kinases in *Arabidopsis*. Plant Cell *19*, 63-73.

Weijers, D., Schlereth, A., Ehrismann, J.S., Schwank, G., Kientz, M., and Jurgens, G. (2006). Auxin triggers transient local signaling for cell specification in *Arabidopsis* embryogenesis. Developmental Cell *10*, 265-270.

Welch, D., Hassan, H., Blilou, I., Immink, R., Heidstra, R., and Scheres, B. (2007). *Arabidopsis* JACKDAW and MAGPIE zinc finger proteins delimit asymmetric cell division and stabilize tissue boundaries by restricting SHORT-ROOT action. Genes Dev. *21*, 2196-2204.

Wildwater, M., Campilho, A., Perez-Perez, J.M., Heidstra, R., Blilou, I., Korthout, H., Chatterjee, J., Mariconti, L., Gruissem, W., and Scheres, B. (2005). The RETINOBLASTOMA-RELATED gene regulates stem cell maintenance in *Arabidopsis* roots. Cell *123*, 1337-1349.

Wu, X., Chory, J., and Weigel, D. (2007). Combinations of *WOX* activities regulate tissue proliferation during *Arabidopsis* embryonic development. Dev. Biol doi:10.1016/j.ydbio.2007.07.019.

Wysocka-Diller, J.W., Helariutta, Y., Fukaki, H., Malamy, J.E., and Benfey, P.N. (2000). Molecular analysis of SCARECROW function reveals a radial patterning mechanism common to root and shoot. Development *127*, 595-603.

Xie, T., Kawase, E., Kirilly, D., and Wong, M.D. (2005). Intimate relationships with their neighbors: tales of stem cells in Drosophila reproductive systems. Dev. Dyn. *232*, 775-790.

Yang, M. and Sack, F.D. (1995). The too many mouths and four lips mutations affect stomatal production in *Arabidopsis*. Plant Cell *7*, 2227-2239.

Chapter 2

SCHIZORIZA encodes a nuclear factor regulating asymmetry of stem cell divisions in the *Arabidopsis* root

Colette A. ten Hove, Viola Willemsen, Wouter J. de Vries, Anja van Dijken, Ben Scheres and Renze Heidstra

Faculty of Science, Department of Biology, section Molecular Genetics, Utrecht University, Padualaan 8, 3584 CH Utrecht, the Netherlands.

Curr Biol (2010), doi:10.1016/j.cub.2010.01.018

Summary

Cell divisions generating daughter cells different in size, shape, identity and function are indispensable for many developmental processes including fate specification, tissue patterning and self-renewal. In animals and yeast, perturbations in factors required for well-described asymmetric cell divisions generally yield cells of equal fate. We here report on SCHIZORIZA (SCZ), a single nuclear factor with homology to heat shock transcription factors that controls the separation of cell fate in a set of stem cells generating different root tissues: root cap, epidermis, cortex and endodermis. Loss-of-function, expression and reconstitution experiments indicate that SCZ acts mainly from within its cortical expression domain in the stem cell niche, exerting both autonomous and non-autonomous effects to specify cortex identity and control the separation of cell fates in surrounding layers. Thus, SCZ defines a novel pathway for asymmetric cell division in plants.

Results and Discussion

Asymmetric cell division is a fundamental and universal mechanism for generating diversity and pattern in multicellular organisms (ten Hove and Heidstra, 2008; Knoblich, 2008). The radial organization of the *Arabidopsis* root is derived from stereotyped asymmetric cell divisions of different stem cells, the initials. These cells and their daughters produce defined tissue layers with distinct cell fates (Figure 1a) (Benfey and Scheres, 2000). The stem cells surround a small group of rarely dividing cells, the quiescent center (QC), required for their maintenance. The QC itself is formed early during embryogenesis when an asymmetric division of the hypophyseal cell forms the lens-shaped QC progenitor cell and future columella root cap (Jürgens and Mayer, 1994). QC fate is specified in parallel by the PLETHORA (PLT) and SHORT-ROOT (SHR), SCARECROW (SCR) transcription factors (Aida et al., 2004; Galinha et al., 2007; Sabatini et al., 2003). SHR and SCR are also required for ground tissue patterning: *shr* and *scr* mutants lack the asymmetric periclinal division in the ground tissue stem cell daughter resulting in a single ground tissue layer. For *shr* this layer lacks endodermal identity, but in *scr* this layer displays mixed cortex/endodermis identity (Di Laurenzio et al., 1996; Helariutta et al., 2000; Nakajima et al., 2001). Several other reports have appeared that suggest plant cells may possess mixed fates (Schnittger et al., 1998; Szymanski and Marks, 1998; Nodine et al., 2007). To our knowledge, the only known example of mixed fate phenotypes in animal development comes from extensive genetic screening approaches in *C. elegans*, which have uncovered mutants in which a single neuronal fate decision is inappropriately executed resulting in a mixed fate phenotype (Sarin et al., 2007). Here we describe the SCZ nuclear factor that is required for plant cell fate separation in several tissues, acting both cell-autonomously and non-cell-autonomously. Our data highlight a novel mechanism of cell fate separation in plants that is particularly relevant for asymmetric cell divisions within stem cell areas.

SCZ encodes a member of the heat shock transcription factor family

To find novel genes involved in QC specification and stem cell maintenance we performed a QC-marker based mutagenesis screen. A line doubly homozygous for *QC25* and *QC46* promoters (Sabatini et al., 2003) fused to $_{ER}$*CFP* and $_{ER}$*YFP*, respectively (Figures 1b,c), was mutagenized and the M2 progeny was analyzed for altered expression. Five phenotypically indistinguishable mutant lines combined reduced *QC25::*$_{ER}$*CFP* and *QC46::*$_{ER}$*YFP* activity with retarded root growth and disorganization of the stem cell niche (Figures 1d,e and see below). Complementation tests showed that all five lines carried allelic mutations. Given the equal allele strength we continued to use one allele, *qc351,* for further analysis.

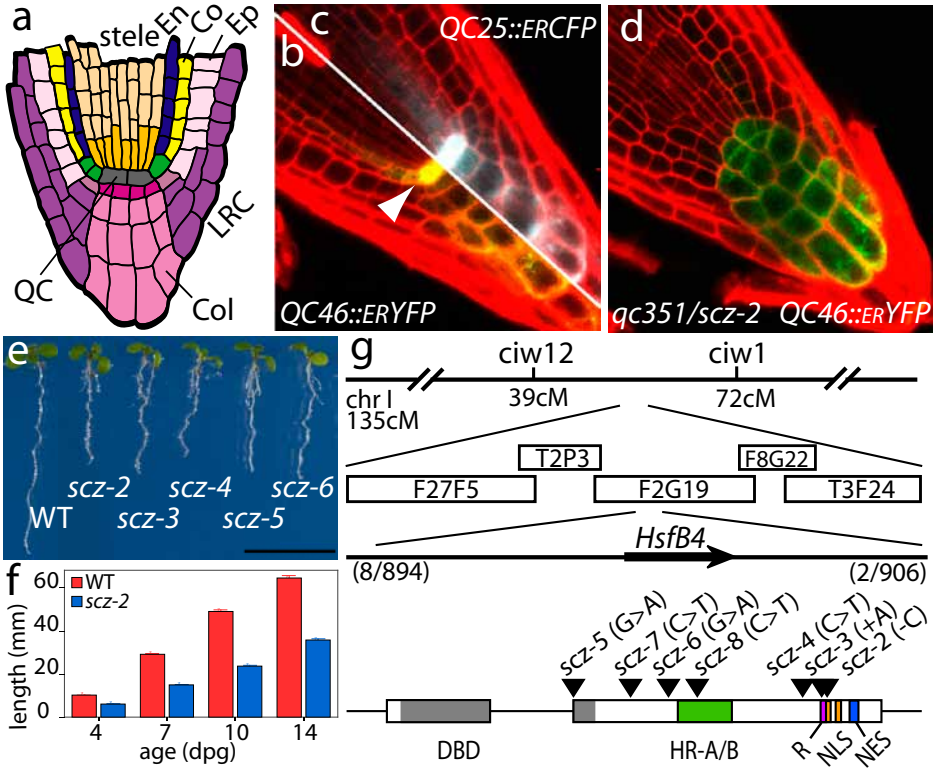

Figure 1. Identification and cloning of *SCZ*. (a) Schematic view of the *Arabidopsis* root meristem. (En) endodermis; (Co) cortex; (Ep) epidermis; (LRC) lateral root cap; (Col) columella; (QC) quiescent center. (b-d) 4-Day-old wild type root expressing both *QC46::$_{ER}$YFP* (b; arrowhead marks QC) and *QC25::$_{ER}$CFP* (c) and 4-day-old *qc351/scz-2* root showing *QC46::$_{ER}$YFP* expression (d; false green). (e) 8-Day-old wild type and *scz-2 – scz-6* seedlings. (f) Root length (in mm) of wild type and *scz-2* seedlings at indicated days post germination (dpg). For each data point $n \geq 57$; error bars, standard error of the mean. (g) Schematic representation of the identification of the *SCZ* gene by positional cloning. *SCZ/HsfB4* location relative to a contig of five BAC clones; the proportion of recombinant seedlings is shown in parenthesis. Boxes indicate coding sequence. Conserved functional domains according to (Nover et al., 2001) are indicated; the conserved DNA binding domain (grey); HR-A/B oligomerization region (green); nuclear localization signal (NLS; orange); nuclear export signal (NES; blue). R (R/KLFGV) motif (purple) (Ikeda and Ohme-Takagi, 2009). The positions of the nucleotide sequence changes are shown for each mutant allele; *scz-7* and *scz-8* are TILLING alleles (Till et al., 2003). See also Figure S1.

Compared to wild type *qc351* roots developed more hairs, lacked the stereotypical pattern of alternating hair and nonhair files and initiated root hairs from subepidermal tissue reminiscent of the *schizoriza* (*scz*) mutant phenotype (Figures S1a,b) (Mylona et al., 2002). Complementation analysis revealed that *qc351* was allelic to *scz*. Accordingly, we renamed our mutant alleles *scz-2* to *scz-6*.

We molecularly characterized the *scz* mutation using a map-based approach. Fine mapping located *SCZ* to a single locus in an area of 70 kb on chromosome 1 (Figure

1g). One of the candidate genes we sequenced was the *heat shock transcription factor B4* (*HsfB4*) locus (At1g46264) based on its stem cell enriched *in silico* root expression pattern (www.arexdb.org) (Birnbaum et al., 2003; Nawy et al., 2005; Brady et al., 2007). Comparison with the corresponding wild type sequence revealed different mutations in the *HsfB4* gene for all *scz* alleles, including two additional TILLING alleles (Figure 1g, Table S1). The identical phenotype indicates that they are likely *HsfB4* mutant null alleles. For *Arabidopsis* the 21 Hsfs are classified into three major groups, A (16 members), B (4 members including *SCZ*) and C (1 member), according to the different flexible linkers in their HR-A/B oligomerization regions (Figure 1g, green). Despite considerable diversification in size and sequence, the basic structure of Hsfs is conserved among eukaryotes (Nover et al., 2001).

SCZ mRNA is first detected at triangular stage embryos in the QC progenitor cells. From heart stage onwards *SCZ* mRNA accumulation expands into ground and vascular tissue progenitors and their immediate daughters (Figures 2a,b,c). This expression pattern is maintained in the postembryonic root with highest *SCZ* mRNA accumulation in QC and ground tissue stem cells and their immediate daughters (Figure 2d). In the *scz-2* mutant, hybridization signal is absent from the subepidermal layer (Figures S2a,b). *SCZ* promoter-reporter fusions essentially corroborate the *in situ* hybridization expression pattern (Figures S2c,d,e). Consistent with its function as a putative transcription factor the complementing *35S::GFP:SCZ* translational fusion localizes to the cell nucleus (see below).

Disturbed asymmetric cell division from embryogenesis onward in *scz*

The reduction in root growth together with altered expression of QC markers *QC25::$_{ER}$CFP* and *QC46::$_{ER}$YFP* in mutants (Figures 1d,e) might indicate a role for *SCZ* in QC/stem cell specification and/or function. However, *scz-2* roots continue to grow in an indeterminate manner with root length lagging by about half behind wild type (Figure 1f). Similarly, root meristem size is reduced but maintained in *scz-2* (Figure S1c). These observations show that *SCZ* is not critically required for stem cell maintenance.

Cells at the position of the QC and columella stem cells in *scz-2* mutant roots are morphologically abnormal and accumulate starch granules, which marks differentiated columella in wild type (Figures 2f,g). QC25, QC46, QC184 markers are displaced from the QC and express diffuse activity in the starch granule containing cells. *WOX5* also marks the QC and the gene product is required to maintain the underlying columella stem cells. *WOX5::$_{ER}$GFP* expression faded from the position of the QC but did not appear in the columella (Figures 2f-i, Figures S2f-i). Apparently, QC and columella fates are present but not separated in *scz-2* roots and the separation defect does not affect stem cell niche activity. Interestingly, this observation

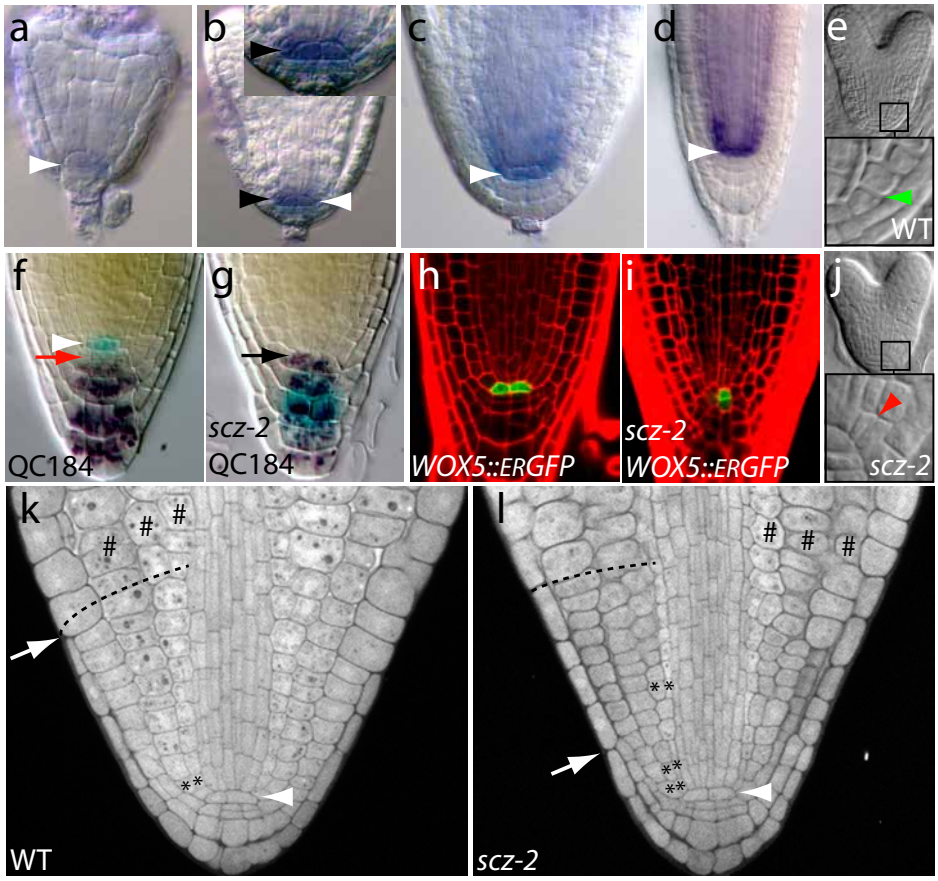

Figure 2. ***SCZ*** **expression and (post-)embryonic mutant stem cell defects.** (a-d) *In situ* hybridization with *SCZ* antisense probe in wild type at triangular (a); heart (b; black arrowhead marks ground tissue accumulation); and torpedo stage embryo (c); and two-day-old seedling (d). (e,j) Heart stage wild type (e) and *scz-2* (j) embryos. Inset shows blowup of normal anticlinally divided ground tissue initial (e; green arrowhead), aberrant periclinally divided ground tissue initial (j; red arrowhead). (f,g) QC184 expression (blue) in 6-day-old wild type (f) shifts in the columella in *scz-2* (g) roots. Red arrow marks columella stem cells devoid of purple starch granules, black arrow; accumulation of starch granules in mutant QC region. (h,i) *WOX5::$_{ER}$GFP* expression in 4-day-old wild type (h) and *scz-2* (i) roots. (k,l) Aniline blue stained wild type (k) and *scz-2* (l) mature embryos. End of lateral root cap layer (white arrow); root/hypocotyl boundary (dashed line); ground tissue layers in hypocotyl (#); ectopic periclinal ground tissue divisions leading to supernumerary mutant layers in *scz-2* (*). See also Figure S2. White arrowhead marks QC.

of mixed fates was reminiscent of the formation of root hairs from subepidermal tissues reported when *scz* mutants were first described (Mylona et al., 2002).

To gain more insight in the possible role for *SCZ* as a fate determination and/or separation factor we traced back the *scz-2* defects to their embryonic origin. The initial defect in *scz-2* occurs in heart stage embryos where ground tissue initial cells perform an aberrant periclinal division (Figure 2j) resulting in the ectopic ground

tissue layer observed at torpedo stage (Mylona et al., 2002) (data not shown). The inner ground tissue daughter cells continue to perform additional periclinal divisions generating more ectopic layers (Figure 2l, asterisk). The organization of QC, columella, pericycle and vasculature appears normal throughout embryogenesis. In wild type mature embryos, an additional cortical layer proximal to the end of the lateral root cap marks the hypocotyl (Figure 2k) (Dolan et al., 1993). Similarly, in *scz-2* the hypocotyl possesses three ground tissue layers (Figure 2l). However, the lateral root cap layer contains fewer cells and epidermal cells below the root-hypocotyl junction appear long and flat, morphologically reminiscent of lateral root cap cells suggestive of mixed fates (Figure 2l, proximal to arrow). These observations are consistent with a role for *SCZ* in cell fate separation from heart stage embryogenesis onward.

Non-cell autonomous regulation of epidermis/lateral root cap fate separation

To probe the identity of the *scz-2* epidermis we analyzed the promoter activity of the *WEREWOLF* gene (*WER*) (Lee and Schiefelbein, 1999) and accumulation of SOMBRERO (SMB):GFP protein (Willemsen et al., 2008) in embryos and roots. *WER* has a role in epidermal cell fate specification and *WER>>$_{ER}$CFP* is expressed in lateral root cap and epidermis including the stem cell in wild type (Figures 3a,b,e,f). SMB represses stem cell-like divisions in the root cap and accordingly *SMB::SMB:GFP* is expressed in nuclei of root cap stem cell daughters and maturing root cap layers (Figures 3a,b,e,f). In *scz-2* embryos SMB:GFP is also expressed in epidermal cells and both markers even extend to the subepidermal cells (Figures 3c,d). In the distal root meristem the epidermal expression overlap is maintained but subepidermal expression is observed only in the distal most cells including the stem cells (Figures 3g,h, arrows). Next we combined *GLABRA2* promoter expression marking developing nonhair cells (*GL2::GUS*) (Masucci et al., 1996) with transverse root sections to examine cell number and shape typical for their differentiation status (Figures 3i-l). Cross sections of *scz-2* root meristems reveal that vascular tissues are normal but a double layer of endodermis-like cells is present (Figure 3k). Epidermal cell number is reduced from the normal ~22 rectangular shaped cells to ~12 ellipsoidal cells resembling the underlying cortex-like cells (Figures 3i,k). An additional layer with lateral root cap morphology surrounds the epidermis. *GL2::GUS* is weakly expressed in almost all epidermal and in few subepidermal cells (Figure 3k). Strikingly, whereas epidermal cell files are tightly connected in the wild type, they separate as tissues mature in *scz-2*, a feature that is restricted to root cap cells in the wild type (Figure 3l). Our data indicate that *scz-2* root epidermal and subepidermal tissues are compromised in fate segregation. Importantly, the nearest tissue expressing *SCZ* is the cortex suggesting that *SCZ* acts non-cell autonomously in epidermis/lateral root cap fate separation.

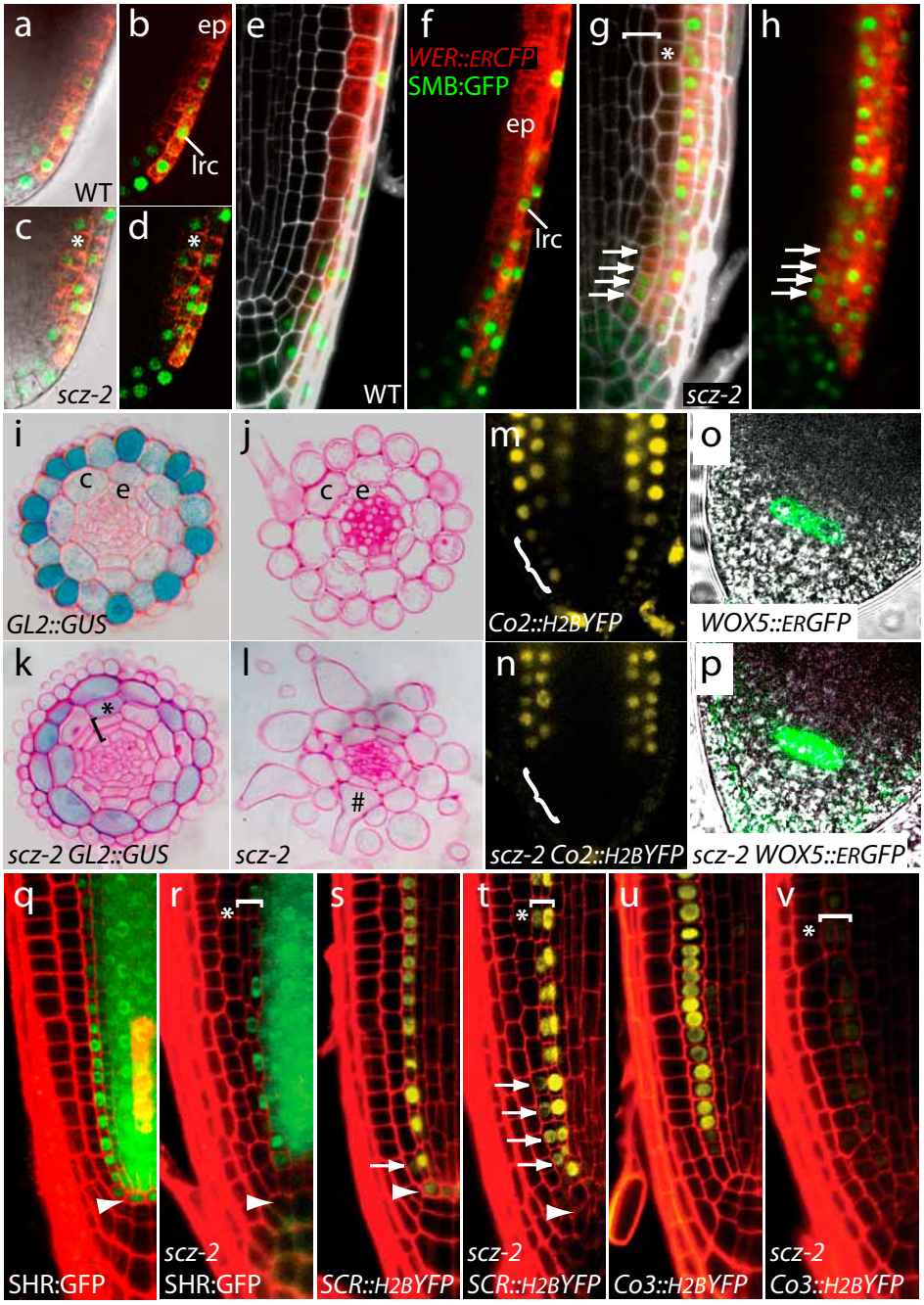

Figure 3. ***SCZ* specifies cortex and segregates cell fates in the root niche.** (a-h) *WER>>*$_{ER}$*CFP* (false red) and SMB:GFP expression in bent cotelydon stage wild type (a,b) and *scz-2* (c,d) embryos, and in 4-day-old wild type (e,f) and *scz-2* (g,h) roots. Arrows indicate *WER>>*$_{ER}$*CFP* and SMB:GFP expression in distal subepidermal cells (g,h). (i-l) Radial root tissue sections of 4-day-old wild type (i,j) and *scz-2* (k,l) roots stained for *GL2::GUS* expression. *scz-2* subepidermal cells express *GL2::GUS* (k, asterisk) and form root hairs (l, hash).

SCZ is required for cortex fate specification

Initial characterization of *scz* revealed ectopic expression of epidermal markers into the ground tissue and misexpression of a ground tissue marker (Mylona et al., 2002). To further investigate the fate of the mutant ground tissue layers we analyzed expression of endodermal markers. *SHR::SHR:GFP* is expressed in stele cells and the protein moves to accumulate in the nuclei of QC, ground tissue stem cells and endodermis where it activates its target *SCR* (Figure 3q) (Nakajima et al., 2001). Upon periclinal asymmetric division of the ground tissue stem cell daughter *SCR* promoter activity is rapidly shut down in the outer cortex cell (Figure 3s, arrow) (Wysocka-Diller et al., 2000). In line with the QC defects by which we selected *scz* mutants, SHR:GFP and *SCR::$_{H2B}$YFP* expression is absent from the QC region (Figures 3r,t, arrowhead). In the *scz-2* ground tissue SHR:GFP is only observed in the innermost layer adjacent to the stele (Figure 3r) whereas *SCR::$_{H2B}$YFP* expression extends into the next layer (Figure 3t). Taking these data together with the cell morphology characteristics we conclude that these layers represent endodermis. In addition, *SCR::$_{H2B}$YFP*, like *WER>>$_{ER}$CFP* and SMB:GFP, even extends into the distal subepidermal tissue (Figure 3t, arrows). Apparently, *SCR::$_{H2B}$YFP* fails to segregate to the endodermis in a timely manner and is maintained independently of SHR presence. This suggests that *SCR* promoter downregulation in wild type is aided by cortically expressed *SCZ*. Similarly the ectopic endodermis division can be explained by coexpression of SHR and SCR resulting in division of the ground tissue, as in wild type, but in the absence of SCZ the outer cell file fails to adopt cortex fate.

To further substantiate a causal link between *SCZ* expression and cortex fate determination we analyzed *Co2::$_{H2B}$YFP* and *Co3::$_{H2B}$YFP* that are highly expressed in the cortex but excluded from the QC and undivided ground tissue stem cells from embryogenesis onward (Figures 3u, Figure S3a). Occasional weak expression in endodermal cells is observed in the wild type. Importantly, in *scz-2* seedling roots, both markers are rarely expressed and if so only the weak endodermal expression is observed (Figure 3v, Figure S3b). Already during embryogenesis *Co2::$_{H2B}$YFP* expression is excluded from the root ground tissue but remains expressed in the hypocotyl ground tissue consistent with the root specific defects in *scz-2* (Figure 3n). We conclude that *SCZ* is necessary for the specification of root cortex cell identity.

(m,n) Embryonic root *Co2::$_{H2B}$YFP* expression in late torpedo stage wild type (m) is absent in *scz-2* embryo (n, bracket). (o,p) *WOX5::$_{ER}$GFP* expression in late torpedo stage wild type (o) and *scz-2* (p) embryos. (q-v) 4-Day-old wild type (q,s,u) and *scz-2* (r,t,v) roots expressing *SHR::SHR:GFP* (q,r); *SCR::$_{H2B}$YFP* (s,t) and *Co3::$_{H2B}$YFP* (u,v). Fading *SCR::$_{H2B}$YFP* expression in periclinally divided ground tissue stem cell daughter (s, arrow) is maintained in *scz-2* subepidermal cell patch (t, arrows). *Co3::$_{H2B}$YFP* expression is lost from the mutant subepidermal layer in *scz-2* (v, asterisk). See also Figure S3.

(ep) Epidermis; (lrc) lateral root cap; (c) cortex; (e) endodermis; (*) mutant subepidermal layer; arrowhead, QC; square bracket indicates ectopic endodermal layers.

To test if *SCZ* is sufficient to determine cortex fate we ectopically expressed *SCZ* from the *35S* promoter. Distal to the QC in *35S::SCZ* roots the presence of an additional columella stem cell layer is apparent by the absence of starch granules and lack of *SMB::SMB:GFP* expression that marks differentiated columella (Figures 4e,f). Examination of radial tissue markers reveals the formation of an ectopic epidermal layer that shows activity of the *WER>>$_{ER}$CFP* and *GL2>>$_{ER}$GFP* epidermal markers (Figures 4g,h, Figures S4a,b). Cross sections reveal occasional misexpression of *GL2>>$_{ER}$GFP* (Figure S4c). In addition, the lateral root cap layer does not slough off in the proximal meristem (Figures S4e,f). We concluded that the overexpression of *SCZ* introduces new cell fate separation defects.

Analysis of SCZ protein expression in *35S::GFP:SCZ* overexpression lines revealed relatively high levels in the columella, lateral root cap and distal epidermal tissues correlating to regions of ectopic cell division (Figure 4i). Interestingly, *WER>>$_{ER}$CFP* expression is lost from the epidermis/lateral root cap stem cell region where it is normally observed (Figure 4g, compare to 3e,f) suggesting inhibition of epidermal/lateral root cap fate. *WER>>$_{ER}$CFP* and *GL2>>$_{ER}$GFP* are (re)expressed in outer layers proximally (Figure 4g, Figure S4b) suggesting transient inhibition of epidermal fate by high levels of SCZ or, alternatively, higher sensitivity of the stem cell region to the SCZ effect. Strikingly, ectopic expression of *Co2::$_{H2B}$YFP* was observed in these high GFP:SCZ expressing root cap cells (Figure 4h) corroborating that *SCZ* expression is sufficient to induce cortex fate and inhibit epidermal and lateral root cap fates.

Cortex expressed SCZ rescues mutant defects

The lack of distal QC and columella fate separation prompted us to examine embryonic QC25, QC46, QC184, *SCR::$_{H2B}$YFP* and *WOX5::$_{ER}$GFP* marker expression. Surprisingly, all markers were appropriately expressed in *scz-2* throughout embryogenesis indicating that cell identities are correctly set up but cannot be maintained, which correlates with reduced stem cell activity and root growth (Figures 3o,p, Figures S3c,d, data not shown). We tested whether compromised stem cell activity might cause the failure to separate cell fates by crossing *scz-2* to *WOX5* overexpressing and *smb-3* knockout mutants that display increased distal stem cell activity and numbers (Willemsen et al., 2008; Sarkar et al., 2007). Interestingly, *scz-2 35S::WOX5* and *scz-2 smb-3* double mutant roots display wild type QC morphology and positioning as visualized by strong re-expression of *QC46::$_{ER}$YFP* and *SCR::$_{H2B}$YFP* in the QC (Figures 4a,b, Figure S4d). Lack of starch staining in *scz-2 smb-3* reveals presence of columella stem cells indicative of improved QC function (Figure 4d). However, the radial cell fate separation defects remain and root growth is not rescued in these double mutant combinations (Figures 4b,d, Figure S4g). Our data indicate that mixed cell fates are not dependent on QC function. The remaining growth defect is reminis-

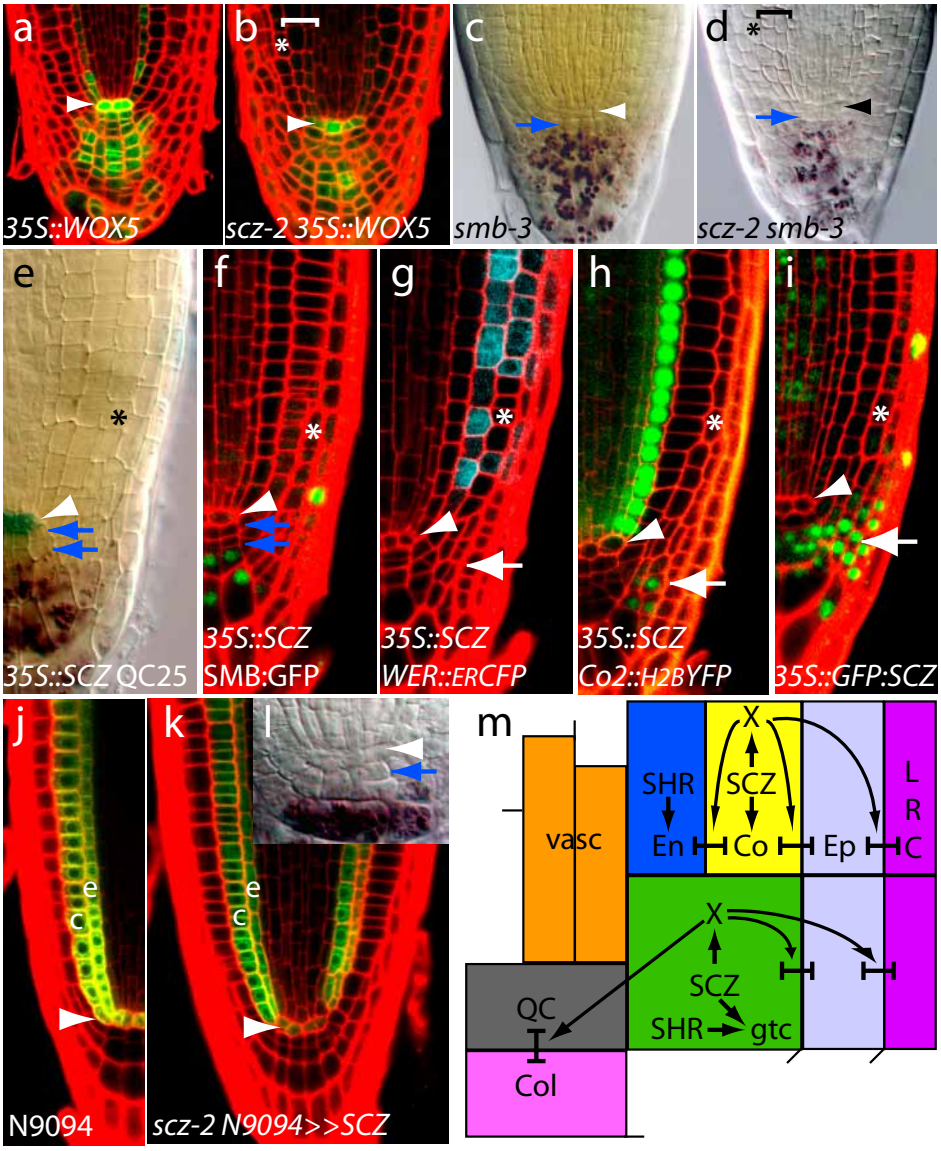

Figure 4. All *SCZ* fate separation functions are enabled from the cortex expression domain. (a,b) 5-Day-old *35S::WOX5* (a) and *scz-2 35S::WOX5* (b) roots expressing *QC46::$_{ER}$YFP*. (c,d) 4-Day-old *smb-3* (c) and *scz-2 smb-3* (d) roots. Introduction of *35S::WOX5* or *smb-3* correctly segregates QC (b,d) and columella stem cell fates (d, blue arrow). (e-h) 4-Day-old *35S::SCZ* roots expressing QC25 (e); SMB:GFP (f); *WER>>$_{ER}$CFP* (g); *Co2::$_{H2B}$YFP* (h; false green). (i) 4-Day-old *35S::GFP:SCZ* roots showing nuclear accumulation GFP:SCZ fusion protein. *SCZ* overexpression induces formation of additional columella stem cells (e,f, blue arrows), an ectopic epidermal layer (e-i, asterisk), and ectopic *Co2::$_{H2B}$YFP* expression (h, white arrow) in progeny of supernumerary epidermis/lateral root cap stem cells (g-i, white arrow). (j) Wild type N9094 root. (k,l) *N9094>>SCZ* complemented *scz-2* roots display normal tissue arrangement and marker expression (k) and correctly segregated QC and columella stem cell fates (l). (m) Role of SCZ in asymmetric division. See text for details. (gtc) ground tissue stem cell. See also Figure S4. Arrowhead marks QC.

cent of that observed when *scr* mutants are complemented by QC-expressed *SCR*, which restores a functional stem cell niche but not cell fate separation and growth (Sabatini et al., 2003).

To determine where *SCZ* acts to promote cell fate separation we reintroduced the gene in specific tissues and examined complementation of the *scz-2* mutant defect. The GAL4VP16-*UAS* transactivation system (Haseloff, 1999) was adopted to drive expression of *SCZ* and the $_{ER}$*GFP* reporter via (i) *WOL* (stele), *WOX5* (QC) and *GL2* (epidermis) promoters in *scz-2* and (ii) *scz-2* N9135 (endodermis and QC) and N9094 (cortex, endodermis and occasional QC) enhancer trap crosses. Strikingly, the *scz-2* mutant could be completely rescued in the *N9094>>SCZ scz-2* line, with restoration of growth, QC function, ground tissue and epidermis (Figures 4j-l, Figures S4g,h). None of the other drivers was able to complement *scz-2* (Figures S4i-l) indicating that *SCZ* activity is required in the cortex to exert its effect on the correct fate segregation in surrounding tissues.

Our studies indicate that *SCZ* acts as a fate determination and separation factor (Figure 4m). *SCZ* action in the ground tissue initial determines its fate from embryogenesis onward and suppresses epidermis and lateral root cap fate in the ground tissue. Non-cell autonomous *SCZ* action maintains QC fate and suppresses columella fate in the QC and in addition segregates epidermis and lateral root cap fate, putatively through a ground tissue derived factor X. After the SHR/SCR induced periclinal division of the ground tissue stem cell daughter takes place, SHR promotes endodermal fate. SCZ action promotes cortex fate and suppresses endodermal fate possibly by downregulation of *SHR*/*SCR* expression in the mature ground tissue. Furthermore, SCZ continues its non-cell autonomous suppression of epidermis and lateral root cap fate in the mature ground tissue. The ability to express differentiated characteristics of both epidermis, lateral root cap, QC and columella cell types implies that the differentiation pathways for these tissues are still intact and do not require a functional *SCZ* gene.

Although *SCZ* belongs to the Hsf family, diverse microarray analyses show that *SCZ* hardly responds during stress situations suggesting that it might be integrated into signaling pathways not directly related to the heat shock response (Miller and Mittler, 2006; Swindell et al., 2007; von Koskull-Doring et al., 2007). The *shepherd* mutant that harbors a mutation of the ER-specific *HSP90* produces floral and shoot meristem phenotypes closely resembling those of the *clavata* (*clv*) mutants, showing more diverse roles for Hsfs and Hsps than solely in stress signaling (Ishiguro et al., 2002). In addition to their role in adaptation to stress, yeast and animal Hsfs and Hsps have been demonstrated to be involved in differentiation and development (reviewed by Morange, 2006). Our discovery that the *Arabidopsis SCZ* gene is crucial for cell fate separation suggests a novel mechanism of asymmetric cell division con-

trol by Hsfs, in which key determinants that are sequestered into both daughter cells are differentially degraded. Recent work on the membrane protein BASL in stomatal precursors cells also indicates that noncanonical mechanisms control plant asymmetric cell division (Dong et al., 2009). Future work will have to establish whether and how such novel factors can be integrated with well-established mechanistic frameworks for asymmetric cell division in other kingdoms of life.

Supplemental Information

Supplemental Information includes four figures, two tables and Experimental Procedures.

Acknowledgements

We are grateful to Monica Pernas and Liam Dolan for sharing results prior to publication. We thank Adriaan van Aelst of the Wageningen University Electron Microscopy Center for help with scanning electron microscopy. This project was (co)financed by the Centre for BioSystems Genomics (CBSG) which is part of the Netherlands Genomics Initiative/Netherlands Organization for Scientific Research (NGI/NWO).

References

Aida, M., Beis, D., Heidstra, R., Willemsen, V., Blilou, I., Galinha, C., Nussaume, L., Noh, Y.S., Amasino, R., and Scheres, B. (2004). The PLETHORA genes mediate patterning of the *Arabidopsis* root stem cell niche. Cell *119*, 109-120.

Benfey, P.N. and Scheres, B. (2000). Root development. Curr Biol *10*, R813-R815.

Birnbaum, K., Shasha, D.E., Wang, J.Y., Jung, J.W., Lambert, G.M., Galbraith, D.W., and Benfey, P.N. (2003). A gene expression map of the *Arabidopsis* root. Science *302*, 1956-1960.

Brady, S.M., Orlando, D.A., Lee, J.Y., Wang, J.Y., Koch, J., Dinneny, J.R., Mace, D., Ohler, U., and Benfey, P.N. (2007). A high-resolution root spatiotemporal map reveals dominant expression patterns. Science *318*, 801-806.

Di Laurenzio, L., Wysocka-Diller, J., Malamy, J.E., Pysh, L., Helariutta, Y., Freshour, G., Hahn, M.G., Feldmann, K.A., and Benfey, P.N. (1996). The SCARECROW gene regulates an asymmetric cell division that is essential for generating the radial organization of the *Arabidopsis* root. Cell *86*, 423-433.

Dolan, L., Janmaat, K., Willemsen, V., Linstead, P., Poethig, S., Roberts, K., and Scheres, B. (1993). Cellular organisation of the *Arabidopsis thaliana* root. Development *119*, 71-84.

Dong, J., MacAlister, C.A., and Bergmann, D.C. (2009). BASL controls asymmetric cell division in *Arabidopsis*. Cell *137*, 1320-1330.

Galinha, C., Hofhuis, H., Luijten, M., Willemsen, V., Blilou, I., Heidstra, R., and Scheres, B. (2007). PLETHORA proteins as dose-dependent master regulators of *Arabidopsis* root development. Nature *449*, 1053-1057.

Haseloff, J. (1999). GFP variants for multispectral imaging of living cells. Methods Cell Biol *58*, 139-151.

Helariutta, Y., Fukaki, H., Wysocka-Diller, J., Nakajima, K., Jung, J., Sena, G., Hauser, M.T., and Benfey, P.N. (2000). The SHORT-ROOT gene controls radial patterning of the *Arabidopsis* root through radial signaling. Cell *101*, 555-567.

Ikeda, M. and Ohme-Takagi, M. (2009). A novel group of transcriptional repressors in *Arabidopsis*. Plant Cell Physiol *50*, 970-975.

Ishiguro, S., Watanabe, Y., Ito, N., Nonaka, H., Takeda, N., Sakai, T., Kanaya, H., and Okada, K. (2002). SHEPHERD is the *Arabidopsis* GRP94 responsible for the formation of functional CLAVATA proteins. EMBO J. *21*, 898-908.

Jürgens, G. and Mayer, U. (1994). *Arabidopsis*. In EMBRYOS, Color Atlas of Development, J.Bard, ed. (London: Mosby-Year Book Limited).

Knoblich, J.A. (2008). Mechanisms of asymmetric stem cell division. Cell *132*, 583-597.

Lee, M.M. and Schiefelbein, J. (1999). WEREWOLF, a MYB-related protein in *Arabidopsis*, is a position-dependent regulator of epidermal cell patterning. Cell *99*, 473-483.

Masucci, J.D., Rerie, W.G., Foreman, D.R., Zhang, M., Galway, M.E., Marks, M.D., and Schiefelbein, J.W. (1996). The homeobox gene GLABRA2 is required for position-dependent cell differentiation in the root epidermis of *Arabidopsis thaliana*. Development *122*, 1253-1260.

Miller, G. and Mittler, R. (2006). Could heat shock transcription factors function as hydrogen peroxide sensors in plants? Ann Bot (Lond) *98*, 279-288.

Morange, M. (2006). HSFs in development. Handb. Exp. Pharmacol. 153-169.

Mylona, P., Linstead, P., Martienssen, R., and Dolan, L. (2002). SCHIZORIZA controls an asymmetric cell division and restricts epidermal identity in the *Arabidopsis* root. Development *129*, 4327-4334.

Nakajima, K., Sena, G., Nawy, T., and Benfey, P.N. (2001). Intercellular movement of the putative transcription factor SHR in root patterning. Nature *413*, 307-311.

Nawy, T., Lee, J.Y., Colinas, J., Wang, J.Y., Thongrod, S.C., Malamy, J.E., Birnbaum, K., and Benfey, P.N. (2005). Transcriptional profile of the *Arabidopsis* root quiescent center. Plant Cell *17*, 1908-1925.

Nodine, M.D., Yadegari, R., and Tax, F.E. (2007). RPK1 and TOAD2 are two receptor-like kinases redundantly required for *arabidopsis* embryonic pattern formation. Dev. Cell *12*, 943-956.

Nover, L., Bharti, K., Doring, P., Mishra, S.K., Ganguli, A., and Scharf, K.D. (2001). *Arabidopsis* and the heat stress transcription factor world: how many heat stress transcription factors do we need? Cell Stress. Chaperones. *6*, 177-189.

Sabatini, S., Heidstra, R., Wildwater, M., and Scheres, B. (2003). SCARECROW is involved in positioning the stem cell niche in the *Arabidopsis* root meristem. Genes Dev. *17*, 354-358.

Sarin, S., O'Meara, M.M., Flowers, E.B., Antonio, C., Poole, R.J., Didiano, D., Johnston, R.J., Jr., Chang, S., Narula, S., and Hobert, O. (2007). Genetic screens for Caenorhabditis elegans mutants defective in left/right asymmetric neuronal fate specification. Genetics *176*, 2109-2130.

Sarkar, A.K., Luijten, M., Miyashima, S., Lenhard, M., Hashimoto, T., Nakajima, K., Scheres, B., Heidstra, R., and Laux, T. (2007). Conserved factors regulate signalling in *Arabidopsis thaliana* shoot and root stem cell organizers. Nature *446*, 811-814.

Schnittger, A., Jurgens, G., and Hulskamp, M. (1998). Tissue layer and organ specificity of trichome formation are regulated by GLABRA1 and TRIPTYCHON in *Arabidopsis*. Development *125*, 2283-2289.

Swindell, W.R., Huebner, M., and Weber, A.P. (2007). Transcriptional profiling of *Arabidopsis* heat shock proteins and transcription factors reveals extensive overlap between heat and non-heat stress response pathways. BMC. Genomics *8*, 125.

Szymanski, D.B. and Marks, M.D. (1998). GLABROUS1 overexpression and TRIPTYCHON alter the cell cycle and trichome cell fate in *Arabidopsis*. Plant Cell *10*, 2047-2062.

ten Hove, C.A. and Heidstra, R. (2008). Who begets whom? Plant cell fate determination by asymmetric cell division. Curr Opin Plant Biol *11*, 34-41.

Till, B.J., Reynolds, S.H., Greene, E.A., Codomo, C.A., Enns, L.C., Johnson, J.E., Burtner, C., Odden, A.R., Young, K., Taylor, N.E., Henikoff, J.G., Comai, L., and Henikoff, S. (2003). Large-scale discovery of induced point mutations with high-throughput TILLING. Genome Res. *13*, 524-530.

von Koskull-Doring, P., Scharf, K.D., and Nover, L. (2007). The diversity of plant heat stress transcription factors. Trends Plant Sci. *12*, 452-457.

Willemsen, V., Bauch, M., Bennett, T., Campilho, A., Wolkenfelt, H., Xu, J., Haseloff, J., and Scheres, B. (2008). The NAC domain transcription factors FEZ and SOMBRERO control the orientation of cell division plane in *Arabidopsis* root stem cells. Dev. Cell *15*, 913-922.

Wysocka-Diller, J.W., Helariutta, Y., Fukaki, H., Malamy, J.E., and Benfey, P.N. (2000). Molecular analysis of SCARECROW function reveals a radial patterning mechanism common to root and shoot. Development *127*, 595-603.

Supplemental Information

SCHIZORIZA encodes a nuclear factor regulating asymmetry of stem cell divisions in the *Arabidopsis* root

Colette A. ten Hove, Viola Willemsen, Wouter J. De Vries, Anja van Dijken, Ben Scheres and Renze Heidstra

Curr Biol (2010), doi:10.1016/j.cub.2010.01.018

Supplemental Figures

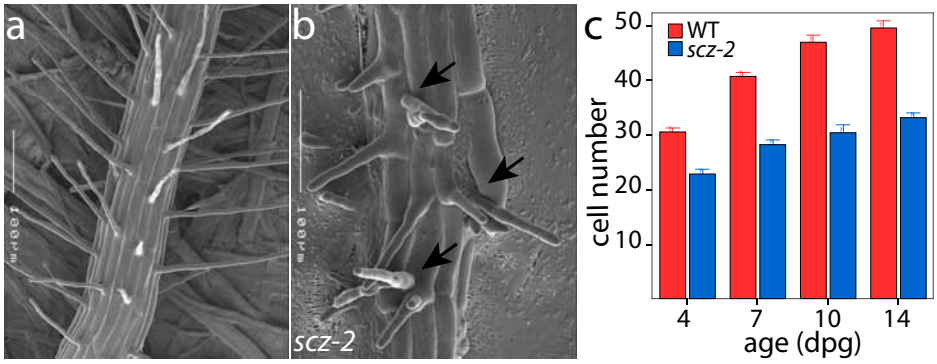

Figure S1. *scz-2* epidermis and growth phenotype, related to Figure 1. (a,b) Scanning electron microscope (SEM) image of the root hair forming zone of a 6-day-old wild type (a) and *scz-2* root (b). Black arrows show root hairs emerging from the *scz-2* subepidermal layer. Bar 100 µm. (c) Root meristem cell number of wild type and *scz-2* seedlings at indicated days post germination. For each data point $n \geq 11$; error bars, standard error of the mean.

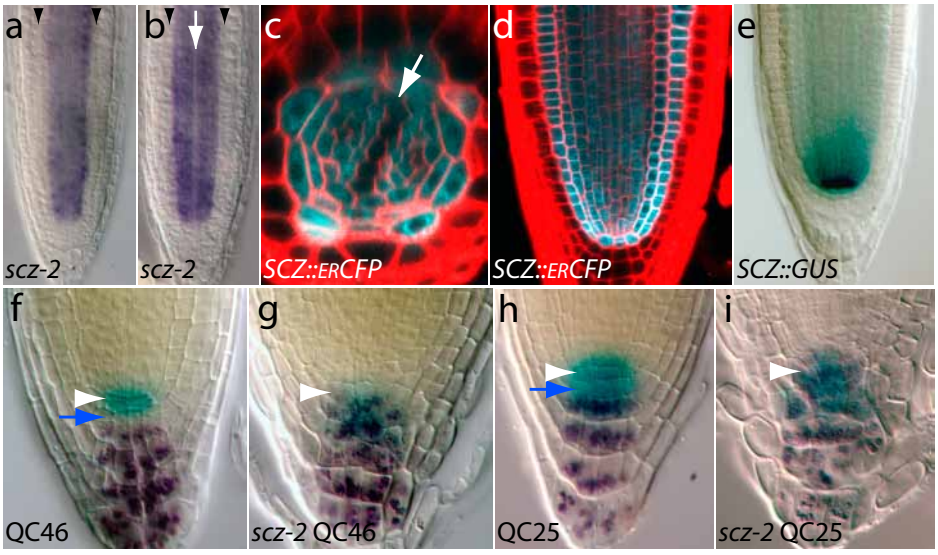

Figure S2. *SCZ* expression and QC/columella fate segregation defects, related to Figure 2. (a,b) *In situ* hybridization with *SCZ* probe in two-day-old *scz-2* seedlings. (c,d,e) Expression from a 2.3 kb *SCZ* promoter fragment driving $_{ER}$*CFP* and a 4.6 kb *SCZ* promoter fragment driving *GUS* (e). *SCZ* antisense probe shows a uniform low hybridization signal in the QC, endodermis and pro-vascular cells but is not expressed in the mutant subepidermal layer (a,b, arrowheads) and excluded from protoxylem cells in wild type and *scz-2* (b,c, arrow). (f,g) QC46 expression (blue) in 6-day-old wild type (f) and *scz-2* (g) roots. (h,i) QC25 expression (blue) in 6-day old wild type (h) and *scz-2* (i) roots. White arrowhead marks the QC (QC region in *scz-2*); blue arrow, columella stem cells; purple, starch granules.

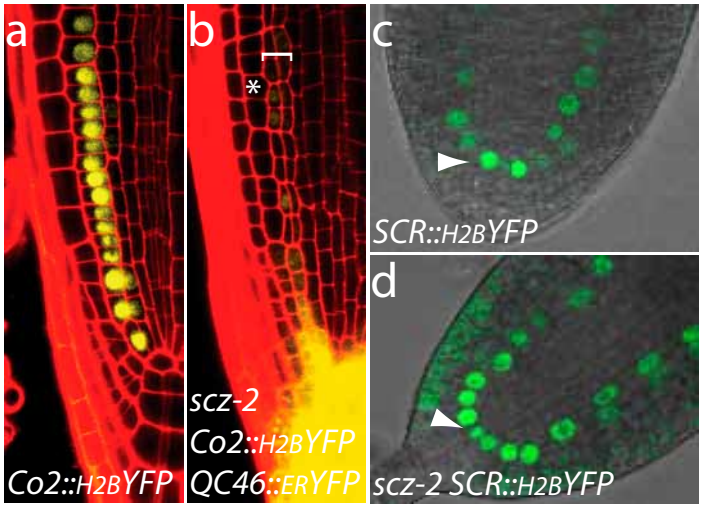

Figure S3. Marker expression analysis in *scz-2*, related to Figure 3. (a,b) *Co2::$_{H2B}$YFP* expression in 4-day-old wild type (a) and *scz-2 QC46::$_{ER}$YFP* (b) roots. (c,d) *SCR::$_{H2B}$YFP* expression in late torpedo stage embryo of wild type (c) and *scz-2* (d). Arrowhead marks QC; square brackets, ectopic endodermal layers; asterisk, subepidermal layer.

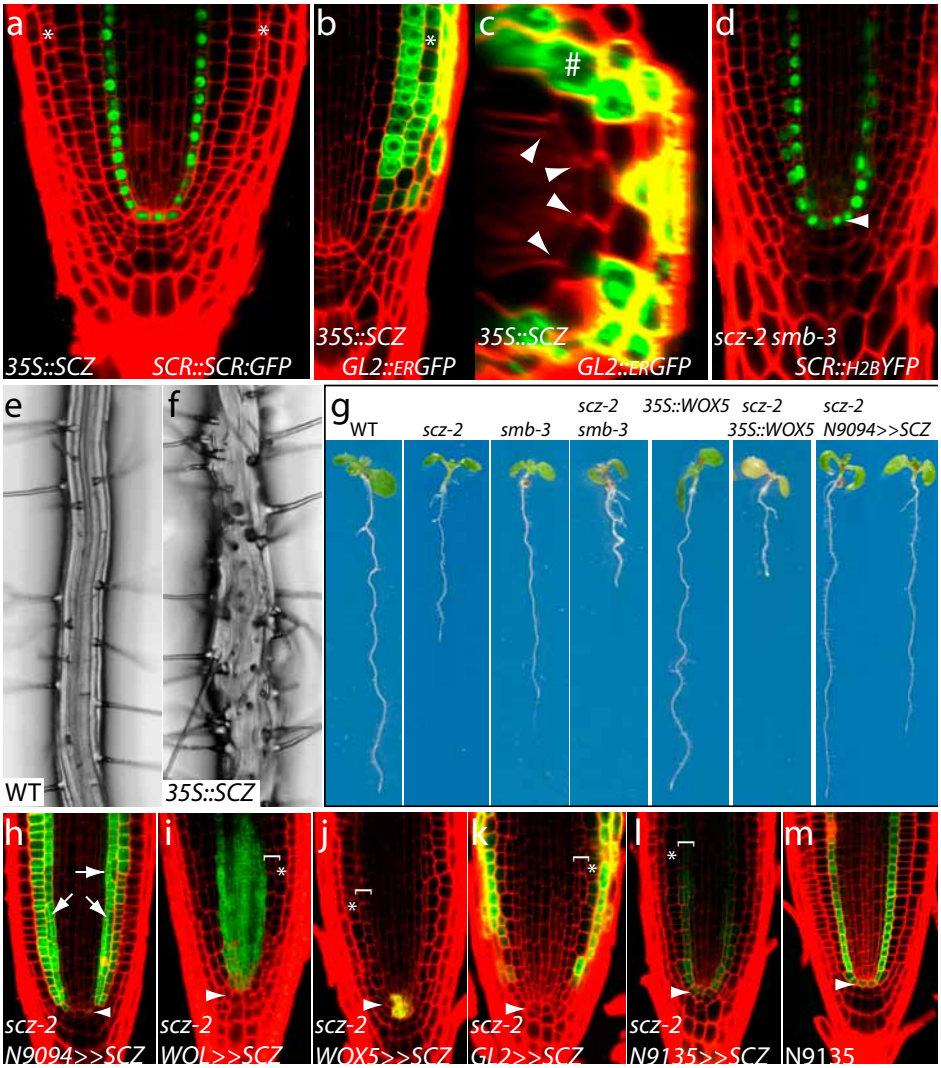

Figure S4. Ectopic *SCZ* expression and complementation analysis in *scz-2*, related to Figure 4. (a,b,c) 4-Day-old *35S:SCZ* roots expressing *SCR::SCR:GFP* (a); *GL2>>*$_{ER}$*GFP* (b,c). Cross section shows misexpression of *GL2>>*$_{ER}$*GFP* in epidermal cell overlying two cortex cells (c, hash) and expression in the ectopic outer epidermis-like layer of *35S::SCZ* roots. Asterisk, mutant layer expressing *GL2>>*$_{ER}$*GFP*; arrowheads, adjoining cortex cells which mark position of developing root hair cells in wild type. (d) *SCR::*$_{H2B}$*YFP* expression in 4-day-old s*cz-2 smb-3* roots. (e,f) Root hair zone of 4-day-old wild type (e) and *35S:SCZ* (f) root. (g) 6-Day-old wild type, *scz-2*, *smb-3*, *scz-2 smb-3*, *35::WOX5*, *scz-2 35S::WOX5* and *scz-2 N9094>>SCZ* seedlings. Note growth restoration in *scz-2 N9094>>SCZ* seedlings. (h) *N9094>>SCZ* partly complemented *scz-2* root. Arrows indicate remaining ectopic endodermal divisions. (i-l) Failed complementation of *scz-2* by *WOL>>SCZ* (i, stele) *WOX5>>SCZ* (j, QC); *GL2>>SCZ* (k, epidermis) and *N9135>>SCZ* (l, endodermis and QC). (m) N9135 expression in wild type root.

Arrowhead marks QC (QC region in *scz-2*); square brackets, ectopic endodermal layers; asterisk, subepidermal layer.

Table S1. Molecular lesions in *scz* alleles

Alelle	Mutation	Predicted effect on protein
scz-2	-C	aa 307: L to F, frameshift, stop at aa 339
scz-3	+A	aa 306: K to K, frameshift, stop at aa 315
scz-4	C to T	aa 299: Q to stop at aa 299
scz-5	G to A	splice acceptor site
scz-6	G to A	aa 171: W to stop at aa 171
scz-7	C to T	aa 132: Q to stop at aa 132
scz-8	C to T	aa 192: Q to stop at aa 192

Table S2. Primers used for cloning and sequencing

Fragment	Primer	Forward primer ('5 - '3)
SCZ promoter (4.6 kb)	*pSCZ2F*	GGGGACAACTTTGTATAGAAAAGTTGCA TTGCGCTAATGAACGTTTTG
SCZ promoter (2.3 kb)	*pSCZ3F*	GGGGACAACTTTGTATAGAAAAGTTGCA AGGAAAGCAGAGCCTCATGT
	pSCZ2R2	GGGGACTGCTTTTTTGTACAAACTTGA TAGAGAGTTCGAGAAAGAGAGAGAC
SCZ gene (1,3 kb)/ cDNA (1.1 kb)	*SCZFattB1*	GGGGACAAGTTTGTACAAAAAAGCAGGCT TGATGGCGATGATGGTCGAG
	SCZRattB2	GGGGACCACTTTGTACAAGAAAGCTGGGTAT TAACGTGTAGAAGCAGTCATGAG
Q46	*p46F2*	AATCAAAGACCAGAGAAAATGAATGTGAGTG
Q25	*p25F*	CATTTTTGTAGTTTGTTTTGACCTCTCTTG
	pGKB5R	AAGGGACTGACCACCCCAAGTGC
Co3 promoter	*Cortex3F*	ATACTCGAGTTTTAATATCGATCGGTTACCTCAA
	Cortex3R	ATGGATCCTGCTTTTGGAGATTTTCTCTTTAT
***SCZ* sequencing primers**		
	HsfB4-1	GTAGTTACACATGAGGACAGATACACA
	HsfB4-2	ACGTGAATGCATTAAATAACTGG
	HsfB4-3	GTGATTACCCATCTCTTAAAGTTCC
	HsfB4-4	GAGGTTGTTGTTGTTGTTGCTTCTG
	HsfB4-5	CGGTGGATTTCGCAGAGT
	HsfB4-6	TTGACACGGCGGCGCAAG

Supplemental Experimental Procedures

Plant materials, growth conditions and mutagenesis

Origins of mutant and transgenic lines: QC25, QC46 and QC184 (Sabatini et al., 2003); *WOX5::$_{ER}$GFP* (Blilou et al., 2005); *smb3*, *SMB::SMB:GFP*, *WER>>$_{ER}$CFP* (Willemsen et al., 2008); *GL2::GUS* (Masucci et al., 1996); *Co2::$_{H2B}$YFP*, *SCR::$_{H2B}$YFP* (Heidstra et al.,

2004); *SHR::SHR:GFP, SCR::SCR:GFP* (Nakajima et al., 2001); *scr-4* (Fukaki et al., 1998); *35S::WOX5* was kindly provided by Thomas Laux (Freiburg University, Germany); *scz-7* (N88021), *scz-8* (N93157) and the enhancer trap lines N9094, N9135 (http://www.plantsci.cam.ac.uk/Haseloff) were obtained from the Nottingham *Arabidopsis* stock center (NASC). Seedlings and embryos were sterilized, plated and grown as described in (Sabatini et al., 2003; Scheres et al., 1995). The *scz-2 – scz-6* alleles were generated by EMS mutagenesis (Willemsen et al., 1998) of approximately 30.000 dry seeds of double homozygous single insertion *QC46::$_{ER}$YFP* and *QC25::$_{ER}$CFP Arabidopsis thaliana* ecotype Columbia-0 plants. Complementation analysis was done by pair-wise crossing of the different alleles.

Map-based cloning

Homozygous *scz-2* plants in Columbia-0 background were crossed to ecotype Landsberg *erecta*. In the F2, *scz-2* mutants were selected and DNA was isolated by using a CTAB method (Lukowitz et al., 1996). *SCZ* was initially mapped to chromosome 1 between *ciw12* (39cM) and *ciw1* (72cM). Primers for further mapping were designed using information from the CEREON collection (http://www.*Arabidopsis*.org/) and Primer 3 software (http://frodo.wi.mit.edu/). The interval was narrowed down to 70 kb spanning one BAC (F2G19). Candidate genes were selected based on expression profiles specific for the ground tissue (Birnbaum et al., 2003) and their genomic regions were sequenced. For primers used to PCR the *SCZ* genomic region for sequencing see Table S2.

Microscopy and *in situ* hybridization

scz-2 was backcrossed to Columbia-0 three times prior to phenotypic and genetic analysis. Light microscopy, starch granule staining, β-glucuronidase activity, measurement of root length and meristematic cell number and aniline blue staining of mature embryos was performed as described (Willemsen et al., 1998; Welch et al., 2007; Bougourd et al., 2000). For confocal microscopy, roots or dissected embryos were mounted in propidium iodide (PI; 20 µg/mL in distilled water) or 4% glucose (+/- PI), respectively. Histological sections were prepared according to (Scheres et al., 1994) and stained with 0.05% Ruthenium Red (Sigma). Whole mount RNA *in situ* hybridization was performed manually as described (Hejatko et al., 2006). For *SCZ*, the whole complementary cDNA fragment was used as probe. Control sense probe did not give any signal. For cryo-scanning electron microscopy, roots were cultured on small pieces of filter paper and examined with a field emission scanning microscope (JEOL 6300F, Japan) on a sample stage at -190°C. The analyses were performed at a working distance of 16 mm, with SE detection at 5 kV.

Constructs and plant transformation

The pGreenII binary vector set (Hellens et al., 2000) (www.pgreen.ac.uk) was used for plant transformation. The *Co3* (At1g73620) marker was generated by cloning a 1516 bp promoter fragment into *pGII124-$_{H2B}$YFP* (methotrexate) as described (Heidstra et al., 2004). *Q25::$_{ER}$CFP* and *Q46::$_{ER}$YFP* markers were constructed by isolation of the T-DNA flanking sequences QC25 and QC46 promoter trap lines by vectorette PCR and subsequently cloning promoter fragments into *pGII227-$_{ER}$CFP* (hygromycin) and *pGII229-$_{ER}$YFP* (basta), respectively. For the *35S::SCZ* and *35S::GFP:SCZ* translational fusions, whole *SCZ* cDNA was fused in the *pMDC32* or *pMDC43* vector, respectively (Curtis and Grossniklaus, 2003). For *SCZ* promoter fusions, *SCZ* promoter fragments were cloned in *pGII229-$_{ER}$CFP* or *pGII229-GUS*. For complementation experiments promoters of *WOX5* (Blilou et al., 2005) and *WOL* (Mahönen et al., 2006) were cloned in *pGII229-GV-U$_{ER}$GFP* in front of the *GAL4VP16* transcriptional activator gene. Subsequently genomic *SCZ* cloned behind the *UAS* element was introduced creating *WOX5>>SCZ* and *WOL>>SCZ*. Plants homozygous for *scz-2* were transformed with these vectors by the floral dip method (Clough and Bent, 1998). For complementation analysis, the genomic sequence of *SCZ* was cloned behind the *UAS* element and fused in *pGII124*. Plants homozygous for *scz-2* carrying N9094, N9135, *WER>>$_{ER}$CFP*, *GL2>>$_{ER}$GFP*, respectively, were transformed with this vector and analyzed for complementation in next generations. Primers used are listed in Table S2.

Supplemental References

Birnbaum, K., Shasha, D.E., Wang, J.Y., Jung, J.W., Lambert, G.M., Galbraith, D.W., and Benfey, P.N. (2003). A gene expression map of the *Arabidopsis* root. Science *302*, 1956-1960.

Blilou, I., Xu, J., Wildwater, M., Willemsen, V., Paponov, I., Friml, J., Heidstra, R., Aida, M., Palme, K., and Scheres, B. (2005). The PIN auxin efflux facilitator network controls growth and patterning in *Arabidopsis* roots. Nature *433*, 39-44.

Bougourd, S., Marrison, J., and Haseloff, J. (2000). Technical advance: an aniline blue staining procedure for confocal microscopy and 3D imaging of normal and perturbed cellular phenotypes in mature *Arabidopsis* embryos. Plant J. *24*, 543-550.

Clough, S.J. and Bent, A.F. (1998). Floral dip: a simplified method for Agrobacterium-mediated transformation of *Arabidopsis thaliana*. Plant J. *16*, 735-743.

Curtis, M.D. and Grossniklaus, U. (2003). A gateway cloning vector set for high-throughput functional analysis of genes in planta. Plant Physiol *133*, 462-469.

Fukaki, H., Wysocka-Diller, J., Kato, T., Fujisawa, H., Benfey, P.N., and Tasaka, M. (1998). Genetic evidence that the endodermis is essential for shoot gravitropism in *Arabidopsis thaliana*. Plant J. *14*, 425-430.

Heidstra, R., Welch, D., and Scheres, B. (2004). Mosaic analyses using marked activation and deletion clones dissect *Arabidopsis* SCARECROW action in asymmetric cell division. Genes Dev. *18*, 1964-1969.

Hejatko, J., Blilou, I., Brewer, P.B., Friml, J., Scheres, B., and Benkova, E. (2006). In situ hybridization technique for mRNA detection in whole mount *Arabidopsis* samples. Nat Protoc. *1*, 1939-1946.

Hellens, R.P., Edwards, E.A., Leyland, N.R., Bean, S., and Mullineaux, P.M. (2000). pGreen: a versatile and flexible binary Ti vector for Agrobacterium-mediated plant transformation. Plant Mol Biol *42*, 819-832.

Lukowitz, W., Mayer, U., and Jurgens, G. (1996). Cytokinesis in the *Arabidopsis* embryo involves the syntaxin-related KNOLLE gene product. Cell *84*, 61-71.

Mahönen, A.P., Higuchi, M., Tormakangas, K., Miyawaki, K., Pischke, M.S., Sussman, M.R., Helariutta, Y., and Kakimoto, T. (2006). Cytokinins regulate a bidirectional phosphorelay network in *Arabidopsis*. Curr Biol *16*, 1116-1122.

Masucci, J.D., Rerie, W.G., Foreman, D.R., Zhang, M., Galway, M.E., Marks, M.D., and Schiefelbein, J.W. (1996). The homeobox gene GLABRA2 is required for position-dependent cell differentiation in the root epidermis of *Arabidopsis thaliana*. Development *122*, 1253-1260.

Nakajima, K., Sena, G., Nawy, T., and Benfey, P.N. (2001). Intercellular movement of the putative transcription factor SHR in root patterning. Nature *413*, 307-311.

Sabatini, S., Heidstra, R., Wildwater, M., and Scheres, B. (2003). SCARECROW is involved in positioning the stem cell niche in the *Arabidopsis* root meristem. Genes Dev. *17*, 354-358.

Scheres, B., Di Laurenzio, L., Willemsen, V., Hauser, M.T., Janmaat, K., Weisbeek, P., and Benfey, P.N. (1995). Mutations affecting the radial organisation of the *Arabidopsis* root display specific defects throughout the embryonic axis. Development *121*, 53-62.

Scheres, B., Wolkenfelt, H., Willemsen, V., Terlouw, M., Lawson, E., Dean, C., and Weisbeek, P. (1994). Embryonic origin of the *Arabidopsis* primary root and root meristem initials. Development *120*, 2475-2487.

Welch, D., Hassan, H., Blilou, I., Immink, R., Heidstra, R., and Scheres, B. (2007). *Arabidopsis* JACKDAW and MAGPIE zinc finger proteins delimit asymmetric cell division and stabilize tissue boundaries by restricting SHORT-ROOT action. Genes Dev. *21*, 2196-2204.

Willemsen, V., Bauch, M., Bennett, T., Campilho, A., Wolkenfelt, H., Xu, J., Haseloff, J., and Scheres, B. (2008). The NAC domain transcription factors FEZ and SOMBRERO control the orientation of cell division plane in *Arabidopsis* root stem cells. Dev. Cell *15*, 913-922.

Willemsen, V., Wolkenfelt, H., de Vrieze G., Weisbeek, P., and Scheres, B. (1998). The HOBBIT gene is required for formation of the root meristem in the *Arabidopsis* embryo. Development *125*, 521-531.

Chapter 3

SCHIZORIZA acts in parallel with the *SHORT-ROOT/SCARECROW* pathway to control *Arabidopsis* root stem cell niche specification

Colette A. ten Hove, Akie Shimothono*, Ikram Blilou*, Ben Scheres and Renze Heidstra

Faculty of Science, Department of Biology, section Molecular Genetics, Utrecht University, Padualaan 8, 3584 CH Utrecht, the Netherlands.

**These authors contributed equally.*

Summary

Arabidopsis root growth is maintained by the activity of the stem cell niche in the heart of the root meristem. The stem cell niche is formed during embryogenesis. Following quiescent center (QC) specification, the surrounding cells are maintained as stem cells. QC fate and stem cell maintenance are controlled by the combinatorial action of *SHORT-ROOT* (*SHR*), *SCARECROW* (*SCR*) and *PLETHORA* (*PLT*) transcription factor genes. Here, we provide evidence that the *SCHIZORIZA* (*SCZ*) transcription factor gene acts in parallel with the *SHR/SCR* pathway for stem cell niche specification in the early embryo.

Introduction

The *Arabidopsis* root meristem is laid down during embryogenesis, where future stem cells (also called initials) are first discerned at late heart stage. The organization of the tissues that make up the root is completed at torpedo stage and maintained in the post-embryonic root by stereotyped asymmetric cell divisions of distinct stem cells. These stem cells surround a small group of rarely dividing cells, the QC, required for their maintenance (Figure 1a) (van den Berg et al., 1997). Acquisition of QC fate and maintenance of the stem cell niche is controlled in parallel by the *SHR, SCR* and *PLT* transcription factor genes (Sabatini et al., 2003; Aida et al., 2004; Galinha et al., 2007).

SHR and *SCR* encode GRAS-type transcription factors. SHR is expressed in the stele but the protein moves one tissue layer outward and activates transcription of its target gene and interacting partner SCR in the QC and endodermis. Apart from their role in QC specification both genes are also required for ground tissue patterning (Di Laurenzio et al., 1996; Helariutta et al., 2000; Nakajima et al., 2001). PLT proteins (PLT1, PLT2, PLT3 and PLT4/BABYBOOM) belong to the double AP2 domain transcription factor family and are expressed in a gradient fashion in the root meristem. PLT activities are largely additive; with added deletion of family members enhancing phenotypic defects, and dose dependent; with high levels of PLT maintaining stem cells, intermediate levels facilitating transient amplifying cell divisions that make up the meristem region and low levels allowing progression of differentiation (Galinha et al., 2007).

We previously showed that *SCZ* plays a role in patterning of the root niche where the gene is expressed in QC, in ground and vascular tissue progenitors and at lower levels in their daughters (ten Hove et al., 2010). Specifically, the *SCZ* transcription factor gene was shown to control the asymmetry of root stem cell divisions. The origin of the *scz* mutant defects were traced back to heart stage embryo when stem cells are believed to be first specified and the root meristem arises (Jürgens and Mayer, 1994; Scheres et al., 1994). However, *SCZ* expression initiates earlier in QC progenitor cells of triangular stage embryos. Expression remains high in the QC from this stage onward and shows overlap with that of the *SHR, SCR* and *PLT* root patterning genes (Aida et al., 2004; Wysocka-Diller et al., 2000), hinting to a potentially broader role for *SCZ* in the stem cell niche. Previous studies did demonstrate a requirement for the *SHR/SCR* pathway for *scz* ectopic divisions. However, QC and stem cell defects in these double mutants were not reported (Mylona et al., 2002).

Here, we investigate the function of *SCZ* in root niche specification during embryogenesis. We provide evidence that *SCZ* functions independently of the SHR, SCR and PLT patterning genes. Importantly, we reveal that *SCZ* acts in parallel with the *SHR/SCR* pathway to specify the QC and stem cells required for root meristem initiation.

Results

Interaction between *SCZ* and *PLT1 and PLT2* genes

Niche activity is compromised in *plt1-4 plt2-2* double mutants and these effects are already visible in the heart stage embryo where the lens-shaped and root cap progenitor cell exhibit aberrant cell divisions (Aida et al., 2004). We investigated the transcriptional and genetic interaction between *SCZ* and *PLT1* and *PLT2* genes. Auxin distribution visualized by $DR5_{rev}$*::GFP* as well as *PLT1* and *PLT2* promoter and protein expression is not affected in *scz-2* (Figure 1b,c,e-h, data not shown). In contrast, *SCZ::*$_{ER}$*CFP* peak expression in the niche is lost as *plt1-4 plt2-2* double mutant roots differentiate (Figure 1j,k). This may indicate a requirement of PLT activity for the maintenance of high *SCZ* transcription levels in the QC or reflect a secondary effect due to the cessation of meristem activity.

We crossed *scz-2* with the *plt1-4 plt2-2* double mutant to test if *SCZ* acts in the *PLT1/PLT2* niche maintenance pathway. In the *scz-2 plt1-4 plt2-2* triple mutant, the *scz* mediated radial patterning defects still occur, indicating that these aspects are *PLT* independent (Figure 1m,bracket). However, growth and meristem dissipation resembles that of *plt1-4 plt2-2* double mutants up to 3 days after germination suggesting epistasis until the early phase of post-embryonic development (Figure 1i,l,m, Figure 2o). Alternatively, the severity of the *plt1 plt2* double mutant may mask the effect of *SCZ* deletion on root growth at early stages, in which case the genes would act independent. The enhanced growth defect at later post-embryonic stages may be explained by the observed compromised *SCR* expression in *scz* background (see below).

SCZ and the *SHR/SCR* pathway specify the stem cell niche in parallel

From early embryogenesis onward *SCZ* gene expression shows overlap with *SHR* and *SCR* gene and protein expression patterns. In addition, root patterning defects occur in the QC and ground tissue of the corresponding mutants (Wysocka-Diller et al., 2000; ten Hove et al., 2010). We therefore investigated the influence of *SCZ* on *SHR*/*SCR* expression and function and vice versa.

SCZ::$_{ER}$*CFP* expression in *shr-2* and *scr-4* mutants is comparable to wild type from embryogenesis onward, indicating that *SHR* and *SCR* are not required for *SCZ* transcription (Figure 2a-f). Expression analyses in *scz-2* embryos and seedling roots indicated that the initiation of *SCR::*$_{H2B}$*YFP* expression is *SCZ* independent but that postembryonic *SHR::SHR:GFP* and *SCR::*$_{H2B}$*YFP* niche expression depends on *SCZ* (ten Hove et al., 2010, Figure 2g,h, l,j,m,n).

scz-2, *shr-2* and *scr-4* single mutants all display shorter roots and meristems compared to wild type (Figure 2o). However, unlike *scz-2* (ten Hove et al., 2010), the

root growth in *shr-2* and *scr-4* is determinate as cells in the meristem differentiate (Sabatini et al., 2003). *scz-2 shr-2* and *scz-2 scr-4* double mutants can be divided in two classes, one showing fully differentiated root poles upon germination and the other entirely lacking primary roots (Figure 2l,o). Seedlings of both classes develop adventitious roots from which lateral roots initiate, indicating that *SCZ* is not required for lateral root formation (Figure 2o and data not shown).

As both double mutant combinations displayed identical phenotypes we continued analysis of *scz-2 shr-2* embryonic development only. The first visible defect in *scz-2* is an aberrant periclinal division of ground tissue initials at heart stage (ten Hove et al., 2010; Figure 3b, arrowhead). *scz-2 shr-2* double mutant embryos resemble *shr-2* up to this stage with a single layer of ground tissue due to defective periclinal ground tissue divisions (Figure 3c,d), confirming previous findings that

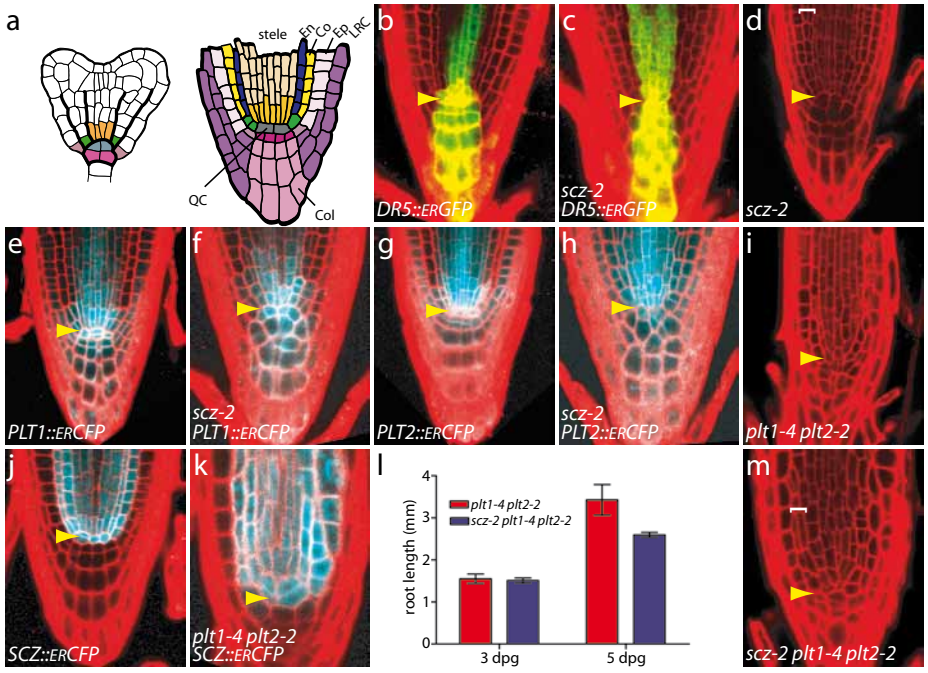

Figure 1. Transcriptional and genetic interactions between *SCZ* and *PLT1* and *PLT2* genes. (a) Schematic representation of the developing *Arabidopsis* root meristem. Left, heart stage embryo; right, seedling root meristem. (En) endodermis; (Co) cortex; (Ep) epidermis; (LRC) lateral root cap; (Col) columella; (QC) quiescent center. (b,c,e-h) 4-Day-old wild type (b,e,g) and *scz-2* (c,f,h) roots expressing *DR5::$_{ER}$GFP* (b,c), *PLT1::$_{ER}$CFP* (e,f) and *PLT2::$_{ER}$CFP* (g,h). (d,i,m) 3-Day-old *scz-2* (d), *plt1-4 plt2-2* (i), *scz-2 plt1-4 plt2-2* (m) roots. *scz* characteristic radial patterning defect (bracket). (j,k) *SCZ::$_{ER}$CFP* expression in 3-day-old wild type (j) and *plt1-4 plt2-2* (k) roots. Yellow arrowhead indicates QC area. (l) Root length measurements (in mm) of *plt1-4 plt2-2* and *scz-2 plt1-4 plt2-2* seedlings. A minimum of 10 seedlings was measured for each time point. Error bars represent standard error of the mean.

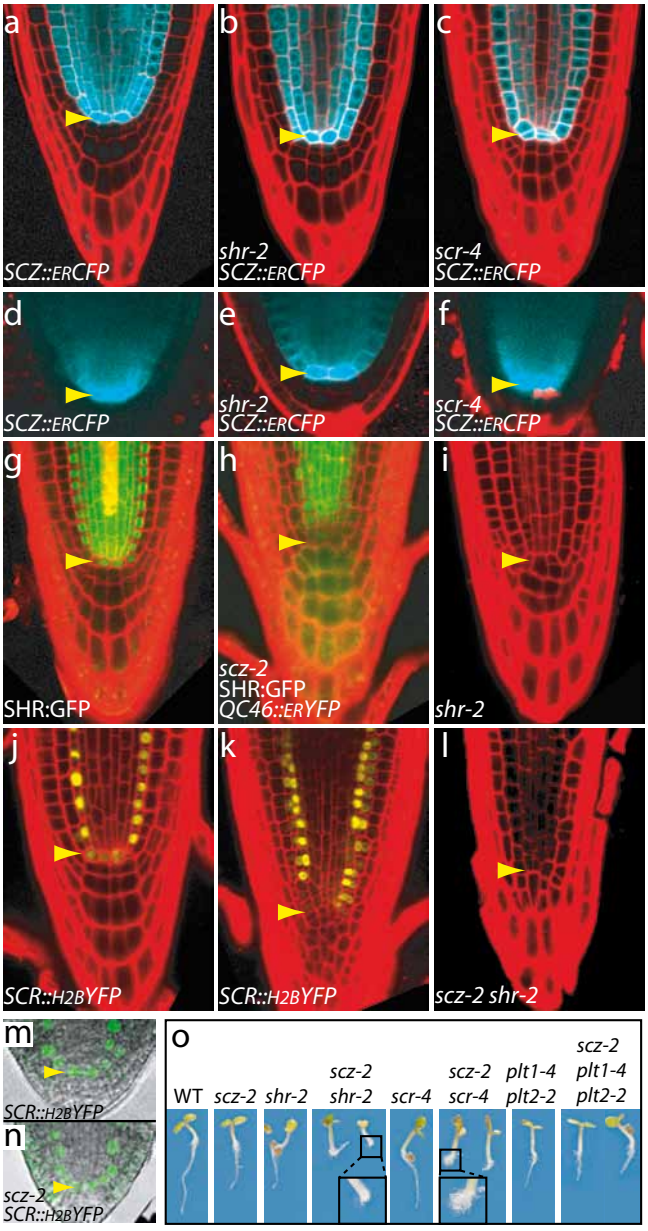

Figure 2. *SCZ* and *SHR/SCR* are together required for root meristem initiation. (a-f) *SCZ::$_{ER}$CFP* expression in 3-day-old wild type (a), *shr-2* (b) and *scr-4* (c) roots and in late torpedo stage wild type (d), *shr-2* (e) and *scr-4* (f) embryos. (g,h) SHR:GFP expression in 5-day-old wild type (g) and *scz-2 QC46::$_{ER}$YFP* (h) roots. (j,k,m,o) *SCR::$_{H2B}$YFP* expression in 5-day-old wild type (j) and *scz-2* (k) roots and in late torpedo stage wild type (m) and *scz-2* (o) embryos. (i,l) 3-Day-old *shr-2* (i) and *scz-2 shr-2* roots (l). Yellow arrowhead indicates QC area. (o) 3-Day-old wild type, *scz-2*, *shr-2*, *scr-4*, *plt1-4 plt2-2*, *scz-2 shr-2*, *scz-2 scr-4* and *scz-2 plt1-4 plt2-2* seedlings. Insets show magnification of *scz-2 shr-2*, *scz-2 scr-4* seedlings lacking a primary root.

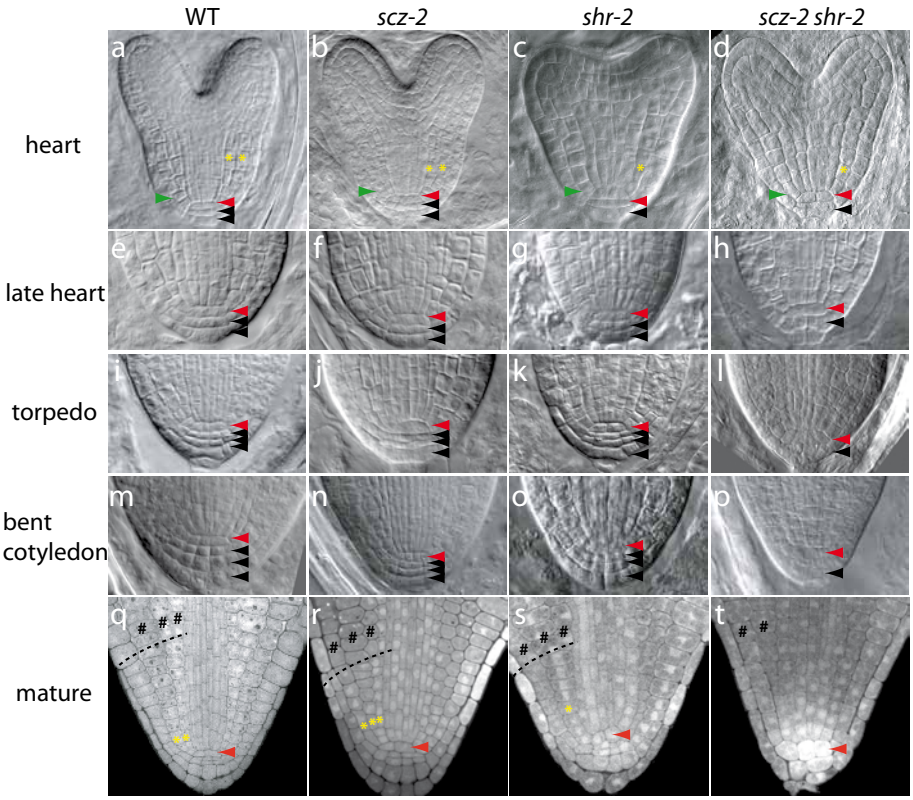

Figure 3. Both *SCZ* and *SHR* are required to set up the root stem cell niche. (a-p) Early heart stage (a-d), late heart stage (e-h), torpedo stage (i-l) and bent cotyledon stage (m-p) wild type (a,e,i,m), *scz-2* (b,f,j,n), *shr-2* (c,g,k,o) and *scz-2 shr-2* (d,h,l,p) embryos. Green arrowhead marks ground tissue initial; red arrowhead marks QC; black arrowhead marks root cap; yellow asterisk marks ground tissue. The *shr-2* younger heart stage has not performed the root cap division yet (c). (q-t) Aniline blue stained wild type (q), *scz-2* (r), *shr-2* (s) and *scz-2 shr-2* (t) mature embryos. Root/hypocotyl boundary (dashed line); ground tissue layers in hypocotyl (hash).

SHR/SCR is required for *scz* ectopic divisions (Mylona et al., 2002). Importantly, the additional phenotypes of the *scz-2 shr-2* double mutant phenotype become apparent at this stage with delayed formative horizontal root cap divisions that are replaced by vertical divisions at late heart stage (Figure 3d,h,l,p,t). Further horizontal root cap divisions are absent in later stage embryos. Most striking in phenotypically strong double mutants (n/total = 16/22) is the vertical division and subsequent longitudinal expansion of the QC cells from torpedo stage onward (Figure 3l,p,t). These elongated cells end up resembling root cap cells by the mature embryo stage according to morphological criteria (Figure 3t). As a result a reduced columella and only few or no lateral root cap-like cells are observed (Figure 3t). The *scz-2 shr-2*

epidermal layer is long and flattened, resembling the mixed epidermis-lateral root cap layer of *scz-2* single mutants. Surprisingly, the mature embryonic root vascular tissue appears to be surrounded by two ground tissue-like layers that continue from the hypocotyl all the way down to the distal root cap tissues (Figure 3t). The typical root-hypocotyl junction can therefore not be distinguished.

The apparent lack of QC and stem cell activity in *scz-2 shr-2* double mutants suggests that *SCZ* and *SHR* function together in specifying the root niche cell types during embryogenesis.

Protein interaction studies in yeast

Despite the strong phenotypes of the double mutants, embryonic expression of SHR and *SCR* is independent of *SCZ* activity and vice versa, opening the possibility that the encoded proteins might interact. SHR and SCR proteins have been shown to functionally interact with each other and members of the JACKDAW family of zinc-finger proteins (Cui et al., 2007; Welch et al., 2007) and a SHR-SCR complex binds *SCR* and *MGP* promoters (Cui et al., 2007). We therefore assessed whether SCZ could influence SHR and/or SCR activity through direct protein-protein interaction. Because the *scz-2 plt1-4 plt2-2* triple mutant phenotype is enhanced over time we also included PLT1 and PLT2 in the interaction assay. However, initial yeast two hybrid interaction studies indicate that there is no direct interaction between SCZ and SHR, SCR or PLT proteins (Table 1).

Table 1. SCZ does not physically interact with PLT, SHR or SCR. Yeast two hybrid interactions. SCZ and SCR serve as bait and PLT1, PLT2, SHR and SCR as prey. SCR-SHR interaction serves as positive control and empty vector as negative control. Positive interaction controls for PLT1 and PLT2 (AS, unpublished data) are not shown. (+) interaction; (-) no interaction; (NA) not analyzed.

bait \ **prey**	PLT1	PLT2	SHR	SCR	empty vector
SCZ	-	-	-	-	-
SCR	NA	NA	+	NA	-

Discussion

During embryogenesis the root stem cell niche is laid down depending on the combinatorial action of the auxin-responsive *PLT* genes and the independently initiated activity of the *SHR* and *SCR* genes. Here, we show that *SCZ* can be added to the list of genes that are required for stem cell niche specification and root initiation. Our studies indicate that *SCZ* operates parallel to the *SHR*/*SCR* and *PLT* pathways. However, *scz-2 plt1-4 plt2-2* triple mutants resemble *plt1-4 plt2-2* up to 3 days post germination and *SCZ* expression is upregulated upon induced *PLT2* overexpression (RH, unpublished data). Therefore, it cannot be excluded that *SCZ* acts downstream of the auxin-dependent *PLT* genes. Expression studies in embryos should clarify whether the reduced *SCZ::*$_{ER}$*CFP* niche expression in *plt1-4 plt2-2* double mutant roots is a secondary effect due to the termination of meristem activity. In addition, analysis of triple and quadruple mutant combinations of *scz* with mutations in additional *PLT* genes may reveal whether *SCZ* and *PLT* genes function independently or not.

Root formation is initiated at the globular stage by an asymmetric division of the hypophysis, forming the lens shaped QC progenitor cell. Auxin response mediated by MONOPTEROS and BODENLOS functions and activity of the protein phosphatases POLTERGEIST (POL) and POL LIKE1 direct this division (Hardtke and Berleth, 1998; Hamann et al., 2002; Gagne and Clark, 2007; Gagne et al., 2008). Expression of WOX5 and its upstream regulator SCR initiated in the hypophysis is maintained in the lens shaped cell (Haecker et al., 2004; Wysocka-Diller et al., 2000) and joined by QC25, QC46 and QC184 expression at heart stage (Aida et al., 2004; Jenik et al., 2005; Sarkar et al., 2007). Defects in *scz-2 shr-2* double mutants were traced back to late heart stage arguing that *SCZ* and *SHR* genes determine the next steps in root formation.

Cell divisions that normally form the root cap at late heart-early torpedo stage are delayed in *scz-2 shr-2* double mutants. Subsequent aberrant cell divisions, especially apparent in the QC and root cap progenitor cells, are indicative of a failure to initiate the stereotypical formative stem cell divisions. These results correlate well with the overlapping expression of *SCZ* and SHR in the QC around these stages of embryogenesis. Further studies using QC specific markers that are still expressed in *shr-2* background (e.g. QC184) should clarify whether QC fate fails to be initiated or is not maintained in the *scz-2 shr-2* double mutant embryo. In addition, *scz-2* displays a compromised ground tissue that lacks cortex attributes and outer tissue layers of mixed identity, whereas *shr-2* mutants display a single ground tissue layer lacking endodermis identity. Therefore, it is of interest to determine the identity of the tissue layers observed outside of the vasculature in *scz-2 shr-2* double mutant

embryos. Tissue specific marker analyses using vascular, ground tissue, epidermal and root cap markers should reveal their identity.

How *SCZ*, *SHR* and *SCR* genes act together remains unclear. From our initial studies it appears that it is not through direct protein interaction. In addition, *SCZ* is not listed as a target of *SHR* in the analysis of Levesque et al., (2006). Future studies to determine downstream effectors should reveal by what mechanisms SCZ acts and how these overlap with SHR targets.

Experimental procedures

Plant materials and growth conditions

Origins of mutant and transgenic lines: *shr-2, SHR::SHR:GFP* (Nakajima et al., 2001); *scr-4* (Fukaki et al., 1998); *SCR::*$_{H2B}$*YFP* (Heidstra et al., 2004); *plt1-4 plt2-2* (Aida et al., 2004); *PLT1::* $_{ER}$*CFP*, *PLT2::* $_{ER}$*CFP* (Galinha et al., 2007); *DR5::*$_{ER}$*GFP* (Benkova et al., 2003). Seedlings and embryos were sterilized, plated and grown as described in (Sabatini et al., 2003; Scheres et al., 1995).

Microscopy

Light microscopy, starch granule staining, measurement of root length and aniline blue staining was performed as described in (Willemsen et al., 1998; Welch et al., 2007; Bougourd et al., 2000). For confocal microscopy, roots and dissected embryos were mounted in propidium iodide (PI; 20 µg/mL in distilled water) or 4% glucose (+/- PI), respectively.

Yeast two hybrid assay

Yeast two hybrid interactions were studied according to (Welch et al., 2007) using the ProQuest Two Hybrid System (Invitrogen Life Technologies) and yeast strains Pj694α and Pj694a. The coding sequence of *SCZ* was amplified and fused into the pDEST32 BD vector whereas the amplified coding sequences of *PLT1*, *PLT2*, *SHR* and *SCR* were recombined into the pDEST22 AD vector. Although pEXP-SCZ did not show auto activation activity, 3 mM 3-AT was used to eliminate any background transcriptional activity. Primers used for *SCZ* are described in (ten Hove et al., 2010), for *SHR* and *SCR* in (Welch et al., 2007) and for *PLT1*, *PLT2* primer sequences are:

PLT1-F: 5'-ggggacaagtttgtacaaaaaagcaggctgtatgaattctaacaactggcttggctttcctct-3',
PLT1-R: 5'ggggaccactttgtacaagaaagctgggtcttactcattccacatagtgaaaacaccaccagg-3',
PLT2-F: 5'-ggggacaagtttgtacaaaaaagcaggctgtatgaattctaacaactggctcgcgttccctc-3',
PLT2-R: 5'-ggggaccactttgtacaagaaagctgggtcttattcattccacatcgtgaaaacacctcctgg-3'.

Acknowledgements

CAtH was co-financed by the Centre for BioSystems Genomics (CBSG), which is part of the Netherlands Genomics Initiative/Netherlands Organization for Scientific Research (NGI/NWO). AS was supported by a long term EMBO fellowship and IB by a VIDI innovational grant from the NWO.

References

Aida, M., Beis, D., Heidstra, R., Willemsen, V., Blilou, I., Galinha, C., Nussaume, L., Noh, Y.S., Amasino, R., and Scheres, B. (2004). The PLETHORA genes mediate patterning of the *Arabidopsis* root stem cell niche. Cell *119*, 109-120.

Benkova, E., Michniewicz, M., Sauer, M., Teichmann, T., Seifertova, D., Jurgens, G., and Friml, J. (2003). Local, efflux-dependent auxin gradients as a common module for plant organ formation. Cell *115*, 591-602.

Bougourd, S., Marrison, J., and Haseloff, J. (2000). Technical advance: an aniline blue staining procedure for confocal microscopy and 3D imaging of normal and perturbed cellular phenotypes in mature *Arabidopsis* embryos. Plant J. *24*, 543-550.

Cui, H., Levesque, M.P., Vernoux, T., Jung, J.W., Paquette, A.J., Gallagher, K.L., Wang, J.Y., Blilou, I., Scheres, B., and Benfey, P.N. (2007). An evolutionarily conserved mechanism delimiting SHR movement defines a single layer of endodermis in plants. Science *316*, 421-425.

Di Laurenzio, L., Wysocka-Diller, J., Malamy, J.E., Pysh, L., Helariutta, Y., Freshour, G., Hahn, M.G., Feldmann, K.A., and Benfey, P.N. (1996). The SCARECROW gene regulates an asymmetric cell division that is essential for generating the radial organization of the *Arabidopsis* root. Cell *86*, 423-433.

Fukaki, H., Wysocka-Diller, J., Kato, T., Fujisawa, H., Benfey, P.N., and Tasaka, M. (1998). Genetic evidence that the endodermis is essential for shoot gravitropism in *Arabidopsis thaliana*. Plant J. *14*, 425-430.

Gagne, J.M. and Clark, S.E. (2007). The Protein Phosphatases POL and PLL1 are Signaling Intermediates for Multiple Pathways in *Arabidopsis*. Plant Signal. Behav. *2*, 245-246.

Gagne, J.M., Song, S.K., and Clark, S.E. (2008). POLTERGEIST and PLL1 are required for stem cell function with potential roles in cell asymmetry and auxin signaling. Commun. Integr. Biol *1*, 53-55.

Galinha, C., Hofhuis, H., Luijten, M., Willemsen, V., Blilou, I., Heidstra, R., and Scheres, B. (2007). PLETHORA proteins as dose-dependent master regulators of *Arabidopsis* root development. Nature *449*, 1053-1057.

Haecker, A., Gross-Hardt, R., Geiges, B., Sarkar, A., Breuninger, H., Herrmann, M., and Laux, T. (2004). Expression dynamics of WOX genes mark cell fate decisions during early embryonic patterning in *Arabidopsis thaliana*. Development *131*, 657-668.

Hamann, T., Benkova, E., Baurle, I., Kientz, M., and Jurgens, G. (2002). The *Arabidopsis* BODENLOS gene encodes an auxin response protein inhibiting MONOPTEROS-mediated embryo patterning. Genes Dev. *16*, 1610-1615.

Hardtke, C.S. and Berleth, T. (1998). The *Arabidopsis* gene MONOPTEROS encodes a transcription factor mediating embryo axis formation and vascular development. EMBO J. *17*, 1405-1411.

Heidstra, R., Welch, D., and Scheres, B. (2004). Mosaic analyses using marked activation and deletion clones dissect *Arabidopsis* SCARECROW action in asymmetric cell division. Genes Dev. *18*, 1964-1969.

Helariutta, Y., Fukaki, H., Wysocka-Diller, J., Nakajima, K., Jung, J., Sena, G., Hauser, M.T., and Benfey, P.N. (2000). The SHORT-ROOT gene controls radial patterning of the *Arabidopsis* root through radial signaling. Cell *101*, 555-567.

Jenik, P.D., Jurkuta, R.E., and Barton, M.K. (2005). Interactions between the cell cycle and embryonic patterning in *Arabidopsis* uncovered by a mutation in DNA polymerase epsilon. Plant Cell *17*, 3362-3377.

Jürgens, G. and Mayer, U. (1994). *Arabidopsis*. In EMBRYOS, Color Atlas of Development, J.Bard, ed. (London: Mosby-Year Book Limited).

Levesque, M.P., Vernoux, T., Busch, W., Cui, H., Wang, J.Y., Blilou, I., Hassan, H., Nakajima, K., Matsumoto, N., Lohmann, J.U., Scheres, B., and Benfey, P.N. (2006). Whole-genome analysis of the SHORT-ROOT developmental pathway in *Arabidopsis*. PLoS. Biol. *4*, e143.

Mylona, P., Linstead, P., Martienssen, R., and Dolan, L. (2002). SCHIZORIZA controls an asymmetric cell division and restricts epidermal identity in the *Arabidopsis* root. Development *129*, 4327-4334.

Nakajima, K., Sena, G., Nawy, T., and Benfey, P.N. (2001). Intercellular movement of the putative transcription factor SHR in root patterning. Nature *413*, 307-311.

Sabatini, S., Heidstra, R., Wildwater, M., and Scheres, B. (2003). SCARECROW is involved in positioning the stem cell niche in the *Arabidopsis* root meristem. Genes Dev. *17*, 354-358.

Sarkar, A.K., Luijten, M., Miyashima, S., Lenhard, M., Hashimoto, T., Nakajima, K., Scheres, B., Heidstra, R., and Laux, T. (2007). Conserved factors regulate signalling in *Arabidopsis thaliana* shoot and root stem cell organizers. Nature *446*, 811-814.

Scheres, B., Di Laurenzio, L., Willemsen, V., Hauser, M.T., Janmaat, K., Weisbeek, P., and Benfey, P.N. (1995). Mutations affecting the radial organisation of the *Arabidopsis* root display specific defects throughout the embryonic axis. Development *121*, 53-62.

Scheres, B., Wolkenfelt, H., Willemsen, V., Terlouw, M., Lawson, E., Dean, C., and Weisbeek, P. (1994). Embryonic origin of the *Arabidopsis* primary root and root meristem initials. Development *120*, 2475-2487.

ten Hove, C.A., Willemsen, V., de Vries, W.J., van Dijken, A., Scheres, B., and Heidstra, R. (2010). *SCHIZORIZA* encodes a nuclear factor regulating asymmetry of stem cell divisions in the *Arabidopsis* root. Current Biology *doi:10.1016/j.cub.2010.01.018*.

van den Berg, C., Willemsen, V., Hendriks, G., Weisbeek, P., and Scheres, B. (1997). Short-range control of cell differentiation in the *Arabidopsis* root meristem. Nature *390*, 287-289.

Welch, D., Hassan, H., Blilou, I., Immink, R., Heidstra, R., and Scheres, B. (2007). *Arabidopsis* JACKDAW and MAGPIE zinc finger proteins delimit asymmetric cell division and stabilize tissue boundaries by restricting SHORT-ROOT action. Genes Dev. *21*, 2196-2204.

Willemsen, V., Wolkenfelt, H., de Vrieze G., Weisbeek, P., and Scheres, B. (1998). The HOBBIT gene is required for formation of the root meristem in the *Arabidopsis* embryo. Development *125*, 521-531.

Wysocka-Diller, J.W., Helariutta, Y., Fukaki, H., Malamy, J.E., and Benfey, P.N. (2000). Molecular analysis of SCARECROW function reveals a radial patterning mechanism common to root and shoot. Development *127*, 595-603.

Chapter 4

SOL3, a new component of the CLE signaling pathway involved in *Arabidopsis* root development

Colette A. ten Hove[1], Raffaele Dello Ioio[2], Sabrina Sabatini[2], Ben Scheres[1] and Renze Heidstra[1]

[1]Faculty of Science, Department of Biology, section Molecular Genetics, Utrecht University, Padualaan 8, 3584 CH Utrecht, the Netherlands.[2]Dipartimento di Genetica e Biologia Molecolare, Laboratory of Functional Genomics and Proteomics of Model Systems, Università La Sapienza, P.le Aldo Moro 5, 00185 Rome, Italy.

Summary

Continuous development and growth of plants is controlled by pools of stem cells located in shoot and root meristems. Shoot stem cells express the CLE family peptide CLAVATA3 (CLV3) that binds to and activates the CLV1 receptor, which is involved in shoot meristem homeostasis. CLV3 overexpression leads to consumption of the shoot apical meristem (SAM). Similarly, overexpression and exogenous application of CLE family peptides terminates the root meristem, suggesting that a CLE signaling pathway involved in meristem maintenance is conserved in shoots and roots. Here, we report on *sol3*, a recessive mutant identified in an activation tagging screen that is able to suppress the CLE19-induced root consumption phenotype. Interestingly, *sol3* mutants display enhanced root growth and meristem size compared to wild type, a phenotype largely unaffected by cytokinin treatment. In addition, the *sol3* root cap contains less columella layers and ground tissue differentiation is delayed. Thus, *SOL3* has a dual role in the root controlling growth and formative cell divisions.

Introduction

Plant postembryonic growth and development is controlled through the activity of meristems that harbor pools of stem cells. Stem cells self-renew and produce daughter cells that give rise to all the different plant organs and structures. A complex network of intercellular signals and regulatory genes is responsible for maintenance of stem cell populations in shoot and root meristems. The CLV-WUSCHEL (WUS) pathway plays an important role in the regulation of stem cell fate in the SAM (reviewed by Sablowski, 2007; Rieu and Laux, 2009). Where *WUS* encodes a homeodomain transcription factor (Laux et al., 1996), *CLV3* belongs to the 31-member-*CLE* (*CLV3/ENDOSPERM SURROUNDING REGION [ESR]*) gene family that encodes small proteins with a conserved 14 amino acid CLE motif at or near the C-terminus (Sharma et al., 2003; Kondo et al., 2006). Stem cells express CLV3 that binds to and activates the membrane-bound leucine-rich repeat receptor-like kinase CLV1 (Ogawa et al., 2008), thereby restricting the *WUS* expression domain. WUS in turn is required for the maintenance of the stem cell population in a non-cell autonomous fashion and a negative feedback loop between CLV3 and WUS ensures a balanced stem cell population in the SAM.

The radial organization of the *Arabidopsis* root is derived from stereotyped asymmetric cell divisions of different stem cells and their daughters (Figure 1a). These stem cells surround a small group of cells in the root meristem, the quiescent center (QC), that is required for their maintenance, thus resembling the SAM organizing center (reviewed by ten Hove and Heidstra, 2008). Combinatorial action of the *SHORT-ROOT* (*SHR*) and *SCARECROW* (*SCR*) genes and the auxin-responsive *PLETHORA* (*PLT*) genes determines the position and maintenance of the stem cell niche (QC and surrounding stem cells) (Sabatini et al., 2003; Aida et al., 2004; Galinha et al., 2007). Stem cell daughters divide a finite number of times in the meristem, before elongating and differentiating. The overall root growth rate and the size of the meristem is determined by the rate of cell division in the meristem, cell expansion and cell differentiation at the transition zone (Beemster and Baskin, 1998; Dello Ioio et al., 2007). Local regulation of the plant hormones cytokinin and auxin partly control the transition from meristematic identity to differentiation. Cytokinin mediated cell differentiation antagonizes auxin-dependent cell division input to control the size of the meristem (Dello Ioio et al., 2007; Dello Ioio et al., 2008b; Ruzicka et al., 2009). Mutants that show increased root growth and meristem cell number include the cytokinin biosynthesis triple mutant *ipt3 ipt5 ipt7* and the cytokinin signaling mutants *ahk3*, *arr1* and *arr12* (Miyawaki et al., 2006; Dello Ioio et al., 2007).

Recent studies point to the existence of analogous signaling mechanisms that control stem cell homeostasis in shoots and roots: (1) application or overexpres-

sion of A-class CLE peptides leads to termination of both shoot and root meristems (Fiers et al., 2005; Whitford et al., 2008); (2) WUS and its family member WOX5 are interchangeable between shoot and root organizers for stem cell maintenance (Sarkar et al., 2007) and; (3) in the root, CLE40 and WOX5 are proposed to form a self-regulating network that controls the proliferation and differentiation of stem cells similar to the CLV3–WUS network in the shoot (Stahl et al., 2009).

CLE-induced arrest of meristem growth has been exploited in suppressor screens using EMS mutagenesis to reveal the identity of additional components of the CLE signaling pathway (Casamitjana-Martinez et al., 2003; Muller et al., 2008). Mutations in *SOL1 (SUPPRESSOR OF LLP1 1)*, a Zn^{2+}-carboxypeptidase, and *SOL2/CORYNE*, a membrane-associated kinase, rendered plants resistant to high levels of CLE peptides (Casamitjana-Martinez et al., 2003; Muller et al., 2008; Miwa et al., 2008).

From an activation tagging screen aimed to identify additional components of a root CLE signaling pathway we isolated several new suppressor mutants that were resistant to high levels of CLE19. In this study, we report on the analysis of one of these mutants, *sol3*. Mutation in *SOL3* leads to resistance to the CLE19 differentiation signal in a recessive manner, and, additionally, results in a reduction in the number of columella layers and transient delay in ground tissue differentiation. Furthermore, *sol3* root and meristem size is increased compared to wild type, a phenotype reminiscent of cytokinin biosynthesis and signaling mutants. Indeed, *sol3* meristems appear less affected than wild type upon cytokinin application.

Results

sol3 suppresses the *RCH1>>CLE19* induced meristem defect

Root-specific overexpression of *CLE19* leads to termination of the root meristem in a dose-dependent manner (Casamitjana-Martinez et al., 2003). To complement reported approaches in finding molecular components involved in CLE-induced root meristem consumption, we performed T-DNA activation tagging on homozygous, single insertion *RCH1>>CLE19* transgenic plants to identify suppressors. A total of 6300 *RCH1>>CLE19* plants were transformed with the *pSKI015* vector and transgenic T1 plants were selected on soil for conferred resistance to the herbicide glufosinate. In the next generation, progeny of individual T-DNA activation tagged plants were screened for recovery of root length and high expression of green fluorescent protein (GFP), indicating root meristem maintenance and homozygosity for the *RCH1>>CLE19* construct (see experimental procedures; Figure 1b). Several long root suppressors with high *RCH1>>CLE19* levels were obtained. One of the suppressors segregating as a single locus was named *sol3* and was analyzed further because of

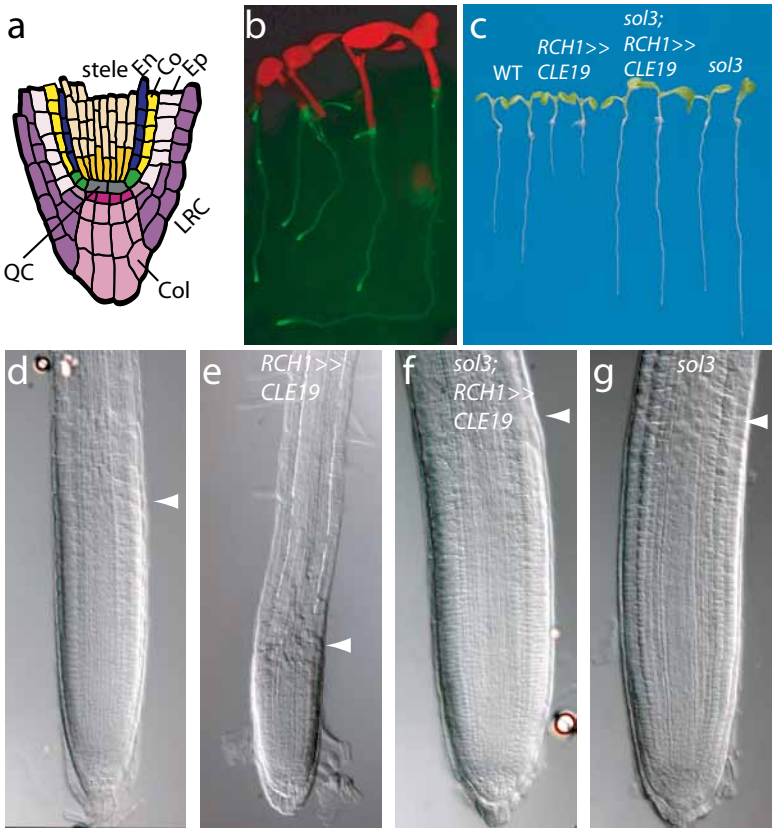

Figure 1. ***sol3* suppresses *RCH1>>CLE19* induced reduction of root meristem size.** (a) Schematic overview of the *Arabidopsis* root meristem. (En) endodermis; (Co) cortex; (Ep) epidermis; (LRC) lateral root cap; (Col) columella; (QC) quiescent center. (b) 4-Day-old *sol3;RCH1>>CLE19* and *RCH1>>CLE19* seedlings. The *sol3;RCH1>>CLE19* suppressor is on the right. (c) 5-Day-old wild type, *RCH1>>CLE19*, *sol3;RCH1>>CLE19* and *sol3* seedlings (d-g) Nomarski images showing the root meristem boundary (white arrowhead) of 4-day-old wild type (d), *RCH1>>CLE19* (e), *sol3;RCH1>>CLE19* (f), and *sol3* (g) roots, respectively.

its additional root phenotypes (see below). The *sol3* mutant suppresses the short root phenotype conferred by *RCH1>>CLE19* (Figure 1b,c,e-g) and is able to maintain complete suppression over time (Figure 2a). In addition, a strong reduction in fertility was observed in *sol3* as anthers released much less pollen grains than wild type (data not shown).

We backcrossed *sol3;RCH1>>CLE19* to *RCH1>>CLE19* to test for the integrity of the construct. The F1 progeny displayed high GFP expression, indicating that *RCH1>>CLE19* is still fully active in the *sol3* background and that the suppression is not due to cosuppression of the *CLE19* transgene (data not shown). The entire F1 progeny displayed short roots, indicating that the activation tagged

sol3;RCH1>>CLE19 mutant carries a recessive mutation. Southern blot analyses revealed that *sol3;RCH1>>CLE19* contained four T-DNA insertions (data not shown). Repeated outcrossing showed linkage between three of these. Attempts to clone *SOL3* using plasmid rescue, thermal asymmetric interlaced polymerase chain reaction (TAIL-PCR) and vectorette PCR were so far unsuccessful.

sol3 enhances root growth and meristem size

Compared to wild type, *sol3;RCH1>>CLE19* displayed enhanced root growth and meristem size (Figure 1c,d,f,g, Figure 2a,b). We also measured root length and meristem size of the *sol3* mutant lacking the *RCH1>>CLE19* construct (*sol3*), which was obtained by repeated outcrossing against Columbia Utrecht. Overall root growth and meristem size of *sol3* was similar to *sol3;RCH1>>CLE19* (Figure 2a,b). In addition to an increase in root growth and root meristem size *sol3;RCH1>>CLE19* and *sol3* roots display an increased root width compared to wild type roots (Figure 1d,f,g, Figure 2c).

Mutants that show increased root growth and meristem cell number include cytokinin biosynthesis and signaling mutants (Miyawaki et al., 2006; Dello Ioio et al., 2007) and the root meristems of these mutants show a reduced response to exogenous cytokinin application (Riefler et al., 2006; Dello Ioio et al., 2007). To address whether the observed *sol3* phenotype involves altered cytokinin biosynthesis or signaling we examined the effect of exogenous cytokinin application on the development of the *sol3;RCH1>>CLE19* root meristem. Wild type and *sol3;RCH1>>CLE19* seedlings were grown for five days on medium without *trans*-zeatin, then transferred and grown for 16 hours on medium supplemented with 5 µM *trans*-zeatin and meristem size was measured. Exogenous application of cytokinins causes a massive decrease in the number of meristematic cells in wild type (40%) and *RCH1>>CLE19* (37%), but leads to only a slight decrease in meristem cell number in *sol3;RCH1>>CLE19* (7%) (Figure 2d). These data suggest that the increased root growth and meristem cell number in *sol3;RCH1>>CLE19* could be related to cytokinin shortage or sensing.

The *SHR*, *SCR*, and *PLT* transcription factor genes have essential roles in QC specification and stem cell and meristem maintenance. *SHR*, *SCR*, and *PLT* gene disruption results in stem cell loss leading to differentiation of the root meristem (Sabatini et al., 2003; Aida et al., 2004; Galinha et al., 2007). To examine whether the increased meristem activity in *sol3* was able to complement *shr* and *scr* single and *plt1 plt2* double mutant roots we constructed *sol3;RCH1>>CLE19 shr-2, sol3;RCH1>>CLE19 scr-4* double and *sol3;RCH1>>CLE19 plt1-4 plt2-2* triple mutants. Growth and meristem dissipation of double and triple mutant combinations resembled that of *shr-2, scr-4* or *plt1-4 plt2-2* mutants, indicating that *sol3;RCH1>>CLE19* could not prevent the premature cessation of root growth observed in these mutants (data not shown).

***SOL3* is required for columella differentiation**

In addition to an increase in root growth *sol3;RCH1>>CLE19* and *sol3* plants display similar defects in root differentiation. In wild type, the columella root cap consists of a single layer of stem cells, located immediately distal to the QC, and 4-5 tiers of differentiated cells that elongate and contain starch granules. *sol3* mutants with or without *RCH1>>CLE19*, however, display less columella root cap layers (Table 1).

The reduction of columella cell layers prompted us to examine QC activity and columella stem cell maintenance. The expression of the QC-specific promoter trap QC25 and *WOX5:*$_{ER}$*GFP* in *sol3;RCH1>>CLE19* and *sol3*, respectively, was comparable to wild type (Figure 3a,b, data not shown). In addition, the layer of columella cells immediately distal to the QC did not accumulate starch granules (Figure 3b), indicating presence of columella stem cells and QC activity.

Other genes involved in columella differentiation are *FEZ*, *SOMBRERO* (*SMB*), *WOX5* and *RETINOBLASTOMA RELATED* (*RBR*). The NAC domain transcription factor genes *FEZ* and *SMB* control the production of root cap cells as well as the division plane of the distal stem cells through a cross regulatory feedback loop (Willemsen et al., 2008). RNAi induced reduction of *RBR* results in excessive stem cell accumulation due to prolonged maintenance of stem cell fate (Wildwater et al., 2005).

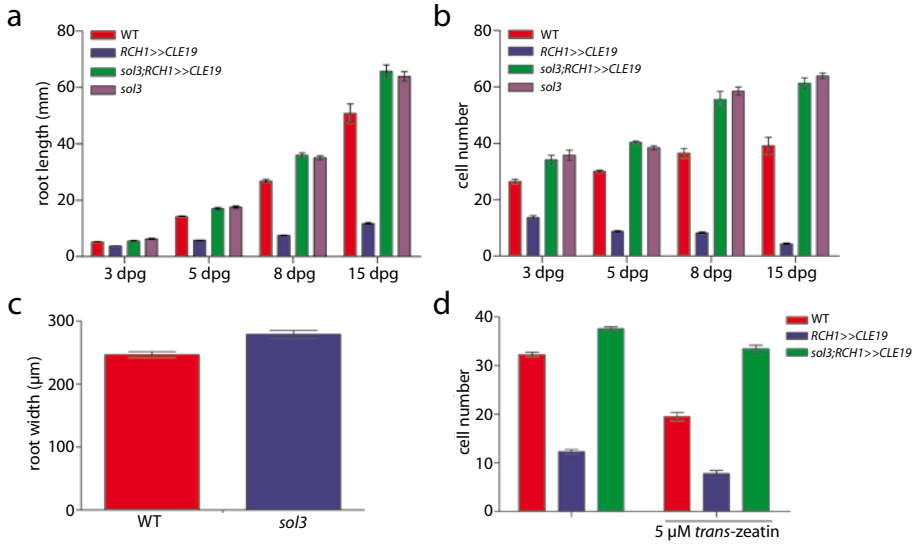

Figure 2. ***sol3* displays an increase in root growth and meristem cell number.** (a,b) Root length (a; in mm) and root meristem cell number (b) of wild type, *RCH1>>CLE19*, *sol3;RCH1>>CLE19* and *sol3* seedlings at different time points. (c) Root width (in μm) of 5-day-old wild type and *sol3;RCH1>>CLE19* seedlings. (d) Root meristem cell number of 5-day-old wild type, *RCH1>>CLE19* and *sol3;RCH1>>CLE19* seedlings grown for 16 h on 5 μM *trans*-zeatin. Error bars indicate the standard error of the mean (sem).

Table 1. Quantification of cell layers.

	No. of columella layers in mature embryos (n) and seedlings (n)[a]		No. of ground tissue stem cells in mature embryos (n) and seedlings (n)[a]	
	Mature embryo	Seedling[a]	Mature embryo	Seedling[a]
WT	4 ± 0 (9)	5,6 ± 0,1 (19)	0,8 ± 0,1 (9)	0,2 ± 0,1 (25)
RCH1>>CLE19	4 ± 0 (3)	NA	1 ± 0,3 (3)	NA
sol3;RCH1>>CLE19	3 ± 0 (30)	NA	3,4 ± 0,2 (30)	NA
sol3	3 ± 0 (13)	3,6 ± 0,1 (29)	6,1 ± 0,3 (13)	2,5 ± 0,3 (28)

Data represented are mean ± sem. Values in parentheses represent sample size. NA; not analyzed, [a]; Four days post germination.

WOX5 is required for columella stem cell maintenance and overexpression blocks differentiation of distal stem cell daughters causing numerous columella stem cell layers (Sarkar et al., 2007). The *sol3* columella phenotype is reminiscent of the *fez* mutant (Willemsen et al., 2008) (Figure 4a,b). *sol3;RCH1>>CLE19 fez-2* double mutants showed a further reduction in the amount of columella layers (Figure 4c). In addition, we crossed *sol3;RCH1>>CLE19* with *smb, 35S::WOX5* and *rRBr* mutants that all display increased distal stem cell activity and numbers (Fig 4c,d,h) (Willemsen et al., 2008; Sarkar et al., 2007; Wildwater et al., 2005). *sol3;RCH1>>CLE19 smb-3*, *sol3;RCH1>>CLE19 35S::WOX5* and *sol3;RCH1>>CLE19 rBRr* double mutants showed additional root cap layers although fewer columella root cap layers than *smb-3, 35S::WOX5* and *rRBr* single mutants (Figure 4e-g,i). Together, these data suggest that *SOL3* forms an independent input into columella differentiation.

SOL3 **is required for ground tissue differentiation**

Cortex and endodermis (collectively called ground tissue) are derived from a shared ground tissue stem cell. This stem cell first divides anticlinally to regenerate a new stem cell and sets off a daughter cell that undergoes a periclinal asymmetric division to generate an outer cortex cell and inner endodermal cell (Figure 1a). In the ground tissue of 4-day-old *sol3;RCH1>>CLE19* and *sol3* seedlings additional anticlinal divisions have taken place before the periclinal division occurs whereas later in development, ground tissue organization is similar to wild type (Table 1, data not shown). To probe the identity of the column of single ground tissue cells we introduced *SCR::SCR:GFP* and *Co2::*$_{H2B}$*YFP* markers in *sol3*. SCR:GFP is expressed in the endodermis, ground tissue stem cells and QC (Figure 3c), whereas *Co2::*$_{H2B}$*YFP* is highly expressed in the cortex, but is excluded from the ground tissue stem cells and their undivided daughters (Figure 3e). In *sol3*, SCR:GFP is expressed in the column of cells at the position of the ground tissue stem cell daughter, whereas *Co2::*$_{H2B}$*YFP* expression is excluded from these cells (Figure 3d,f). These data suggest that the ground tissue stem cell status is temporarily expanded in *sol3*.

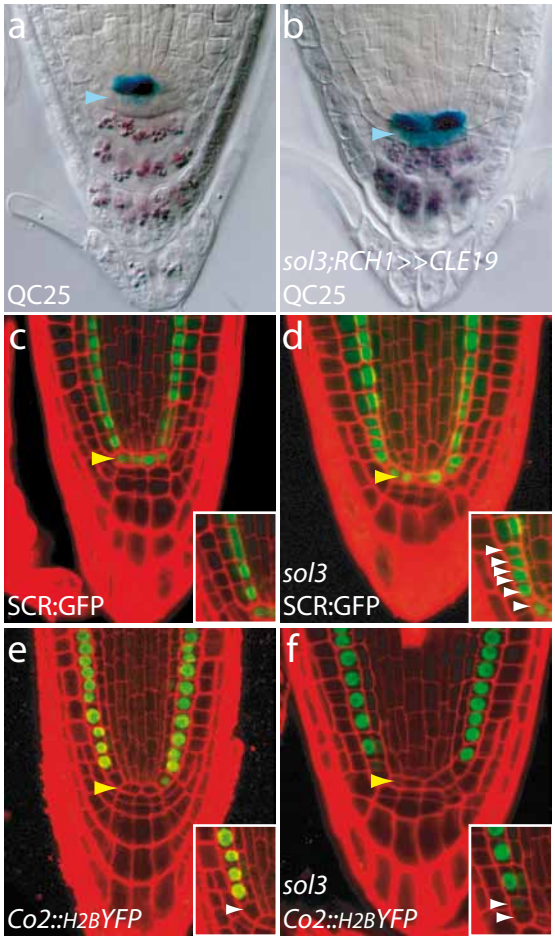

Figure 3. Ground tissue stem cell status is expanded in *sol3*. (a-b) QC25 expression in 6-day-old wild type (a) and *sol3;RCH1>>CLE19* (b) roots. Starch granule staining (purple) marks differentiated columella cells. Blue arrowhead marks columella stem cells. (c-f) 5-Day-old wild type (c,e) and *sol3* (d,f) roots showing SCR:GFP (c,d) and *Co2::$_{H2B}$YFP* (e,f) expression. The inserts (c-f) show a blow-up of ground tissue stem cells (white arrowheads) expressing SCR:GFP (d) and lacking *Co2::$_{H2B}$YFP* expression (e,f). Yellow arrowhead marks QC.

sol3 embryonic patterning defects

To trace back the defects observed in *sol3* seedling roots we analyzed embryonic patterning. In wild type and *RCH1>>CLE19* mature embryos, 4 layers of columella are observed, whereas in *sol3* there are only 3 columella layers present (Figure 5a-d, Table 1), a number that is maintained in the seedling root. Additionally, a column of anticlinally divided cells is observed in the ground tissue of *sol3* before the periclinal division takes place. These embryonic phenotypes are identical in *sol3;RCH1>>CLE19*

and *sol3* except that *sol3* displays more undivided ground tissue cells (Figure 5a-d, Table 1). The organization of other cell types does not appear to be affected in *sol3*.

These data suggest that *SOL3* promotes periclinal divisions of the columella and the ground tissue in the root.

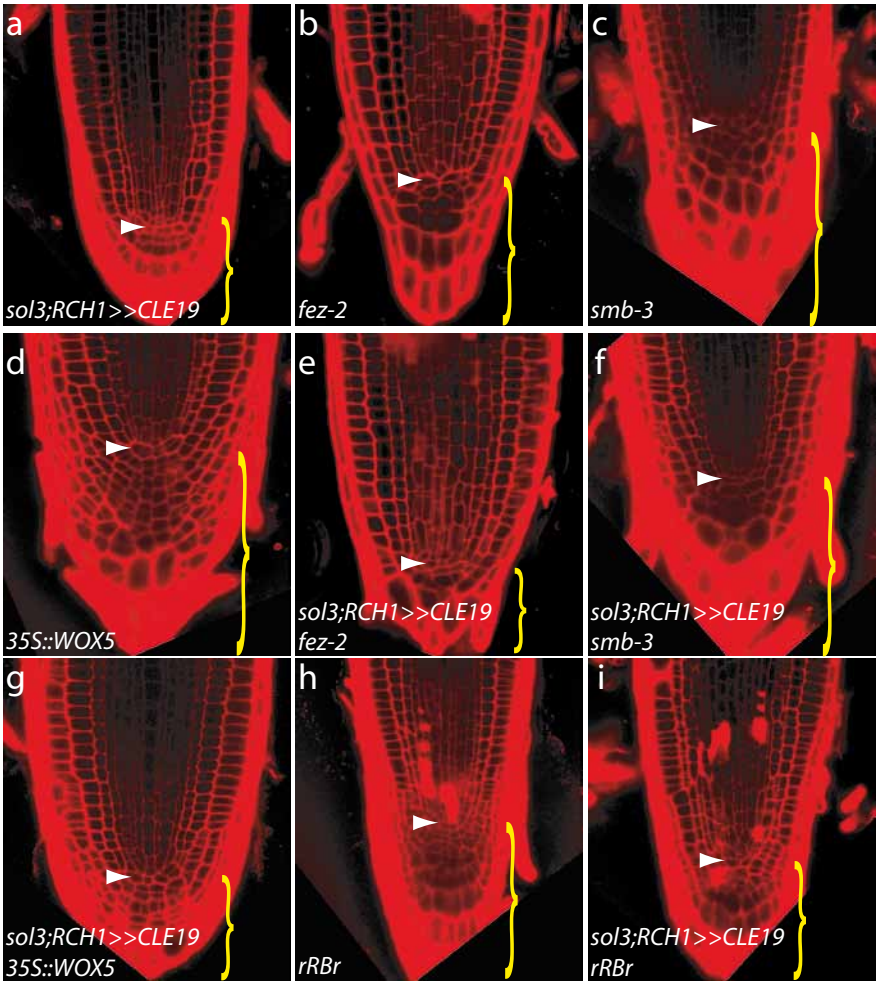

Figure 4. *SOL3* operates independent of columella patterning genes. (a-i) 6-Day-old roots of *sol3;RCH1>>CLE19* (a), *fez-2* (b), *smb-3* (c), *sol3;RCH1>>CLE19 fez-2* (e), *sol3;RCH1>>CLE19 smb-3* (f), 5-day-old *35S::WOX5* (d), *sol3 35S::WOX5* (g), 8-day-old *rBRr* (h) and *sol3;RCH1>>CLE19 rBRr* (i) single mutant and double mutant combinations. QC (white arrowhead); root cap columella (yellow bracket).

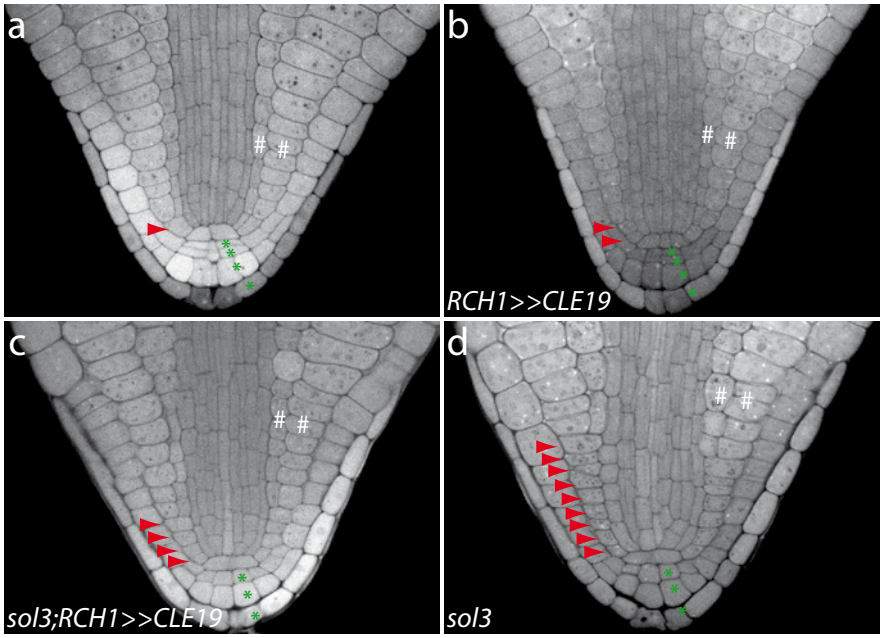

Figure 5. *sol3* embryonic defects. (a-d) Aniline blue stained wild type (a), *RCH1>>CLE19* (b), *sol3;RCH1>>CLE19* (c) and *sol3* (d) mature embryos. Ground tissue stem cells (red arrowheads); ground tissue (white hash); columella cells (green asterisk).

Discussion

Several studies hint at the possible existence of analogous signaling machinery in shoots and roots in controlling meristem size (Casamitjana-Martinez et al., 2003; Sarkar et al., 2007; Stahl et al., 2009). We applied T-DNA activation tagging to *RCH1>>CLE19* transgenic plants in an attempt to obtain gain-of-function mutations showing resistance to CLE19-induced arrest of root growth. In this screen, we identified a new recessive CLE19-resistant mutant, *sol3*.

sol3 displays less columella layers from embryogenesis onward, suggesting that *SOL3* controls the number of periclinal cell divisions in the columella. These relatively rare tissue-forming divisions are referred to as formative divisions as opposed to proliferative divisions that serve to increase cell number within a tissue. Double mutant combinations of *sol3;RCH1>>CLE19* with *fez-2* showed a further decrease in columella layers, whereas double mutant combinations with *smb-3*, *35S::WOX5* and *rBRr* showed additional root cap layers, although fewer columella root cap layers than the single mutants. Thus, *SOL3* can be added to this list of genes that appear to control the number of formative cell divisions in the columella through independent mechanisms.

In wild type, the formative ground tissue asymmetric periclinal division always occurs immediately in the stem cell daughter, a process tightly regulated by the *SHR/SCR* pathway (reviewed by ten Hove and Heidstra, 2008). *sol3* mutant roots develop a column of anticlinally divided ground tissue cells before the asymmetric periclinal division is observed. Absence of *Co2::$_{H2B}$YFP* expression in these cells suggests that these cells retain ground tissue stem cell fate characteristics. A column of ground tissue stem cells is visible up to one week, indicating that the asymmetric periclinal ground tissue division is delayed. Our observations suggest that *SOL3* controls the timing of periclinal ground tissue division. Previously, it was shown that wild type roots displayed a column of anticlinally divided cells at the position of the ground tissue stem cell daughter upon CLV3, CLE19 and CLE40 peptide treatment (Fiers et al., 2005). However, tissue marker analysis using *SCR::$_{ER}$GFP* and *Co2::$_{H2B}$YFP* showed that this CLE-induced column of anticlinally divided cells had adopted a shared cortex/endodermis identity, indicating that only *SOL3* is involved in fate determination. Other recent studies showed that CLE40, and its putative receptor ACR4, a receptor-like kinase belonging to the Crinkly4 class, restrict formative divisions in daughter cells of columella stem cells in the root apex (De Smet et al., 2008; Stahl et al., 2009; Stahl and Simon, 2009). Differentiation of columella stem cells is delayed in *cle40* and *acr4* mutants ultimately giving rise to a distorted root cap. Future work will have to clarify the relation between *SOL3* and CLE-mediated signaling on control of formative cell division in the root.

Remarkably, *sol3* does not only suppress CLE19-induced arrest of root growth but also exhibits a larger root and meristem size. Nevertheless, *sol3;RCH1>>CLE19* could not complement the root length and the root meristem maintenance defect of *plt1-4 plt2-2*, *shr-2* and *scr-4* mutants. An increased root and meristem size phenotype is also observed in the cytokinin biosynthesis triple mutant *ipt3 ipt5 ipt7* and the cytokinin signaling mutants *ahk2*, *ahk3* and *ahk4* (Dello Ioio et al., 2008a). The same effect was observed for cytokinin depletion by CYTOKININ OXIDASE/DEHYDROGENASE (CKX) overexpression in the vascular tissue transition zone, but not when cytokinin was depleted in the root meristem, indicating that cytokinin acts at the vascular tissue transition zone to control meristem size (Werner et al., 2003; Dello Ioio et al., 2007). Similar to *ipt3 ipt5 ipt7* and *ahk2*, *ahk3* and *ahk4* (Dello Ioio et al., 2007; Riefler et al., 2006), the *sol3* root shows a reduced response to exogenous cytokinin application, implying that *SOL3* may act in the vascular tissue transition zone to control meristem size. Measurement of cytokinin levels in *sol3* together with the generation of double mutant combinations with signaling mutants *ahk3*, *arr1* and *arr12* could help clarify whether *sol3* is involved in regulating cytokinin levels (e.g. by directing *IPT* gene expression) or sensing. Vice versa, it would be of

interest to learn how the root meristems of these cytokinin biosynthesis and signaling mutants respond to exogenous CLE peptide treatment.

In the shoot, high cytokinin levels are necessary to preserve shoot meristem activity, in contrast to its role in root meristem maintenance (Shani et al., 2006). Interestingly, components of the shoot meristem gene regulatory network have been found to be involved in regulating cytokinin levels and signaling. SHOOT MERISTEMLESS induces the expression of the cytokinin biosynthesis *IPT* genes (Yanai et al., 2005), whereas WUS enhances cytokinin activity in the organizer by directly repressing the expression of several negative acting type-A *ARR* genes (Leibfried et al., 2005). In the root, *SOL3* activity may be involved in regulation of cytokinin levels or signaling thereby connecting the root CLE signaling pathway to cytokinin in root meristem homeostasis. Cloning of *SOL3* should reveal its relationship to cytokinin and its function in the CLE signaling pathway controlling meristem maintenance and formative cell divisions in the root.

Experimental procedures

Plant materials and growth conditions

Origins of mutant and transgenic lines: *RCH1>>CLE19* (Casamitjana-Martinez et al., 2003); SCR:GFP (Nakajima et al., 2001); *Co2::$_{H2B}$YFP* (Heidstra et al., 2004); QC25 (Sabatini et al., 1999; Sabatini et al., 2003); *fez-2*, *smb-3* (Willemsen et al., 2008); *35S::WOX5* was kindly provided by Thomas Laux (Freiburg University, Germany); *rRBr* (Wildwater et al., 2005). Seeds were gas-sterilized in a desiccator for 2 hours with 100 mL of bleach (4% NaClO) mixed with 3 mL of HCl in a beaker or surface-sterilized in 20% bleach for 20 minutes. Seedlings were plated and grown as described in (Sabatini et al., 2003).

Generation of an activation tagging mutant population and molecular analysis

For activation tagging mutagenesis, approximately 6300 plants homozygous for a single copy of *RCH1>>CLE19* (ecotype Columbia Utrecht) were transformed with the *pSKI015* T-DNA activation tagging plasmid (Weigel et al., 2000) using the floral dip method (Clough and Bent, 1998). Seeds were sown on soil and were grown in a plant chamber at 22°C, 70% humidity with a 16 hour light and 8 hour dark cycle. Herbicide-resistant plants were selected by spraying twice a week for 3 weeks with DL-phosphinotricin (also known as PPT, glufosinate ammonium or Basta; Duchefa, Haarlem). T2 seedlings were individually harvested and were screened on plates containing half strength Murashige and Skoog (MS) salt mixture, 1% sucrose and 0.5 g/L (N-morpholino) ethanesulfonic acid (MES), pH5.8, in 0.8% agar for recovery

of root length and high GFP expression using a Leica MZFLIII stereomicroscope. Suppressors were crossed to *RCH1>>CLE19* to check for preservation of a functional *RCH1>>CLE19* construct after T-DNA activation tagging and for dominant or recessive traits. If the F1 showed the phenotype of *RCH1>>CLE19*, the suppressor was considered functional and not dominant. Suppressors were also crossed to *sol1* and *sol2* to test for possible allelism. We established cosegregation of *sol3* developmental and suppression phenotypes by verifying that the suppressor phenotype in a *sol3* segregating population correlates to the root patterning defect and vise versa. Plasmid rescue, TAIL-PCR and vectorette PCR were performed as described (Weigel et al., 2000; Liu and Whittier, 1995; Arnold and Hodgson, 1991).

Microscopy

sol3 was backcrossed to *RCH1>>CLE19* or Columbia Utrecht three times prior to phenotypic and genetic analysis. Fluorescent reporters were crossed to *sol3* and not *sol3;RCH1>>CLE19* as the *RCH1>>CLE19* construct harbored GFP and would interfere with the analyses. Light microscopy, starch granule staining, measurement of root length or number of meristematic cells was performed as described in (Willemsen et al., 1998) and (Welch et al., 2007). Root width was measured just above the QC. Aniline blue staining of mature embryos was performed as described in (Bougourd et al., 2000). For confocal microscopy, roots were mounted in 20 µg/mL propidium iodide.

Acknowledgements

This project was financed by the Centre for BioSystems Genomics (CBSG), which is part of the Netherlands Genomics Initiative/Netherlands Organization for Scientific Research (NGI/NWO). SS is supported by a Giovanni Armenise-Harvard Foundation career development grant.

References

Aida, M., Beis, D., Heidstra, R., Willemsen, V., Blilou, I., Galinha, C., Nussaume, L., Noh, Y.S., Amasino, R., and Scheres, B. (2004). The PLETHORA genes mediate patterning of the *Arabidopsis* root stem cell niche. Cell *119*, 109-120.

Arnold, C. and Hodgson, I.J. (1991). Vectorette PCR: a novel approach to genomic walking. Genome Research *1*, 39-42.

Beemster, G.T. and Baskin, T.I. (1998). Analysis of cell division and elongation underlying the developmental acceleration of root growth in *Arabidopsis thaliana*. Plant Physiol *116*, 1515-1526.

Bougourd, S., Marrison, J., and Haseloff, J. (2000). Technical advance: an aniline blue staining procedure for confocal microscopy and 3D imaging of normal and perturbed cellular phenotypes in mature *Arabidopsis* embryos. Plant J. *24*, 543-550.

Casamitjana-Martinez, E., Hofhuis, H.F., Xu, J., Liu, C.M., Heidstra, R., and Scheres, B. (2003). Root-specific CLE19 overexpression and the sol1/2 suppressors implicate a CLV-like pathway in the control of *Arabidopsis* root meristem maintenance. Curr. Biol. *13*, 1435-1441.

Clough, S.J. and Bent, A.F. (1998). Floral dip: a simplified method for Agrobacterium-mediated transformation of *Arabidopsis thaliana*. Plant J. *16*, 735-743.

De Smet, I., Vassileva, V., De, R.B., Levesque, M.P., Grunewald, W., Van, D.D., Van, N.G., Naudts, M., Van, I.G., De, C.R., Wang, J.Y., Meuli, N., Vanneste, S., Friml, J., Hilson, P., Jurgens, G., Ingram, G.C., Inze, D., Benfey, P.N., and Beeckman, T. (2008). Receptor-like kinase ACR4 restricts formative cell divisions in the *Arabidopsis* root. Science *322*, 594-597.

Dello Ioio, R., Linhares, F.S., and Sabatini, S. (2008a). Emerging role of cytokinin as a regulator of cellular differentiation. Curr. Opin. Plant Biol. *11*, 23-27.

Dello Ioio, R., Linhares, F.S., Scacchi, E., Casamitjana-Martinez, E., Heidstra, R., Costantino, P., and Sabatini, S. (2007). Cytokinins determine *Arabidopsis* root-meristem size by controlling cell differentiation. Curr. Biol. *17*, 678-682.

Dello Ioio, R., Nakamura, K., Moubayidin, L., Perilli, S., Taniguchi, M., Morita, M.T., Aoyama, T., Costantino, P., and Sabatini, S. (2008b). A genetic framework for the control of cell division and differentiation in the root meristem. Science *322*, 1380-1384.

Fiers, M., Golemiec, E., Xu, J., van der, G.L., Heidstra, R., Stiekema, W., and Liu, C.M. (2005). The 14-amino acid CLV3, CLE19, and CLE40 peptides trigger consumption of the root meristem in *Arabidopsis* through a CLAVATA2-dependent pathway. Plant Cell *17*, 2542-2553.

Galinha, C., Hofhuis, H., Luijten, M., Willemsen, V., Blilou, I., Heidstra, R., and Scheres, B. (2007). PLETHORA proteins as dose-dependent master regulators of *Arabidopsis* root development. Nature *449*, 1053-1057.

Heidstra, R., Welch, D., and Scheres, B. (2004). Mosaic analyses using marked activation and deletion clones dissect *Arabidopsis* SCARECROW action in asymmetric cell division. Genes Dev. *18*, 1964-1969.

Kondo, T., Sawa, S., Kinoshita, A., Mizuno, S., Kakimoto, T., Fukuda, H., and Sakagami, Y. (2006). A plant peptide encoded by CLV3 identified by in situ MALDI-TOF MS analysis. Science *313*, 845-848.

Laux, T., Mayer, K.F., Berger, J., and Jurgens, G. (1996). The WUSCHEL gene is required for shoot and floral meristem integrity in *Arabidopsis*. Development *122*, 87-96.

Leibfried, A., To, J.P., Busch, W., Stehling, S., Kehle, A., Demar, M., Kieber, J.J., and Lohmann, J.U. (2005). WUSCHEL controls meristem function by direct regulation of cytokinin-inducible response regulators. Nature *438*, 1172-1175.

Liu, Y.G. and Whittier, R.F. (1995). Thermal asymmetric interlaced PCR: automatable amplification and sequencing of insert end fragments from P1 and YAC clones for chromosome walking. Genomics *25*, 674-681.

Miwa, H., Betsuyaku, S., Iwamoto, K., Kinoshita, A., Fukuda, H., and Sawa, S. (2008). The receptor-like kinase SOL2 mediates CLE signaling in *Arabidopsis*. Plant Cell Physiol *49*, 1752-1757.

Miyawaki, K., Tarkowski, P., Matsumoto-Kitano, M., Kato, T., Sato, S., Tarkowska, D., Tabata, S., Sandberg, G., and Kakimoto, T. (2006). Roles of *Arabidopsis* ATP/ADP isopentenyltransferases and tRNA isopentenyltransferases in cytokinin biosynthesis. Proc. Natl. Acad. Sci. U. S. A *103*, 16598-16603.

Muller, R., Bleckmann, A., and Simon, R. (2008). The receptor kinase CORYNE of *Arabidopsis* transmits the stem cell-limiting signal CLAVATA3 independently of CLAVATA1. Plant Cell *20*, 934-946.

Nakajima, K., Sena, G., Nawy, T., and Benfey, P.N. (2001). Intercellular movement of the putative transcription factor SHR in root patterning. Nature *413*, 307-311.

Ogawa, M., Shinohara, H., Sakagami, Y., and Matsubayashi, Y. (2008). *Arabidopsis* CLV3 peptide directly binds CLV1 ectodomain. Science *319*, 294.

Riefler, M., Novak, O., Strnad, M., and Schmulling, T. (2006). *Arabidopsis* Cytokinin Receptor Mutants Reveal Functions in Shoot Growth, Leaf Senescence, Seed Size, Germination, Root Development, and Cytokinin Metabolism. Plant Cell *18*, 40-54.

Rieu, I. and Laux, T. (2009). Signaling pathways maintaining stem cells at the plant shoot apex. Seminars in Cell & Developmental Biology *20*, 1083-1088.

Ruzicka, K., Simaskova, M., Duclercq, J., Petrasek, J., Zazimalova, E., Simon, S., Friml, J., Van Montagu, M.C., and Benkova, E. (2009). Cytokinin regulates root meristem activity via modulation of the polar auxin transport. Proc. Natl. Acad. Sci. U. S. A *106*, 4284-4289.

Sabatini, S., Beis, D., Wolkenfelt, H., Murfett, J., Guilfoyle, T., Malamy, J., Benfey, P., Leyser, O., Bechtold, N., Weisbeek, P., and Scheres, B. (1999). An auxin-dependent distal organizer of pattern and polarity in the *Arabidopsis* root. Cell *99*, 463-472.

Sabatini, S., Heidstra, R., Wildwater, M., and Scheres, B. (2003). SCARECROW is involved in positioning the stem cell niche in the *Arabidopsis* root meristem. Genes Dev. *17*, 354-358.

Sablowski, R. (2007). Flowering and determinacy in *Arabidopsis*. J. Exp. Bot. *58*, 899-907.

Sarkar, A.K., Luijten, M., Miyashima, S., Lenhard, M., Hashimoto, T., Nakajima, K., Scheres, B., Heidstra, R., and Laux, T. (2007). Conserved factors regulate signalling in *Arabidopsis thaliana* shoot and root stem cell organizers. Nature *446*, 811-814.

Shani, E., Yanai, O., and Ori, N. (2006). The role of hormones in shoot apical meristem function. Curr. Opin. Plant Biol *9*, 484-489.

Sharma, V.K., Ramirez, J., and Fletcher, J.C. (2003). The *Arabidopsis* CLV3-like (CLE) genes are expressed in diverse tissues and encode secreted proteins. Plant Mol. Biol. *51*, 415-425.

Stahl, Y. and Simon, R. (2009). Is the *Arabidopsis* root niche protected by sequestration of the CLE40 signal by its putative receptor ACR4? Plant Signal. Behav. *4*, 634-635.

Stahl, Y., Wink, R.H., Ingram, G.C., and Simon, R. (2009). A signaling module controlling the stem cell niche in *Arabidopsis* root meristems. Curr. Biol. *19*, 909-914.

ten Hove, C.A. and Heidstra, R. (2008). Who begets whom? Plant cell fate determination by asymmetric cell division. Curr Opin Plant Biol *11*, 34-41.

Weigel, D., Ahn, J.H., Blazquez, M.A., Borevitz, J.O., Christensen, S.K., Fankhauser, C., Ferrandiz, C., Kardailsky, I., Malancharuvil, E.J., Neff, M.M., Nguyen, J.T., Sato, S., Wang, Z.Y., Xia, Y., Dixon, R.A., Harrison, M.J., Lamb, C.J., Yanofsky, M.F., and Chory, J. (2000). Activation tagging in *Arabidopsis*. Plant Physiol *122*, 1003-1013.

Welch, D., Hassan, H., Blilou, I., Immink, R., Heidstra, R., and Scheres, B. (2007). *Arabidopsis* JACKDAW and MAGPIE zinc finger proteins delimit asymmetric cell division and stabilize tissue boundaries by restricting SHORT-ROOT action. Genes Dev. *21*, 2196-2204.

Werner, T., Motyka, V., Laucou, V., Smets, R., Van, O.H., and Schmulling, T. (2003). Cytokinin-deficient transgenic *Arabidopsis* plants show multiple developmental alterations indicating opposite functions of cytokinins in the regulation of shoot and root meristem activity. Plant Cell *15*, 2532-2550.

Whitford, R., Fernandez, A., De, G.R., Ortega, E., and Hilson, P. (2008). Plant CLE peptides from two distinct functional classes synergistically induce division of vascular cells. Proc. Natl. Acad. Sci. U. S. A *105*, 18625-18630.

Wildwater, M., Campilho, A., Perez-Perez, J.M., Heidstra, R., Blilou, I., Korthout, H., Chatterjee, J., Mariconti, L., Gruissem, W., and Scheres, B. (2005). The RETINOBLASTOMA-RELATED gene regulates stem cell maintenance in *Arabidopsis* roots. Cell *123*, 1337-1349.

Willemsen, V., Bauch, M., Bennett, T., Campilho, A., Wolkenfelt, H., Xu, J., Haseloff, J., and Scheres, B. (2008). The NAC domain transcription factors FEZ and SOMBRERO control the orientation of cell division plane in *Arabidopsis* root stem cells. Dev. Cell *15*, 913-922.

Willemsen, V., Wolkenfelt, H., de Vrieze G., Weisbeek, P., and Scheres, B. (1998). The HOBBIT gene is required for formation of the root meristem in the *Arabidopsis* embryo. Development *125*, 521-531.

Yanai, O., Shani, E., Dolezal, K., Tarkowski, P., Sablowski, R., Sandberg, G., Samach, A., and Ori, N. (2005). *Arabidopsis* KNOXI proteins activate cytokinin biosynthesis. Curr. Biol. *15*, 1566-1571.

Chapter 5

Probing the roles of LRR RLK genes in *Arabidopsis thaliana* roots using a custom T-DNA insertion set

Colette A. ten Hove[1], Zoltán Bochdanovits[2], Vera M. A. Jansweijer[1], Fenne G. Koning[1], Lidija Berke[3], Gabino F. Sanchez-Perez[3], Ben Scheres[1] and Renze Heidstra[1]

[1]Faculty of Science, Department of Biology, section Molecular Genetics, Utrecht University, Padualaan 8, 3584 CH Utrecht, the Netherlands. [2]Department of Clinical Genetics, section Medical Genomics, VU University Medical Center, Van der Boechorststraat 7, 1081 BT Amsterdam, the Netherlands. [3]Faculty of Science, Department of Biology, section Theoretical Biology and Bioinformatics, Utrecht University, Padualaan 8, 3584 CH Utrecht, the Netherlands.

Summary

Leucine-rich repeat receptor-like protein kinases (LRR RLKs) represent the largest group of *Arabidopsis* RLKs with approximately 235 members. A minority of these LRR RLKs have been assigned to diverse roles in development, pathogen resistance and hormone perception. Using a reverse genetics approach, a collection of homozygous T-DNA insertion lines for 69 root expressed LRR RLKs was screened for root developmental defects and altered response after exposure to environmental, hormonal/chemical and abiotic stress. The obtained data demonstrate that LRR RLKs play a role in a wide variety of signal transduction pathways related to hormone and abiotic stress responses. The described collection of T-DNA insertion mutants provides a valuable tool for future research into the function of LRR RLK genes.

Introduction

Multicellular organisms sense and respond to both external and internal signals in an intricate and accurate way for survival and coordinate development. A multi-step signal transduction set up, involving receptor protein kinases using phosphorylation status to transduce external messages into the cell, creates the needed complexity for sophisticated response regulation (Wang et al., 2007).

The receptor-like protein kinases (RLKs) are the largest class of *Arabidopsis* protein kinases forming a monophyletic group that contains both transmembrane and cytoplasmic protein kinases (Shiu and Bleecker, 2001a; Shiu and Bleecker, 2001b; Shiu and Bleecker, 2003). The *Arabidopsis* genome contains over 600 RLK genes representing about 2.5% of the protein encoding genes. RLKs can function as homo and heterodimers, adding to their signaling, sensing and regulatory potential, indicating that *Arabidopsis* is able to perceive a wide range of signals (Johnson and Ingram, 2005). The best studied RLKs are those containing extracellular leucine-rich repeats (LRRs). LRRs are tandem repeats of approximately 24 amino acids with conserved leucines. The group of LRR RLKs is the largest RLK class with over 200 members, divided over 13 subfamilies (LRR I to XIII), classified according to the organization of LRRs in the extracellular domain (Shiu and Bleecker, 2001a; Shiu and Bleecker, 2003).

Over the years an increasing number of RLKs have been assigned functions in development, pathogen resistance and hormone perception (Dievart and Clark, 2004; Morillo and Tax, 2006). In addition, many RLKs show a transcriptional response upon hormone treatment (Chae et al., 2009). Two of the best characterized LRR RLKs in *Arabidopsis* are CLV1 and BRI1 (Rieu and Laux, 2009; Aker and de Vries, 2008). The CLV pathway regulates stem cell proliferation and differentiation in the shoot apical meristem (SAM). CLV2 encodes a LRR receptor-like protein required for the stability of CLV1 that is the receptor for CLV3, a small secreted CLE family peptide ligand (Ogawa et al., 2008). Mutations in any of these three *CLV* genes cause an ectopic accumulation of stem cells and a progressive enlargement of the shoot meristem. Downstream of CLV1 signaling is the homeobox transcription factor WUSCHEL (WUS) that forms a negative feedback loop with CLV3 to maintain meristem size (Sablowski, 2007). Brassinosteroid (BRs) signaling through the BRI1 receptor regulates plant growth and development through a complex signal transduction pathway. Binding of BRs to BRI1, releases its negative regulator BKI1, thereby increasing the affinity for the BAK1/SERK3 co-receptor, and allowing downstream signaling to the phosphorylation sensitive BES and BZR1 transcription factors (Vert et al., 2005; Aker and de Vries, 2008).

Roots form from stereotyped embryonic divisions and harbor a clearly discernible stem cell set. The radial organization of the *Arabidopsis* root is maintained by

asymmetric cell divisions of different stem cells and their daughters that are located in the root meristem (ten Hove and Heidstra, 2008). These stem cells surround a small group of cells, the quiescent center (QC), required for their maintenance. The current hypothesis is that the angiosperm root meristem has evolved from the SAM (Stahl et al., 2009). In addition, roots respond sensitively to plant growth factors and to environmental signaling (Wolters and Jurgens, 2009; Iyer-Pascuzzi et al., 2009). Key regulatory themes in the shoot have been found to be significant in the development and regulation of the root, involving phytohormones, transcription factors as well as peptide ligands and their receptors. Several observations suggest that a signaling pathway involving CLV1-like LRR RLKs may function in root stem cell maintenance: (1) the similarity between the two apical meristems (Scheres, 2007); (2) the fact that overexpression or application of A-class CLE peptides causes differentiation of shoot and root meristems (Ito et al., 2006; Kinoshita et al., 2007; Whitford et al., 2008); and (3) the fact that WUS and its family member WOX5 can substitute for each other in stem cell maintenance (Sarkar et al., 2007).

To study possible conservation of LRR RLK function in shoot and root meristem maintenance, a collection of homozygous T-DNA insertion lines for root expressed LRR RLKs was generated and investigated for root developmental phenotypes. In addition, these lines were screened for altered response to a series of hormone/chemical and abiotic stress treatments. Despite the absence of new developmental phenotypes under normal growth conditions we implicate several previously characterized as well as uncharacterized LRR RLKs in hormone and abiotic stress responses.

Results

A homozygous T-DNA insertion mutant collection for root expressed LRR RLKs

Starting from the assumption that a conserved CLV-like pathway for *Arabidopsis* root meristem maintenance exists, we investigated LRR RLK function in root development by taking a reverse genetics approach. We first analyzed the expression patterns in the different tissues of the root meristem of all LRR RLKs from subfamilies II, III, IV, VII, VIII-2, X, XI and XIII using the *in silico* expression database of the *Arabidopsis* root (The *Arabidopsis* Expression Database; www.arexdb.org) (Birnbaum et al., 2003; Brady et al., 2007), We also included 6 kinases that belong to the same monophyletic group as the LRR RLKs but originate from different classes (L-lectin, SD-1, URK1) that were identified as putative targets of root expressed transcription factors (RH, unpublished data). 87 RLKs of mostly unknown function (Table 1) were expressed in different tissues of the root meristem (Figure 1). Comparison with the

GENEVESTIGATOR database indicated that all kinases were also expressed in other tissues (https://www.genevestigator.com/gv/index.jsp, data not shown).

We collected putative T-DNA insertion lines for all root expressed RLKs (see experimental procedures), which were subsequently tested by PCR based genotyping and built a collection of 134 homozygous T-DNA lines representing 69 RLK genes, harboring insertions in: (1) exons (98 lines); (2) introns (10 lines); (3) within 500 nucleotides upstream of the open reading frame (15 lines); and (4) between 500 and 1000 nucleotides upstream of the open reading frame (11 lines) (Table 1). For 18 RLK genes we failed to generate homozygous T-DNA insertion lines and these genes were excluded from our study. Together this collection makes up around 30% of the LRR RLKs present in the *Arabidopsis* genome.

Developmental phenotype analysis of LRR RLK T-DNA insertion mutants

To identify LRR RLKs involved in root growth and development we phenotypically analyzed 4 to 8-day-old roots of the homozygous T-DNA insertion mutants using both confocal microscopy and nomarski optics. We tested the integrity of the stem cell niche based on morphology and absence of starch accumulation in columella stem cells. Two lines appeared to have a root developmental defect. *rlk902* showed a reduced root length and meristem size and was further characterized (Chapter 6). The SALK_009453c line, homozygous for a T-DNA insertion in *At2g31880,* segregated in a recessive manner for a short root phenotype. This suggests that a mutation unlinked to the T-DNA is responsible for the observed phenotype. When compared to wild type plants grown under long day conditions for 4-8 weeks no obvious above ground defects were observed apart from previously reported phenotypes for a number of mutants in these genes (e.g. *erecta*). Together, these results suggest that the LRR RLKs analyzed are functionally redundant for developmental pathways or function only under specific stimuli and/or in other than root tissues.

All tested LRR RLK T-DNA insertion mutants are susceptible to CLE peptide treatment

Overexpression and exogenous application of CLV3 and other A-class CLE peptides leads to general loss of meristematic activity, suggesting that these peptides act in controlling shoot and root meristem size, whereas B-class CLE peptides (CLE41-CLE44) suppress the differentiation of xylem cells from stem cell-like procambial cells and promote cell division (Ito et al., 2006; Kinoshita et al., 2007; Whitford et al., 2008). In the SAM, the CLE peptide CLV3 is the ligand for the CLV1 receptor (Ogawa et al., 2008). To identify putative receptors involved in the perception of CLE peptides in roots, we treated the LRR RLK mutants with synthetic CLV3 and/or CLE19 peptides. Compromised receptors should not be able to transduce any signal

Table 1. List of the examined LRR RLK genes and corresponding T-DNA insertion lines.

Nr	AGI code	Family	Gene name	Function	T-DNA lines/ gene	T-DNA line	Location	References
1	At4g33430	LRR II	BAK1 / SERK3	perception of BR, innate immunity	2	N534523	Intron	Nam and Li, (2002); Li et al., (2002); Chinchilla et al., (2007); Heese et al., (2007)
						N616202	Exon	
2	At1g25320	LRR III			2	N610111	Exon	
						N653321/ SALK_082100C	Exon	
3	At1g48480	LRR III	RKL1		3	N599094	Exon	Ohtake et al., (2000); Tarutani et al., (2004)
						N874554/ SAIL_525_D09	Exon	
						N876722/ SAIL_772_B09	Exon	
4	At1g60630	LRR III			0			
5	At1g67510	LRR III			1	N640207	Exon	
6	At1g68400	LRR III			1	N872562/ SAIL_256_E01	300-UTR5	
7	At2g01210	LRR III			2	N521338	Exon	
						N661769/ SALK_021338C	Exon	
8	At2g15300	LRR III			1	N584900	1000-Promotor	
9	At2g23300	LRR III			1	N601079	Exon	
10	At2g26730	LRR III			0			
11	At2g27060	LRR III			1	N586912	Exon	
12	At2g36570	LRR III			1	N634974	Exon	
13	At2g42290	LRR III			1	N617410	1000-Promotor	
14	At3g02880	LRR III			2	N501905	1000-Promotor	
						N519840	Exon	
15	At3g08680	LRR III			1	N606115	300-UTR5	
16	At3g17840	LRR III	RLK902		2	GABI_114_B09	300-UTR5	Tarutani et al., (2004)
						rlk902	Intron	
17	At3g24660	LRR III	TMKL1		0			Valon et al., (1993)
18	At3g50230	LRR III			1	N872131/ SAIL_209_C11	300-UTR5	
19	At3g51740	LRR III	IMK2		1	N529864	Exon	Fujita et al., (2003)
20	At3g56100	LRR III	MRLK / IMK3	phosphorylates and binds AGL24	1	N524031	Exon	Fujita et al., (2003)
21	At3g57830	LRR III			1	N558587	Exon	

22	At4g23740	LRR III			1	N505132	Exon	
23	At4g31250	LRR III			0			
24	At4g34220	LRR III			0			
25	At4g37250	LRR III			1	N563572	Exon	
26	At5g07620	LRR III			2	N572205	300-UTR5	
						N644635	Exon	
27	At5g10020	LRR III			0			
28	At5g16590	LRR III			1	N553366	1000-Promotor	
29	At5g43020	LRR III			2	N513455	300-UTR5	
						N535437	Exon	
30	At5g53320	LRR III			1	N556616	Exon	
31	At5g58300	LRR III			2	N347264/ GABI_822B12	Exon	
						N347265/ GABI_822B12	Exon	
32	At5g67200	LRR III			1	N592099	Exon	
33	At5g67280	LRR III			2	N580358	Exon	
						N620462	1000-Promoter	
34	At2g45340	LRR IV			2	N611584	Exon	
						N659297	300-UTR5	
35	At1g75640	LRR VII			1	N601029/ N800023	Exon	
36	At2g24230	LRR VII			1	N659661/ SALK_010569C	1000-Promotor	
37	At3g28040	LRR VII			4	N553567/ N800014	Exon	
						N553567	Exon	
						N593475/ N800022	Exon	
						N521579	300-UTR5	
38	At3g56370	LRR VII	IRK		1	N538787	Exon	Kanamoto et al., (2002); Hattan et al., (2004)
39	At4g36180	LRR VII			2	N542323/ N800009	Exon	
						N564666/ N800016	Exon	
40	At5g01890	LRR VII			2	N518730/ N800005	Exon	
						N555351	Exon	
41	At5g45800	LRR VII	MEE62	calmodulin binding	3	N551073/ N800013	Exon	Charpenteau et al., (2004)
						N608935/ N800025	Exon	
						N633510	Exon	
42	At5g58150	LRR VII			1	SALK_093781C	1000-Promotor	

43	At1g53440	LRR VIII-2			4	N557812	300-UTR5	
						N630548	Exon	
						N663996/ SALK_030548C	Exon	
						N648231	Intron	
44	At1g27190	LRR X			3	N616632/ N800027	Exon	
						N632078	Exon	
						N661081/ SALK_110440C	Exon	
45	At1g74360	LRR X			0			
46	At2g02220	LRR X	PSKR1	cellular longevity and growth	4	N508585	Exon	Matsubayashi et al., (2006);
						N508585/ N800002	Exon	Matsubayashi et al., (2006)
						N571659	1000-Promotor	
						N662917/ SALK_071659C	1000-Promotor	
47	At3g13380	LRR X	BRL3	perception of BR, leaf patterning	2	N506024	Exon	Cano-Delgado et al., (2004)
						N506024/ N800036	Exon	
48	At2g01950	LRR X	BRL2 / VH1	leaf patterning	4	N516024/ N800004	Exon	Clay and Nelson, (2002)
						N570890	300-UTR5	
						N642625	Exon	
						SALK_142625C	Exon	
49	At3g28450	LRR X			0			
50	At5g42440	LRR X			0			
51	At5g48380	LRR X	BIR1	innate immunity	0			Gao et al., (2009)
52	At5g53890	LRR X			3	N524464/ N859716	Exon	
						N524464/ N800006	Exon	
						N640876	Exon	
53	At1g08590	LRR XI			1	N655622/ SALK_074344C	Exon	
54	At5g61480	LRR XI			1	N800037	Exon	
55	At1g09970	LRR XI			2	N594492	Exon	
						SALK_120595c	Exon	
56	At1g17750	LRR XI			2	N536564/ N800008	Exon	
						N598161	Exon	
57	At1g28440	LRR XI	HSL1		2	N608127	Exon	Stenvik et al., (2008b)

						N654434/ SALK_141756C	Intron	
58	At1g34110	LRR XI			2	N500143/ N800032	Intron	
						N558918	Exon	
59	At1g72180	LRR XI			3	N500022/ N800031	1000-Promotor	
						N514533	Exon	
						N581193	300-UTR5	
60	At1g73080	LRR XI	PEPR1	innate immunity	4	N514538	Exon	Yamaguchi et al., (2006)
						N514538/ N800003	Exon	
						N559281/ N800015	Exon	
						N560002	300-UTR5	
61	At2g31880	LRR XI	SOBIR	innate immunity	2	N550715	Exon	Gao et al., (2009)
						N661434/ SALK_009453C	Exon	
62	At2g33170	LRR XI			7	N554914	1000-Promotor	
						N569849/ N800019	Exon	
						N615856/ N800026	Exon	
						N615856	Exon	
						N659440/ SALK_069849C	Exon	
						N659493/ SALK_092719C	Exon	
						N859736/ SALK_092719	Exon	
63	At3g24240	LRR XI	RCH2		1	N520659	Exon	Casamitjana-Martínez (2003)
64	At3g49670	LRR XI	BAM2	organ, meristem, gametophyte, ovule and vascular development	0			DeYoung et al., (2006, 2008); Hord et al., (2006)
66	At4g20270	LRR XI	BAM3		2	N544433/ N800012	Exon	DeYoung et al., (2006, 2008); Hord et al., (2006)
						bam3-2	Exon	
65	At4g20140	LRR XI	GSO1	embryo development	1	N543282	Exon	Tsuwamoto et al., (2008)
67	At4g28650	LRR XI			2	N536232/ N800045	Exon	
						N614354	Exon	

68	At5g25930	LRR XI			0			
69	At5g44700	LRR XI	GSO2	embryo development	0			Tsuwamoto et al., (2008)
70	At5g48940	LRR XI	RCH1		3	N504583/ N800034	Intron	Casamitjana-Martínez (2003)
						N538309/ N800048	Exon	
						N597109/ N800047	Exon	
71	At5g49660	LRR XI			0			
72	At5g56040	LRR XI			2	N537932/ N800047	Exon	
						N537932	Exon	
73	At5g63930	LRR XI			1	N874087/ SAIL_429_B07	Exon	
74	At5g65700	LRR XI	BAM1	meristem, gametophyte, ovule and vascular development	2	N607016	300-UTR5	DeYoung et al., (2006, 2008); Hord et al., (2006)
						bam1-1	Exon	
75	At5g65710	LRR XI	HSL2	floral organ abscission	2	N530520/ N800042	Exon	Stenvik et al., (2008a,b); Cho et al., (2008)
						N557117/ N800051	Exon	
76	At1g31420	LRR XIII	FEI1	cell wall function	0			Xu et al., (2008)
77	At2g26330	LRR XIII	ER	meristem, organ, ovule, anther, stomatal development, pathogen resistance	4	N544110/ N800010	Intron	Torii et al., (1996); Gross-Hardt and Laux.,(2003); Shpak et al., (2004, 2005); Pillitteri et al., (2007); Hara (2007); Hord et al., (2008)
						N566455/ N800017	Intron	
						N566455	Intron	
						er-105	Exon	
78	At2g35620	LRR XIII	FEI2	cell wall function	1	N544226/ N800011	Exon	Xu et al., (2008)
79	At5g07180	LRR XIII	ERL2	organ, ovule, anther, stomatal development	6	N507643/ N800001	Exon	Shpak et al., (2004, 2005); Pillitteri et al., (2007); Hara (2007); Hord et al., (2008)
						N526292	Exon	
						N619164/ N800028	Intron	
						N630647/ N800030	Intron	

						N661394	Exon	
						erl2-1	Exon	
80	At5g62230	LRR XIII	ERL1	organ, ovule, anther, stomatal development	3	N581669/ N800021	Exon	Shpak et al., (2004, 2005); Pillitteri et al., (2007); Hara (2007); Hord et al., (2008)
						N584012	300-UTR5	
						erl1-2	Exon	
81	At5g62710	LRR XIII	AIK3		1	N585175	Exon	
82	At3g19300	URK I			1	N638829	Exon	
83	At4g21400	DUF26			0			
84	At4g03230	SD-1			1	N589055	Exon	
85	At5g13290	N. A.			0			
86	At3g53380	L-Lectin			0			
87	At3g55550	L-Lectin			1	N559967	300-UTR5	

upon ligand binding and mutant plant meristems should be similar to untreated wild type meristems. Only the N585175 line, homozygous for a T-DNA insertion in *AIK3,* displayed resistance to both CLV3 and CLE19 peptide treatment, albeit in a Mendelian fashion (~25% resistance, corresponding to a recessive phenotype). PCR analysis confirmed that the T-DNA insertion in *AIK3* did not co-segregate with the observed CLE peptide resistance, indicating the presence of an additional mutation. The results indicate that none of the tested RLKs are involved in CLE perception.

Analysis of LRR RLK T-DNA insertion mutants for conditional phenotypes

In addition to developmental phenotyping, we undertook a broad-spectrum panel of environmental assays on the T-DNA insertion lines to test the involvement of individual LRR RLKs in the response to these stimuli (Table 2). We produced dose response curves for conditions not yet published using the online *Arabidopsis* Gantlet Project database (http://thale.biol.wwu.edu/index.html). Quantifiable traits as root length and germination were used and threshold doses were established to test for sensitivity and saturation doses for insensitivity. No consistent differential responsiveness was observed in comparison to wild type plants for treatments with ACC, ABA, MeJa, EBL, low NaCl, sucrose, low and high temperature or gravitropism (data not shown).

LRR RLK mutants affected in auxin response

Hormonal signaling plays a critical role in almost every aspect of plant development, from embryogenesis to senescence. Although the molecular details of hormone

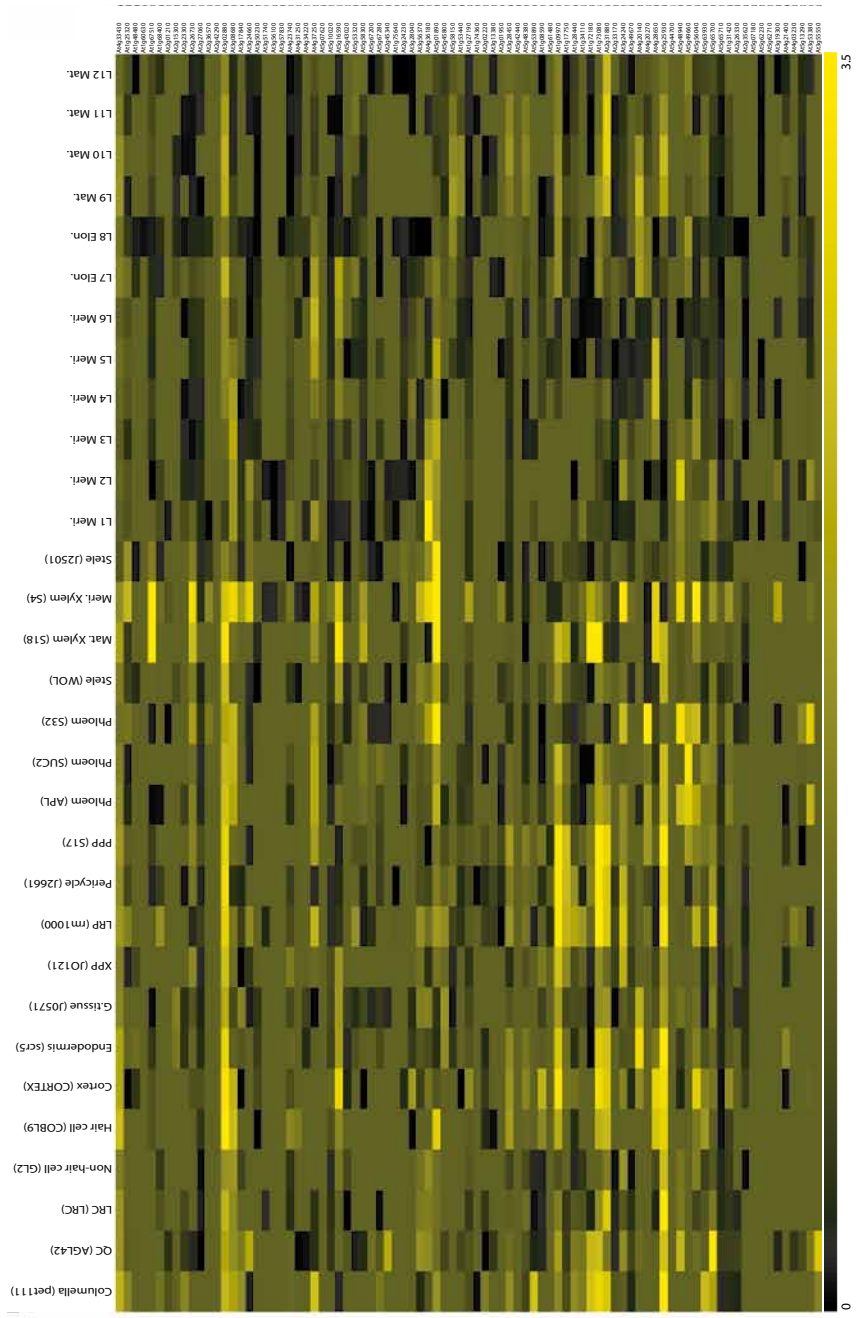

Figure 1. LRR RLK root expression profiles.

Heat map of the expression patterns of the 87 LRR RLKs in the root based on several root markers and longitudinal sections. The expression indices for each marker/section were obtained from (Brady et al., 2007) and were visualized in MultiExperiment Viewer (MeV) v4.5.0 (Saeed et al., 2003). Colors indicate lowered (black) or increased (yellow) transcript accumulation relative to the respective controls within a 0 to +3.5 range.

Table 2. Conditional phenotype assays applied to LRR RLK mutants.
See experimental procedures for details on stress conditions and assays.

Condition	Concentration	Assay
Hormone sensitivity/resistance		
ACC (1-aminocyclopropane-1-carboxylic acid)	0 µM, 0,5 µM and 10 µM	vertical, dark, triple response assay
ABA (abscisic acid) sensitivity	0,3 µM	vertical, light, germination assay
ABA resistance	3 µM	vertical, light, germination assay
MeJa (methyl jasmonate)	1 µM	vertical, light, root length assay
EBL (epi-brassinolide)	0,1 µM	vertical, light, root length assay
NPA (1-naphthylphthalamic acid)	5 µM	vertical, light, root length assay
IAA (indole-3-acetic acid)	0,2 µM	vertical, light, root length assay
6-BAP (6-benzylaminopurine)	0,1 µM	vertical, light, root length assay
Peptide sensitivity		
CLE19p	10 µM	vertical, light, root length assay
CLV3p	5 µM	vertical, light, root length assay
Abiotic stress		
NaCl: salt stress tolerance	200 mM	vertical, light, germination assay
NaCl: salt stress hypersensitivity	50 mM	vertical, light, root length assay
Mannitol: osmotic stress	400 mM	vertical, light, germination assay
Sucrose: metabolites	4,5% w/v	vertical, light, germination assay
Others		
Gravitropism (90° rotation)		vertical, light, root length assay
Dark		vertical, dark, germination assay
Temperature (15°C and 30°C)		vertical, light, general growth assay

action remain largely unknown, receptors for the major hormones have now been identified (Bishopp et al., 2006; Wolters and Jurgens, 2009). The plant hormone auxin plays a key role in many aspects of plant growth and development. Auxin transport is facilitated by auxin influx and efflux carriers, integral plasma membrane proteins that transport auxin molecules into and out of the cell, respectively (Petrášek and Friml, 2009). The nuclear localized receptors AFB1, AFB2, AFB3 and TIR1, which are the F-box subunits of the E3-ubiquitin ligase complexes SCF-TIR1 and SCF-AFB bind auxin. This results in the degradation of the Aux/IAA transcriptional repressor proteins by the 26S proteasome and subsequent ARF dependent activation of transcription (Dharmasiri et al., 2005). However, not all auxin-regulated processes

can be easily attributed to this type of signaling. Another putative auxin receptor is ABP1 that binds auxin and is implicated in a set of early auxin responses such as rapid activation of ion fluxes at the plasma membrane (Badescu and Napier, 2006; Tromas et al., 2009).

To identify LRR RLKs involved in auxin signaling we screened seedling root growth response to the natural auxin IAA and the phytotropin polar auxin transport inhibitor NPA. We tested the T-DNA insertion mutants using concentrations that slightly inhibit root growth in wild type seedlings, i.e. 0,2 µM IAA and 5 µM NPA. For the IAA treatment, 19 T-DNA insertion lines corresponding to 16 RLK genes showed a consistent enhanced root length compared to wild type, indicative of increased resistance to IAA (Table 3). In contrast, 2 T-DNA insertion lines corresponding to *BAK1/SERK3* and *IRK* genes showed a consistent enhanced root growth inhibition, indicative of increased sensitivity to IAA. 23 T-DNA insertion lines corresponding to 22 RLK genes were found to be resistant to NPA treatment (Table 3). Reversely, 3 T-DNA insertion lines, corresponding to *BAK1/SERK3* and *PSKR1* genes, were more sensitive to NPA.

Resistance to the phytohormone auxin and polar auxin transport inhibitors frequently coincides (Fujita and Syono, 1997). These observations are confirmed in our study as we observed an overlap between IAA and NPA resistance observed for T-DNA insertions in 7 genes: *At1g67510*, *At5g43020*, *At1g53440*, *At4g03230*, *PEPR1*, *BAM1* and *ERL2*, whereas the T-DNA insertion line N534523 (*BAK1/SERK3*) showed increased sensitivity for both IAA and NPA. Together, our results suggest that a number of LRR RLKs are involved in auxin signaling and/or response.

LRR RLK mutants affected in cytokinin response

Cytokinins, generally acting antagonistically to auxin (Bishopp et al., 2006), have been shown to play a key role in the regulation of root growth and meristem size (Dello Ioio et al., 2007). Plants respond to cytokinins via a two-component signaling pathway involving the transmembrane histidine kinases *AHK2*, *AHK3* and *AHK4/CRE1* (Dello Ioio et al., 2008). These receptors transfer the signal via phosphorelay to the nucleus, thereby activating negative (type-A) and positive (type-B) regulators (ARRs) of the cytokinin response. Type B ARRs act as transcription factors activating the transcription of cytokinin primary response genes, including type-A ARRs, thereby forming a negative feedback loop to control cytokinin responses (Bishopp et al., 2006).

To explore whether LRR RLKs are involved in cytokinin signaling and/or response we screened seedling root growth response to the synthetic cytokinin 6-benzylaminopurine (6-BAP). We tested the T-DNA insertion mutants using concentrations that slightly inhibit root growth in wild type seedlings, i.e. 0,1 µM 6-BAP. One

Table 3. Results of conditional tests.
(R) resistant; (S) sensitive; (-) similar to wild type. See experimental procedures for details on stress conditions and assays.

AGI code	Gene name	T-DNA line	Location	0,2 µM IAA	5 µM NPA	0,1 µM 6-BAP	Dark	200 mM NaCl	400 mM mannitol
At4g33430	BAK1/ SERK3	N534523	Intron	S	S	-	-	-	-
		N616202	Exon	-	S	S	-	-	-
At1g25320		N610111	Exon	-	-	-	-	-	R
		N653321/ SALK_082100C	Exon	-	R	-	-	-	-
At1g48480	RKL1	N599094	Exon	-	-	-	-	-	-
		N874554/ SAIL_525_D09	Exon	-	-	-	-	-	-
		N876722/ SAIL_772_B09	Exon	-	-	-	-	-	-
At1g67510		N640207	Exon	R	R	-	-	-	-
At1g68400		N872562/ SAIL_256_E01	300-UTR5	-	-	-	-	-	-
At2g01210		N521338	Exon	-	-	-	-	-	-
		N661769/ SALK_021338C	Exon	-	R	-	-	-	-
At2g15300		N584900	1000-Promotor	-	-	-	-	-	-
At2g23300		N601079	Exon	-	R	-	-	-	-
At2g27060		N586912	Exon	-	R	-	-	R	-
At2g36570		N634974	Exon	-	-	-	-	R	R
At2g42290		N617410	1000-Promotor	R	-	-	-	R	-
At3g02880		N501905	1000-Promotor	-	-	-	-	-	-
		N519840	Exon	R	-	-	-	-	R
At3g08680		N606115	300-UTR5	-	-	-	-	-	R
At3g17840	RLK902	GABI_114_B09	300-UTR5	-	R	-	-	-	-
		rlk902	Intron	-	-	-	-	-	-
At3g50230		N872131/ SAIL_209_C11	300-UTR5	-	-	-	-	-	-
At3g51740	IMK2	N529864	Exon	-	R	-	-	-	R
At3g56100	MRLK/ IMK3	N524031	Exon	-	-	-	-	R	R
At3g57830		N558587	Exon	-	R	-	-	-	-
At4g23740		N505132	Exon	-	-	-	-	-	R
At4g37250		N563572	Exon	-	-	-	-	-	-
At5g07620		N572205	300-UTR5	-	-	-	-	R	R
		N644635	Exon	-	-	-	-	R	-
At5g16590		N553366	1000-Promotor	-	-	-	-	-	-
At5g43020		N513455	300-UTR5	-	-	-	-	R	R

		N535437	Exon	R	R	-	-	-	-
At5g53320		N556616	Exon	R	-	-	-	R	-
At5g58300		N347264/ GABI_822B12	Exon	-	-	-	S	-	-
		N347265/ GABI_822B12	Exon	-	-	-	-	-	-
At5g67200		N592099	Exon	-	-	-	-	R	R
At5g67280		N580358	Exon	-	R	-	-	-	-
		N620462	1000-Promoter	-	-	-	-	-	-
At2g45340		N611584	Exon	-	R	-	-	-	-
		N659297	300-UTR5	-	-	-	-	-	-
At1g75640		N601029/ N800023	Exon	-	-	-	-	-	-
At2g24230		N659661/ SALK_010569C	1000-Promotor	-	-	-	-	-	R
At3g28040		N553567/ N800014	Exon	-	-	-	S	-	-
		N553567	Exon	-	-	-	-	-	-
		N593475/ N800022	Exon	-	-	-	-	-	-
		N521579	300-UTR5	-	-	-	S	-	R
At3g56370	IRK	N538787	Exon	S	-	-	-	-	R
At4g36180		N542323/ N800009	Exon	-	-	-	-	-	-
		N564666/ N800016	Exon	-	-	-	-	-	-
At5g01890		N518730/ N800005	Exon	-	-	-	-	-	R
		N555351	Exon	-	-	-	S	-	-
At5g45800	MEE62	N551073/ N800013	Exon	R	-	-	-	-	-
		N608935/ N800025	Exon	-	R	-	-	-	-
		N633510	Exon	-	-	-	-	-	R
At5g58150		SALK_093781C	1000-Promotor	-	-	-	-	R	R
At1g53440		N557812	300-UTR5	R	-	-	-	-	-
		N630548	Exon	R	-	-	-	-	-
		N663996/ SALK_030548C	Exon	R	R	-	-	-	-
		N648231	Intron	R	-	-	-	R	-
At1g27190		N616632/ N800027	Exon	-	-	-	-	-	-
		N632078	Exon	-	-	-	-	-	R
		N661081/ SALK_110440C	Exon	-	-	-	-	-	-
At2g02220	PSKR1	N508585	Exon	-	-	-	-	-	-

		N508585/ N800002	Exon	-	S	-	-	-	-
		N571659	1000-Promotor	-	-	-	-	-	-
		N662917/ SALK_071659C	1000-Promotor	-	-	-	-	R	-
At3g13380	BRL3	N506024	Exon	-	-	-	S	R	-
		N506024/ N800036	Exon	-	-	-	-	R	R
At2g01950	BRL2/ VH1	N516024/ N800004	Exon	-	-	-	-	-	R
		N570890	300-UTR5	R	-	-	-	R	R
		N642625	Exon	-	-	-	-	R	-
		SALK_142625C	Exon	-	-	-	-	-	-
At5g53890		N524464/ N859716	Exon	-	-	-	-	-	R
		N524464/ N800006	Exon	-	-	-	-	-	-
		N640876	Exon	-	-	-	-	-	-
At1g08590		N655622/ SALK_074344C	Exon	-	-	-	-	-	-
At5g61480		N800037	Exon	-	-	-	-	-	-
At1g09970		N594492	Exon	-	-	-	-	-	-
		SALK_120595c	Exon	-	-	-	-	-	-
At1g17750		N536564/ N800008	Exon	-	-	-	-	-	-
		N598161	Exon	-	-	-	S	R	-
At1g28440	HSL1	N608127	Exon	R	-	-	-	-	R
		N654434/ SALK_141756C	Intron	-	R	-	-	-	-
At1g34110		N500143/ N800032	Intron	-	-	-	-	-	-
		N558918	Exon	-	-	-	-	-	-
At1g72180		N500022/ N800031	1000-Promotor	-	-	-	-	-	R
		N514533	Exon	-	R	-	-	-	R
		N581193	300-UTR5	-	-	-	-	R	-
At1g73080	PEPR1	N514538	Exon	-	-	-	S	-	-
		N514538/ N800003	Exon	-	-	-	-	-	R
		N559281/ N800015	Exon	-	-	-	-	-	R
		N560002	300-UTR5	R	R	-	-	-	R
At2g31880	SOBIR	N550715	Exon	R	-	-	-	-	-
		N661434/ SALK_009453C	Exon	-	-	-	-	R	-
At2g33170		N554914	1000-Promotor	-	-	-	-	-	-

		N569849/ N800019	Exon	-	-	-	-	-	-
		N615856/ N800026	Exon	R	-	-	-	-	R
		N615856	Exon	-	-	-	-	-	-
		N659440/ SALK_069849C	Exon	-	-	-	-	-	-
		N659493/ SALK_092719C	Exon	-	-	R	S	-	-
		N859736/ SALK_092719	Exon	-	-	R	-	-	-
At3g24240	RCH2	N520659	Exon	-	-	-	-	R	-
At4g20140	GSO1	N543282	Exon	-	-	-	-	R	R
At4g20270	BAM3	N544433/ N800012	Exon	-	-	-	S	-	-
		bam3-2	Exon	-	-	-	-	-	-
At4g28650		N536232/ N800045	Exon	-	-	-	-	-	-
		N614354	Exon	-	-	-	-	-	-
At5g48940	RCH1	N504583/ N800034	Intron	-	-	-	S	-	-
		N538309/ N800048	Exon	-	R	-	-	-	-
		N597109/ N800047	Exon	-	-	-	-	-	-
At5g56040		N537932/ N800047	Exon	-	-	-	-	-	-
		N537932	Exon	-	-	-	-	-	-
At5g63930		N874087/ SAIL_429_B07	Exon	-	-	-	-	-	-
At5g65700	BAM1	N607016	300-UTR5	R	R	-	-	R	R
		bam1-1	Exon	-	-	-	-	-	R
At5g65710	HSL2	N530520/ N800042	Exon	R	-	-	-	-	-
		N557117/ N800051	Exon	-	-	-	-	-	-
At2g26330	ER	N544110/ N800010	Intron	-	-	-	-	-	-
		N566455/ N800017	Intron	-	R	-	-	R	-
		N566455	Intron	-	-	-	-	-	-
		er-105	Exon	-	-	-	-	-	R
At2g35620	FEI2	N544226/ N800011	Exon	-	-	-	-	-	-
At5g07180	ERL2	N507643/ N800001	Exon	R	R	-	-	-	-
		N526292	Exon	-	-	-	-	-	-

		N619164/ N800028	Intron	-	-	-	-	-	-
		N630647/ N800030	Intron	-	-	-	S	-	-
		N661394	Exon	-	R	-	-	-	-
		erl2-1	Exon	-	-	-	-	-	-
At5g62230	ERL1	N581669/ N800021	Exon	-	-	-	-	-	-
		N584012	300-UTR5	-	R	-	-	-	-
		erl1-2	Exon	-	-	-	-	R	R
At5g62710	AIK3	N585175	Exon	-	-	-	-	-	-
At3g19300		N638829	Exon	-	-	-	-	-	R
At4g03230		N589055	Exon	R	R	-	-	R	R
At3g55550		N559967	300-UTR5	-	-	-	-	R	R

homozygous T-DNA insertion line showed a consistent increased (*At2g33170*) and one showed a consistent reduced (*BAK1/SERK3*) root length compared to wild type (Table 3). These results suggest that *At2g33170* and *BAK1/SERK3* mediate cytokinin control on root growth.

Identification of LRR RLKs involved in light signaling and/or response

Light is one of the key external factors controlling seed germination and dormancy (Penfield and King, 2009). Perception and response to this stimulus ensures that seedling emergence and growth occur at the most advantageous time. The effect of light on seed germination is mainly conveyed by photoreceptors called phytochromes. Additionally, different hormones favor (GA, ethylene, BR) or repress (ABA) germination.

The LRR RLK T-DNA insertion mutants were screened for light requirement by analyzing their germination potential (measured by radicle emergence) in the absence of light. We scored mutants as light sensitive when they showed germination levels of lower than 25% at 25°C in the dark. High germination levels were observed for all T-DNA insertion lines and co-plated wild type controls in the light. 11 T-DNA insertion lines showed dark germination levels lower than 25% (Table 3), implicating involvement of the corresponding 10 RLK genes in light signaling and/or response.

LRR RLK mutants affected in salt and osmotic stress tolerance

Plants vary greatly in their tolerance to abiotic stress such as salt (Xiong and Zhu, 2002). Whereas halophytes can complete their life cycle under saline conditions, glycophytes are more sensitive to salt stress, although their tolerance varies widely between species and even among varieties. *Arabidopsis thaliana* is a glycophytic,

salt intolerant plant. It is assumed that salt is perceived by specific receptors of various types, including RLKs, two component histidine kinases and G-protein-associated receptors (Xiong and Zhu, 2001). Recently, the LRR RLK encoding *SRLK* was implicated in the regulation of the adaptation of *Medicago truncatula* roots to salt stress (de Lorenzo et al., 2009).

To determine whether any of the *Arabidopsis* LRR RLKs play a role in the perception of abiotic stress, we have tested the T-DNA insertion lines for their ability to germinate compared to co-plated wild type control seeds on medium containing 200 mM NaCl or 400 mM mannitol. A 1.8 fold increase in germination percentage to wild type was chosen to be called NaCl or mannitol resistant (see experimental procedures). 26 T-DNA insertion lines displayed enhanced NaCl tolerance corresponding to 23 RLK genes (Table 3). For mannitol treatment, 36 T-DNA lines corresponding to 31 RLK genes showed enhanced resistance to mannitol (Table 3).

High salinity causes both hyperionic and hyperosmotic stress effects, whereas mannitol induces hyperosmotic stress (Hasegawa et al., 2000). To assess whether the altered response to NaCl treatment was due to altered tolerance towards ionic and/or osmotic stress effects we analyzed the overlap in T-DNA insertion lines with altered NaCl and mannitol responses. 13 T-DNA insertion lines for 13 genes: *At3g55550*, *At2g36570*, *At5g07620*, *At5g43020*, *At5g67200*, *At5g58150*, *At4g03230*, *BAM1*, *BRL2/VH1*, *BRL3*, *ERL1*, *GSO1* and *MRLK1/IMK3* were tolerant to both ionic effects and osmotic pressure, suggesting that these mutants are primarily osmotolerant. Together, our results suggest that these kinases play a role in plant salt and/or osmotic stress tolerance.

Bioinformatic analyses to uncover trends in altered conditional responses

We next investigated whether there was a possible link between the obtained functional data and LRR RLK phylogeny. A neighborhood joining tree of the 69 tested LRR RLKs was constructed using the kinase domain with each treatment depicted on the branches for each of the kinases (Figure 2). No patterns emerged that connect LRR RLK phylogeny and mutant response.

We next investigated a possible link between LRR RLK behavior at the transcriptome level with the functional characterization of corresponding mutants. A hierarchical clustering of the 69 studied LRR RLKs was performed based on their behavior in different public microarray experiments using conditional stresses comparable to those described here. We then compared the transcriptomic data with our functional characterization of the mutants and analyzed whether there was an overlap. LRR RLK gene clusters with similar behavior at the transcriptome level upon different stress treatments can be distinguished (Figure 3). However, comparison of

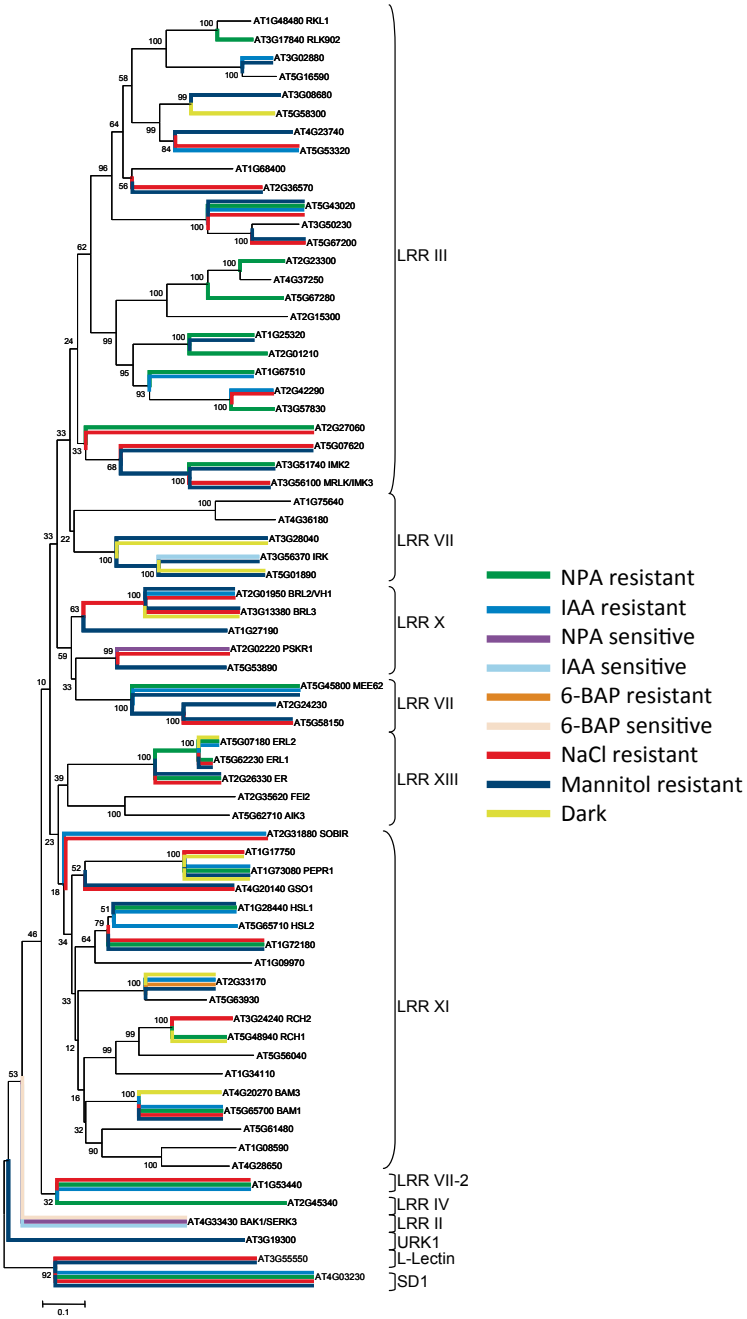

Figure 2. Combination of LRR RLK phylogeny with functional data. Neighborhood joining tree of the 69 LRR RLKs tested. Subfamilies are indicated. Positive and negative response to tested conditions was color coded on the branches for each of the kinases as indicated. The numbers on the base of the branch indicate bootstrap support out of 500 replicates.

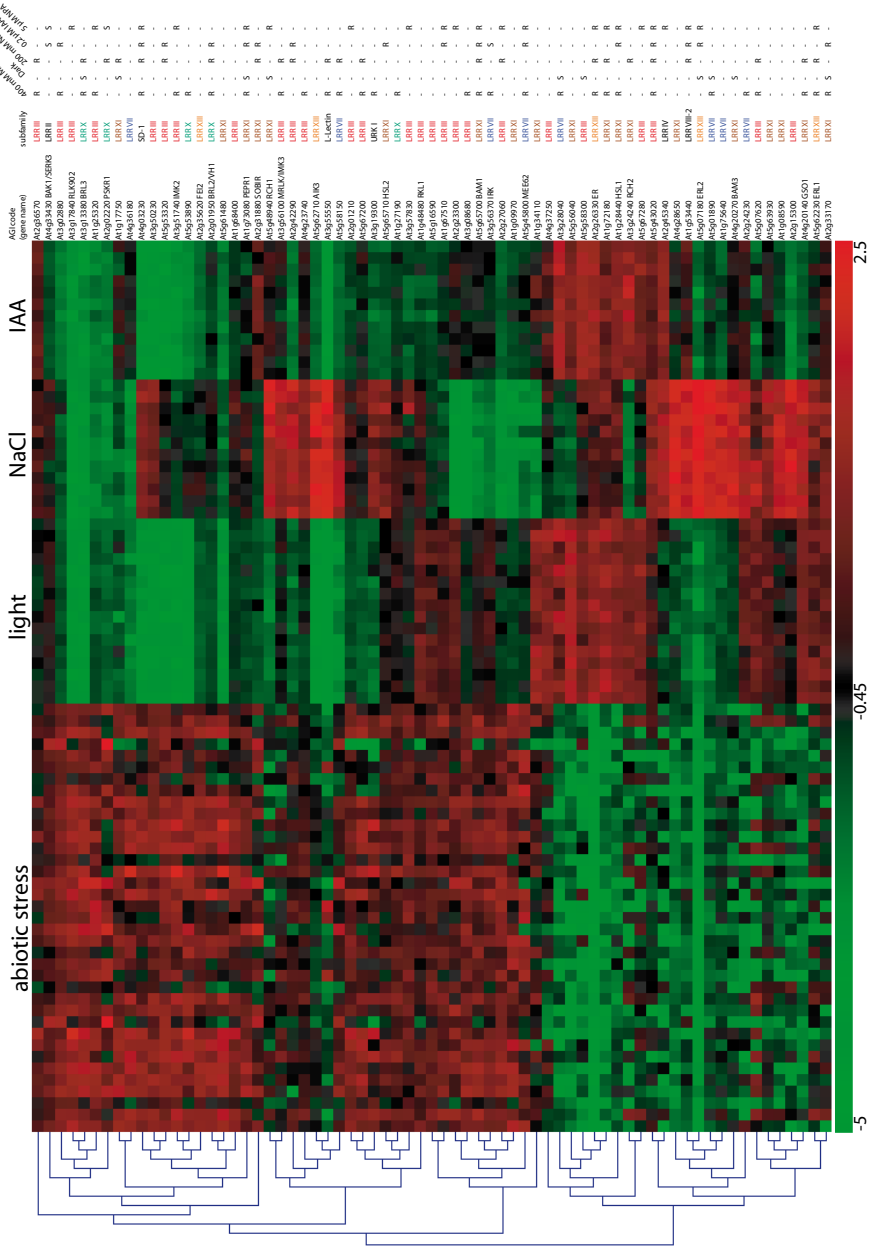

Figure 3. Combination of cluster analysis of the studied LRR RLKs with functional data.
The 69 studied LRR RLKs are clustered based on their behavior during different public microarray experiments upon a range of abiotic stress, light, NaCl and IAA treatment (see experimental procedures). Each column represents the results from one microarray condition. Colors indicate lowered (green) or increased (red) transcript accumulation relative to the respective controls within a -5.5 to +2.5 range. The results of the conditional tests for mannitol, dark, NaCl and IAA (modified from Table 3) are depicted on the right, (R) resistant; (S) sensitive; (-) similar to wild type.

these clustered expression patterns to RLK phylogeny and function in these stress responses did not reveal any significant correlation (Figure 3).

Discussion

Here, we have have undertaken a reverse genetics approach concentrating on root meristem expressed LRR RLKs with two objectives: first, to investigate the function of CLV1 paralogs in root meristem maintenance; and second, to gain a broader understanding of the function of LRR RLKs in root growth in general. We generated a collection of 134 homozygous T-DNA insertion mutants for 69 LRR RLK genes that comprise around 30% of the LRR RLKs present in the *Arabidopsis* genome.

Assuming conservation of the CLV pathway in the root, we expected the kinase involved in root meristem homeostasis to be closely related to CLV1 and/or a member of the LRR RLK class. However, in our screen we did not obtain CLV1 paralogs involved in root development nor in CLE signaling. Recently, different types of receptors putatively involved in CLE signaling were implicated to play a role in regulating root growth. Mutations in CRN/SOL2, a membrane bound receptor kinase lacking an extracellular domain, and the CLV2 receptor-like protein can both prevent CLE induced consumption of the root meristem (Muller et al., 2008; Miwa et al., 2008). Other recent work assigned ACR4, a receptor of the Crinkly4 class, in controlling distal stem cell proliferation in the root meristem (De Smet et al., 2008). CLE40 is the putative ligand of ACR4 and together they regulate *WOX5* expression, thus resembling the activity of the CLV3-CLV1-WUS shoot module (Stahl et al., 2009; Stahl and Simon, 2009). Although these studies demonstrated recruitment of receptors other than the LRR class in controlling root meristem maintenance, they certainly do not exclude that LRR RLKs operate in this process.

The degree of specificity and redundancy among RLKs has been a matter of debate. Lack of identification of biological functions for RLK genes can be explained by functional redundancy that complicates studies employing reverse genetic strategies. Two emerging themes are that receptor kinases are part of a cellular network of regulatory proteins that includes physical interactions with other RLKs, and that multiple receptor kinases are involved in similar or overlapping processes. Double and triple mutants have been found that display phenotypes supporting this hypothesis, e.g. synergistic actions of *ER*, *ERL1* and *ERL2* control organ growth and cell proliferation whereas *BAM1*, redundantly with *BAM2* and *BAM3*, balances cell division and differentiation in the shoot meristem (Shpak et al., 2004c; Deyoung et al., 2006). In addition, receptors can potentially participate in different receptor complexes and this explains why some of these receptors play roles in diverse processes.

ER is the best example as a pleiotropic regulator of developmental, physiological processes as well as a modulator of responses to environmental stimuli (van Zanten et al., 2009). Strategies employing RNA interference to knockdown the expression of several RLKs simultaneously should help in overcoming functional redundancy among RLK genes. *clv1* null alleles show a weak phenotype and all intermediate and strong alleles appeared dominant negative most likely interfering with the signaling function (Dievart et al., 2003). Similar observations have been made for *bak1* and *har1* mutants (Dievart and Clark, 2003). Generating dominant negative mutations for RLKs e.g. by removing their kinase domain could possibly lead to a better understanding of their function.

To gain a broader understanding of the function of LRR RLKs in root growth in general, we screened the T-DNA lines for altered response to environmental, hormonal/chemical and abiotic stress. Of the 69 mutant LRR RLKs tested 16 are involved in response to one type of treatment whereas 36 are involved in response to two or more types of treatment. 24 of the 69 LRR RLKs have been assigned a name of which many have been implicated in various biological programs. Three characterized LRR RLKs mutants were known to respond to the conditions tested in this study, and this was confirmed by us, demonstrating the validity of our screen: the *elg* mutant allele of *BAK1/SERK3* was reported hypersensitive to IAA treatment (Whippo and Hangarter, 2005) and; a T-DNA line for the RLK *IRK* was found to be more sensitive to IAA treatment. Although the function of *IRK* is elusive, its expression is increased by auxin treatment (Kanamoto et al., 2002). Seemingly contrasting our results, the *vh1* mutant was previously reported hypersensitive to low concentrations of the synthetic auxin analog 2,4-dichlorophenoxyacetic acid (2,4-D; 25 and 50 mM), while responding as wild type at higher concentrations (Ceserani et al., 2009). The observed discrepancy may be due to the type of mutation or to the use of different auxin molecules.

In addition, we identified several novel conditional phenotypes linked with mutations in LRR RLK genes. T-DNA lines for *BAK1/SERK3* showed an increased sensitivity for IAA and NPA treatment as well as an increased sensitivity to 6-BAP. These results are in line with the known interdependency of brassinosteroid (BR) and auxin signaling in *Arabidopsis* (Nemhauser et al., 2004). The antagonistic interaction between auxin and cytokinins is known but no relationship has been reported between BRs and cytokinin so far. Our studies provide a link for crosstalk between these three pathways.

In this study, novel phenotypes were found for 52 RLKs. 21 of these concerned RLKs with previously characterized phenotypes but 31 provide functions for hitherto uncharacterized RLKs. We could not detect a clear relationship between conditional phenotypes and phylogeny. This suggests that these transmembrane

receptor kinases, despite a fairly similar domain organization, can readily acquire different functions compared to their closest paralogs during evolution. We showed that there are LRR RLK gene clusters with similar behavior at the transcriptome level upon different stress treatments. However, RLK clusters did not correlate with the functional characterization of the mutants. Similarly, a large scale analysis of the transcriptional response of the 604-member RLK gene family to a range of known environmental and developmental stimuli demonstrated a broad response of these kinases to multiple treatments (Chae et al., 2009). Our observations that many T-DNA insertion lines respond to more than one treatment supports the existence of extensive cross talk and signal integration among different signaling pathways. With respect to hormones, for which receptors are identified, resistance or sensitivity may indicate a function of receptor signaling in secondary signaling events. Our study represents a preliminary view of processes in which the studied kinases may be involved. Additionally, the generated collection of LRR RLK T-DNA insertion mutants can be easily applied for the analysis of other developmental aspects, function in defense and additional stress conditions and thus forms a valuable resource for future investigations into the biological role of LRR RLKs.

Experimental Procedures

Plant materials

The T-DNA Express database of the SALK Institute Genomic Analysis Laboratory (SIGnAL; http://signal.salk.edu/cgi-bin/tdnaexpress) was employed to identify putative T-DNA insertion mutants. We aimed to select T-DNA insertions within the coding region of the gene to enhance the likelihood of successful disruption of gene function. When unavailable, lines were selected with predicted intron or promoter (1000 bp promoter and 500 bp 5'UTR) insertions. Available lines of interest generated by The Salk Institute for Biological Studies (SALK) (Alonso et al., 2003), the German plant genomics research program (GABI) (Rosso et al., 2003), and Syngenta *Arabidopsis* Insertion Library (SAIL) (Sessions et al., 2002) were obtained from the *Arabidopsis* Biological Resource Center (ABRC; http://abrc.osu.edu/), the Nottingham *Arabidopsis* Stock Centre (NASC; http://arabidopsis.info/) or Syngenta. *rlk902* (Tarutani et al., 2004) was kindly donated by Dr. Yoshihito Suzuki (University of Tokyo, Japan), *bam1-1* and *bam3-2* (Deyoung et al., 2006) by Dr. Steven Clark (University of Michigan, USA) and *er-105*, *erl1-2* and *erl2-1* (Shpak et al., 2004b) by Dr. Keiko Torii (University of Washington, USA). All T-DNA mutants used were of Columbia ecotype. The authenticity of T-DNA mutations was verified by PCR. Genomic DNA was isolated from approximately 10 individual plants per T-DNA line.

Table 4. Primers used for PCR based genotyping.

T-DNA	Gene-specific primer pair Forward primer 5′ - 3′	Gene-specific primer pair Reverse primer 5′ - 3′	T-DNA primer 5′ - 3′
N534523	tgacacacgagaacaaccaaaaaga	ataaggtgcttcaaagttgggatgc	gcgtggaccgcttgctgcaact
N616202	atgtgtgtctttgtagtccatgagttttg	tgtctttgtctttgaaatgttattcaactg	gcgtggaccgcttgctgcaact
N610111	tttgactagattgcaaggaactctt	atttcctaagcatacacaaaaacca	gcgtggaccgcttgctgcaact
N653321/ SALK_082100C	tttttcaagctcacaattctttaac	cttcagtgactcgtaacaaaaacg	gcgtggaccgcttgctgcaact
N599094	gtgtcaaatgcgagagtaacagagt	tcttcaagatcaaaaaccttagtcg	gcgtggaccgcttgctgcaact
N874554/ SAIL_525_D09	tttcactccttttacagctctcttc	ttgattgttgagatatcaacagctc	tagcatctgaatttcataaccaatctcgatacac
N876722/ SAIL_772_B09	tcttccatcaactcaagatctcaac	tcttcaagatcaaaaaccttagtcg	tagcatctgaatttcataaccaatctcgatacac
N640207	cgtcgcgttgaataattgagtagga	gcaatcaattacacatgccaccatac	gcgtggaccgcttgctgcaact
N872562/ SAIL_256_E01	aaaaagatttgtcatgaaattaaggg	agtgaggttagtgatgagattgacc	tagcatctgaatttcataaccaatctcgatacac
N521338	gtctctagggtttctctccagtctc	ctttagcagctcctccaggtta	gcgtggaccgcttgctgcaact
N661769/ SALK_021338C	gtctctagggtttctctccagtctc	ctttagcagctcctccaggtta	gcgtggaccgcttgctgcaact
N584900	gagatggtgaaccactgcaagtaatg	tttaaggatgttggactgtaatgggg	gcgtggaccgcttgctgcaact
N601079	ccggtttacggaagatctactattt	ggggatactagctataaccgagcta	gcgtggaccgcttgctgcaact
N586912	atcttgaagaggaagagaaccagag	agtgatgagtctgttttcacagcta	gcgtggaccgcttgctgcaact
N634974	acatttcaagtcttcaactatcagaaaccc	acatctgaaactttggtaatactctggtgg	gcgtggaccgcttgctgcaact
N617410	ttcttgtccatatactatggtttga	ataagcttgagatgaatcagagtgc	gcgtggaccgcttgctgcaact
N501905	catagccatgaagaagaggttaaga	atatatcgacttttcggatatggg	gcgtggaccgcttgctgcaact
N519840	cttccgagcataatcagaatcaatctagg	gaaccctaaaaataaacaaatgcacaaatg	gcgtggaccgcttgctgcaact
N606115	tgcttttgactttagctctagcttc	tctcaaatgttttctctggtaaagg	gcgtggaccgcttgctgcaact
GABI_114_B09	catgtaatcgtgtaacatgtg	ctcgtggcttagactatcttca	atattgaccatcatactcattgc
rlk902	gatatcatgcgactcttcttcacac	gatatcctttcatctgatggtcttac	cagtggtcccaaagatggacc
N872131/ SAIL_209_C11	aaatgaaaatctaacaattgcgatg	ctcggtgagagagtatagaagcttg	tagcatctgaatttcataaccaatctcgatacac
N529864	gcatccataatcacaatttatttcg	aacgagaacatgatccatgagaat	gcgtggaccgcttgctgcaact
N524031	ccacactacaaaaattctccactct	gaaagatcaccaaaagtcaaaaaga	gcgtggaccgcttgctgcaact
N558587	gaggtatttttccggtgagattatt	tcacagagcaacaacacattatttt	gcgtggaccgcttgctgcaact
N505132	atcttcaagaactgctttgtacgtc	ggagttacttgtaatcaagacggat	gcgtggaccgcttgctgcaact
N563572	ccactatcttgttcttcttgcatct	tggagaggaatctcttgtaataacg	gcgtggaccgcttgctgcaact
N572205	tagagtaccatagcttgattttccg	ggagttgtatgtacttgccttcaat	gcgtggaccgcttgctgcaact
N644635	cttacaaggccaagaaatcataaagtcaac	ggaatggtaaattatccaggaagattctaag	gcgtggaccgcttgctgcaact
N553366	cttcccaaaaattttcgatatgagt	cttcttcttacccaaagcttaatcc	gcgtggaccgcttgctgcaact
N513455	aactaactagcttttaagtgtcaaccacca	tattgaaggagaaatcgagagttcttaacc	gcgtggaccgcttgctgcaact
N535437	ctttaccattgttgcttcttcttcttcttc	tcttctatctcactctcttgttctatcgcc	gcgtggaccgcttgctgcaact
N556616	gcagagtcctcgagatcaaccttgt	aacgtctgcatagaagcagagacga	gcgtggaccgcttgctgcaact
N592099	cggtagttacgaagaagaaaggtaa	tgataagtacacaaaaacccttcaca	gcgtggaccgcttgctgcaact
N580358	aaacagtttttgagacttgccgttgactc	gtgaagcaacctctccacctccatc	gcgtggaccgcttgctgcaact

N620462	ttcctattcgtaaattatgctgacg	atcagtctaactctcgtgagtcgtg	gcgtggaccgcttgctgcaact
N611584	gctaaattctcatgcttcaacagtgtcag	caagattcataaattcttcagattctaaaccg	gcgtggaccgcttgctgcaact
N601029/ N800023	atgattgataaagaatgcaagaagg	taatagtttaaagggtcacattccg	gcgtggaccgcttgctgcaact
N553567/ N800014	ctccttgttcatggagttacgtcaaatg	ctttaagctgaacaatcataagctctttgc	gcgtggaccgcttgctgcaact
N553567	ctccttgttcatggagttacgtcaaatg	ctttaagctgaacaatcataagctctttgc	gcgtggaccgcttgctgcaact
N593475/ N800022	ctaggttttgggaacttcctcttac	gaactcgtactaagaaccgaaac	gcgtggaccgcttgctgcaact
N521579	acagaattaccaaacagaaaattcg	atttgacgtaactccatgaacaag	gcgtggaccgcttgctgcaact
N538787	tcattccaagaaagcgaactattac	ttaactgtgttctgtttcatgcttc	gcgtggaccgcttgctgcaact
N542323/ N800009	ggtgagataccagctagtgtaggcaatc	aaaacgacaggagccagagtcaaa	gcgtggaccgcttgctgcaact
N564666/ N800016	gataatctctagtggaccactcgag	tcacagtccttagaggttactacgc	gcgtggaccgcttgctgcaact
N518730/ N800005	gactttatgccatttcaaatttttg	ctcttgatccacgagtttgtttc	gcgtggaccgcttgctgcaact
N555351	ctctgtaccttgccactcaagac	gtttcttcaacaccatccctctct	gcgtggaccgcttgctgcaact
N551073/ N800013	tcaatggtagtgttaaaccgatttc	aaaaacggaaaatattttgttacatta	gcgtggaccgcttgctgcaact
N608935/ N800025	actaaccacagtttttcgttacgtc	atccttgaaagtcagattcatcaac	gcgtggaccgcttgctgcaact
N633510	gtgttcttgatctctccaacaactctctc	atcagatccttgaaagtcagattcatcaac	gcgtggaccgcttgctgcaact
SALK_093781C	acggggcatagaggtgatgatagtt	ttgatcttcgaacagaggaaaaggtc	gcgtggaccgcttgctgcaact
N557812	tcatttaccgcttcttctaccggat	tgtttgttttatttgcgggactttg	gcgtggaccgcttgctgcaact
N630548	acaaacgtaataccaacaagaggtgtttac	aagtctttgtttctctgtgcctgttaaatc	gcgtggaccgcttgctgcaact
N663996/ SALK_030548C	acaaacgtaataccaacaagaggtgtttac	aagtctttgtttctctgtgcctgcctgttaaatc	gcgtggaccgcttgctgcaact
N648231	agattagaaagcagtcgacgaaccc	aactggccaaattgcacatgtattg	gcgtggaccgcttgctgcaact
N616632/ N800027	tgttcttcaaagattcatacacctg	cgttggtttagttatattctggtgg	gcgtggaccgcttgctgcaact
N632078	gtatcacacagtcaatgaccattcttcttc	caatccaatcactatcatccttagacttcc	gcgtggaccgcttgctgcaact
N508585	gcttggaagctcttgatctctctaataacc	cttacatgcgtctcgtaaggactcatcagc	gcgtggaccgcttgctgcaact
N508585/ N800002	gcttggaagctcttgatctctctaataacc	cttacatgcgtctcgtaaggactcatcagc	gcgtggaccgcttgctgcaact
N571659	aatgaagatgaagaagcaagagaga	cgaagcttttatcggaaactaaag	gcgtggaccgcttgctgcaact
N662917/ SALK_071659C	aatgaagatgaagaagcaagagaga	cgaagcttttatcggaaactaaag	gcgtggaccgcttgctgcaact
N506024	actcacgacggtgcttaagaaatca	ttaggtaactggagatacgggtcgg	gcgtggaccgcttgctgcaact
N506024/ N800036	actcacgacggtgcttaagaaatca	ttaggtaactggagatacgggtcgg	gcgtggaccgcttgctgcaact
N516024/ N800004	agtattaatgtagcgacgtttcagc	gagatcttcatgttgttacaagctg	gcgtggaccgcttgctgcaact
N570890	tcaagagaggtgaaagcattgaagg	attctacaacggacaattccttccg	gcgtggaccgcttgctgcaact
N642625	ctttaccggaatgtaagaatggaaacaatc	acatctgaaactttggtaatactctggtgg	gcgtggaccgcttgctgcaact
SALK_142625C	ctttaccggaatgtaagaatggaaacaatc	acatctgaaactttggtaatactctggtgg	gcgtggaccgcttgctgcaact

N524464/ N859716	gattgctcaagttcttgcttaactc	tactgtttattgggattcgattttc	gcgtggaccgcttgctgcaact
N524464/ N800006	gattgctcaagttcttgcttaactc	tactgtttattgggattcgattttc	gcgtggaccgcttgctgcaact
N640876	atcttacaatcatctctacggttcg	tgagcttcaaacttctcatctaaca	gcgtggaccgcttgctgcaact
N594492	tctcctctaaccaaatttcccgatg	aagtttccgaatccggtaggaagtt	gcgtggaccgcttgctgcaact
N536564/ N800008	gtgaacaaaatacgaacgtgttatg	tcaacatatccaacaacaagttgac	gcgtggaccgcttgctgcaact
N598161	caaactcatcgatcgtttcttaaat	actgacaaatagctcaccaagattc	gcgtggaccgcttgctgcaact
N608127	ttataaccggttttccggttcagttcctac	gtttgtaacctttctctggatcacaatctc	gcgtggaccgcttgctgcaact
N558918	tcgcctctctactctccagttccttatatt	tcttctggtattcttcctgttagcttgttc	gcgtggaccgcttgctgcaact
N500022/ N800031	gacttcttctgctttttgttgtttc	cactggaattcccacctacatag	gcgtggaccgcttgctgcaact
N514533	attgcaagagccaagaacaagagtg	gctcgacacggttgatatatctgaaaa	gcgtggaccgcttgctgcaact
N581193	tttaaacctccaatactctcaggaa	gcacccattcttcttacaaaatct	gcgtggaccgcttgctgcaact
N514538	aatcgttggtatacagagagaccaaacatc	caaaagattgagactttcaggtaatgaacc	gcgtggaccgcttgctgcaact
N514538/ N800003	aatcgttggtatacagagagaccaaacatc	caaaagattgagactttcaggtaatgaacc	gcgtggaccgcttgctgcaact
N559281/ N800015	agagttgacagcttcttaagctcag	atttgtcatacaatgaattcgaagg	gcgtggaccgcttgctgcaact
N560002	cattcttattgccgcttagtacatt	ccaaatgcttcagaagagagagtag	gcgtggaccgcttgctgcaact
N550715	caagcaataagaggatcagaaaaac	ggatcatccaaagtacagtaacagg	gcgtggaccgcttgctgcaact
N554914	ccaaagcaaaaaccttacttatccttctc	tgaccatcactattcaaactctctgaagtc	gcgtggaccgcttgctgcaact
N615856/ N800026	agcttgtggcttatactaataacttgaccg	gttttgatccaactcaatagcagaaagg	gcgtggaccgcttgctgcaact
N615856	agcttgtggcttatactaataacttgaccg	gttttgatccaactcaatagcagaaagg	gcgtggaccgcttgctgcaact
N520659	tgttctcaggatcgatacctacttc	ccattaggcatgtaatcatacatca	gcgtggaccgcttgctgcaact
N543282	acccctctctcctctctctctagatctctc	aacacagtgagatcagagcagtttcctaac	gcgtggaccgcttgctgcaact
N544433/ N800012	gcaatctcactatgtttctgtgtctgattc	cttcaaaacaacttttttgactggaga	gcgtggaccgcttgctgcaact
N536232/ N800045	actcaaatggcaatgttgagaag	attctaacacgaactagtgattggc	gcgtggaccgcttgctgcaact
N614354	cgttcttggtaatgaactaaggagtcaagt	taatgcttcctatctctcttggaattgttc	gcgtggaccgcttgctgcaact
N504583/ N800034	atatctcactaagcatagcagccac	tcaaggcaaataatattctgattgg	gcgtggaccgcttgctgcaact
N538309/ N800048	aaatatccggttctttacctgtttc	ggttgagtgaaatgagatgacctag	gcgtggaccgcttgctgcaact
N597109/ N800047	tcttgatctcagcagtaataacatctctgg	ccaaactcccatttgacatataatcataca	gcgtggaccgcttgctgcaact
N537932	aagttaagttcttgacgatgtcgtc	gagtctctttctcaatgtcaagagc	gcgtggaccgcttgctgcaact
N874087/ SAIL_429_B07	aggaccagttaagctgttgtatgag	gcttgagcttctttatctttttgag	tagcatctgaatttcataaccaatctcgatacac
N607016	tatgacctcttgtatcttttgaggg	gtgacaccaatccatgtacagaag	gcgtggaccgcttgctgcaact
N530520/ N800042	ctaggttttgggaacttcctct	gaactcgtactaagaaccg	gcgtggaccgcttgctgcaact

N557117/ N800051	ccaaacaaacacttaagaaagaaactgtca	gaatcggactaggatcaaaactgatgtaag	gcgtggaccgcttgctgcaact
N566455/ N800017	tgggtttctcttctgcttgagcttag	caacatgaacacacttcatcaaataaaacc	gcgtggaccgcttgctgcaact
N566455	tgggtttctcttctgcttgagcttag	caacatgaacacacttcatcaaataaaacc	gcgtggaccgcttgctgcaact
N544226/ N800011	ggtagagcgactgagaaaaccgatg	atgggaactttgctcagatggattt	gcgtggaccgcttgctgcaact
N507643/ N800001	ccttctagtatttggaccaaacaag	gttcttggaaccattggatatattg	gcgtggaccgcttgctgcaact
N526292	cagtgactgttcctgagagagcaaaa	gccaaaatcaggcaaagattacaca	gcgtggaccgcttgctgcaact
N619164/ N800028	taatgttagatggaatcagccctac	cttttactctcaacctcagatttcg	gcgtggaccgcttgctgcaact
N630647/ N800030	cgaaatctgaggttgagagtaaaag	ataacgttagcctcaatgttgtctc	gcgtggaccgcttgctgcaact
N661394	ccttctagtatttggaccaaacaag	gttcttggaaccattggatatattg	gcgtggaccgcttgctgcaact
N581669/ N800021	atgtttttgtttccagagatctgtc	aactgcaaggaaaatcatacatagg	gcgtggaccgcttgctgcaact
N584012	ttcagtttctctacatcgcttccca	acacagacgattttagattcaaactttcaga	gcgtggaccgcttgctgcaact
N585175	gcaaaagagaaatcaagaatcagaa	ataatatctcctagcattgggaagc	gcgtggaccgcttgctgcaact
N638829	accatcttctgtggattagggacca	ctgaatttccgaaaaccaaacgaat	gcgtggaccgcttgctgcaact
N589055	ctcttctccagcaacacaatagcca	agacacggttactggtggaactgaa	gcgtggaccgcttgctgcaact
N559967	tgatcaacccccgataacctctagt	gagttagcgaggaaatagccagcag	gcgtggaccgcttgctgcaact

Primers (Table 4) were generated using the T-DNA primer design tool (http://signal.salk.edu/tdnaprimers.2.html) and used in two separate PCR reactions. Reaction one contained a T-DNA specific and gene-specific primer to check for the presence of an insertion whereas reaction two contained two gene-specific primers spanning the putative insertion site to check for nondisrupted alleles. Plants were considered homozygous for the T-DNA insertion when only PCR reaction one yielded a product, which was subsequently confirmed in their progeny.

Plant growth conditions and microscopy

All seeds (wild type control and T-DNA insertion mutants) used in the assays were obtained from plants harvested at similar time points. Seeds were gas-sterilized in a desiccator for 2 hours with 100 ml of bleach (4% NaClO) mixed with 3 ml of HCl in a beaker or were surface-sterilized in 20% bleach for 20 minutes. Sterilized seeds were imbibed in sterile water containing 0.1% agarose for 3-4 days at 4°C in the dark. For phenotypic analysis of root growth, seeds were germinated on half strength Murashige and Skoog (MS) salt mixture, 1% sucrose and 0.5 g/L 2-(N-morpholino) ethanesulfonic acid (MES), pH5.8, in 0.8% agar (standard medium). Plates were incubated in a near vertical position at 22°C with a cycle of 16 h light/8 h dark. Roots were analyzed after 4-8 days using Nomarski optics and confocal microscopy.

Starch granules were visualized as described (Willemsen et al., 1998). For confocal microscopy, roots were mounted in propidium iodide (PI; 20 µg/mL in distilled water). Seedlings were transferred to soil for further phenotypic analysis of general growth and development. Soil grown plants were cultured in a growth chamber at 22°C, 70% relative humidity and a cycle of 16 h light/8 h dark. For temperature assays, seedlings were grown on plates in a near vertical position and a cycle of 8 h light/16 h dark and analyzed after 7 days (30°C) or 14 days (15°C), respectively. Root gravitropism was studied by growing seedlings on plates at near vertical position that were rotated 90° after 3 days of growth. After 1-2 days, the bending angle of the root was measured.

Conditional phenotypes assays

20 seeds per T-DNA insertion line and 20 wild type control seeds were plated for each experiment. To minimize plate position effects, seeds were plated in alternate groups, i.e. one row 10 wild type followed by 10 mutant seeds, and a second row of 10 mutant followed by 10 wild type seeds. For vertical, light germination assays, seed germination was determined by recording the presence of a radicle. For vertical, light, root length and general root growth assays, uniformity of germination was analyzed after 1-2 days and only seedlings that germinated at the same time were taken along for qualitative root length or general growth measurements. To test whether LRR RLK genes are involved in responsiveness to stress, seeds were directly sown on standard medium supplemented with hormones ACC, ABA, MeJa, EBL, 6-BAP or with CLE peptides, respectively, at concentrations listed in Table 3. For NPA treatment, seedlings were transferred three days after germination to standard medium supplemented with NPA. For abiotic stress experiments, seeds were directly sown on standard medium amended with 200 mM NaCl or 400 mM mannitol, respectively. The ratio of mutant germination percentage over wild type germination percentage exhibited a bimodal distribution. Based on this distribution, a 1.8 fold increase in germination percentage relative to wild type was chosen as threshold to be called NaCl or mannitol resistant. This threshold identifies only the T-DNA insertion lines that comprise the distinct upper part of the distribution as resistant. Susceptibility to salt stress was tested by sowing seeds on standard medium and transferring seedlings to standard medium supplemented with 50 mM NaCl after 3 days, followed by a 180° rotation. Root growth was measured after 1-2 days. To test for altered responses to sucrose, seeds were sown on standard medium lacking sucrose and transferred after 3 days to standard medium supplemented with 3.5% sucrose.

Kinase phylogeny and coexpression analysis

From the 69 LRR RLKs from *Arabidopsis thaliana* analyzed in this study 352 positions were aligned automatically corresponding to the kinase domain using the program ClustalW implemented in the Bioedit Software (Hall, 1999). The phylogenetic tree was reconstructed using a neighbor-joining method in the MEGA package v4.0 (Tamura et al., 2007) with 500 bootstrap resampling. In order to detect coregulation between the kinases, we selected several microarray experiments showing differential expression for at least a subset of the 69 LRR RLKs analyzed. Processed data for microarray experiments were obtained from ArrayExpress (http://www.ebi.ac.uk/microarray-as/ae/) i.e. E-GEOD-3709 for abiotic stress, E-GEOD-5617 for light, E-GEOD-7643 for NaCl and E-GEOD-18975 for IAA. Genes were clustered based on the expression profiles to find coexpressed gene clusters. Hierarchical clustering of microarray data was performed in MultiExperiment Viewer (MeV) v4.5.0 (Saeed et al., 2003), using Pearson correlation and Average Linkage Clustering algorithm.

Acknowledgements

We are grateful to ABRC, NASC, Syngenta, Dr. Yoshihito Suzuki, Dr. Steven Clark and Dr. Keiko Torii for providing plant material and to Hiroo Fukuda (University of Tokyo, Japan) for providing CLV3 peptide. This research was funded by the Centre for BioSystems Genomics (CBSG), which is part of the Netherlands Genomics Initiative/ Netherlands Organization for Scientific Research (NGI/NWO).

References

Aker, J. and de Vries, S.C. (2008). Plasma membrane receptor complexes. Plant Physiol *147*, 1560-1564.

Alonso, J.M., Stepanova, A.N., Leisse, T.J., Kim, C.J., Chen, H., Shinn, P., Stevenson, D.K., Zimmerman, J., Barajas, P., Cheuk, R., Gadrinab, C., Heller, C., Jeske, A., Koesema, E., Meyers, C.C., Parker, H., Prednis, L., Ansari, Y., Choy, N., Deen, H., Geralt, M., Hazari, N., Hom, E., Karnes, M., Mulholland, C., Ndubaku, R., Schmidt, I., Guzman, P., guilar-Henonin, L., Schmid, M., Weigel, D., Carter, D.E., Marchand, T., Risseeuw, E., Brogden, D., Zeko, A., Crosby, W.L., Berry, C.C., and Ecker, J.R. (2003). Genome-wide insertional mutagenesis of *Arabidopsis thaliana*. Science *301*, 653-657.

Badescu, G.O. and Napier, R.M. (2006). Receptors for auxin: will it all end in TIRs? Trends in Plant Science *11*, 217-223.

Birnbaum, K., Shasha, D.E., Wang, J.Y., Jung, J.W., Lambert, G.M., Galbraith, D.W., and Benfey, P.N. (2003). A gene expression map of the *Arabidopsis* root. Science *302*, 1956-1960.

Bishopp, A., Mahonen, A.P., and Helariutta, Y. (2006). Signs of change: hormone receptors that regulate plant development. Development *133*, 1857-1869.

Brady, S.M., Orlando, D.A., Lee, J.Y., Wang, J.Y., Koch, J., Dinneny, J.R., Mace, D., Ohler, U., and Benfey, P.N. (2007). A high-resolution root spatiotemporal map reveals dominant expression patterns. Science *318*, 801-806.

Cano-Delgado, A., Yin, Y., Yu, C., Vafeados, D., Mora-Garcia, S., Cheng, J.C., Nam, K.H., Li, J., and Chory, J. (2004). BRL1 and BRL3 are novel brassinosteroid receptors that function in vascular differentiation in *Arabidopsis*. Development *131*, 5341-5351.

Casamitjana-Martinez, E. Receptor kinase signaling in *Arabidopsis* root meristem maintenance. *3*, 49-70. 2003. Thesis/Dissertation.

Ceserani, T., Trofka, A., Gandotra, N., and Nelson, T. (2009). VH1/BRL2 receptor-like kinase interacts with vascular-specific adaptor proteins VIT and VIK to influence leaf venation. Plant J. *57*, 1000-1014.

Chae, L., Sudat, S., Dudoit, S., Zhu, T., and Luan, S. (2009). Diverse transcriptional programs associated with environmental stress and hormones in the *Arabidopsis* receptor-like kinase gene family. Mol. Plant *2*, 84-107.

Charpenteau, M., Jaworski, K., Ramirez, B.C., Tretyn, A., Ranjeva, R., and Ranty, B. (2004). A receptor-like kinase from *Arabidopsis thaliana* is a calmodulin-binding protein. Biochem. J. *379*, 841-848.

Chinchilla, D., Zipfel, C., Robatzek, S., Kemmerling, B., Nurnberger, T., Jones, J.D., Felix, G., and Boller, T. (2007). A flagellin-induced complex of the receptor FLS2 and BAK1 initiates plant defence. Nature *448*, 497-500.

Cho, S.K., Larue, C.T., Chevalier, D., Wang, H., Jinn, T.L., Zhang, S., and Walker, J.C. (2008). Regulation of floral organ abscission in *Arabidopsis thaliana*. Proc. Natl. Acad. Sci. U. S. A *105*, 15629-15634.

Clay, N.K. and Nelson, T. (2002). VH1, a provascular cell-specific receptor kinase that influences leaf cell patterns in *Arabidopsis*. Plant Cell *14*, 2707-2722.

de Lorenzo, L., Merchan, F., Laporte, P., Thompson, R., Clarke, J., Sousa, C., and Crespi, M. (2009). A novel plant leucine-rich repeat receptor kinase regulates the response of Medicago truncatula roots to salt stress. Plant Cell *21*, 668-680.

De Smet, I., Vassileva, V., De, R.B., Levesque, M.P., Grunewald, W., Van, D.D., Van, N.G., Naudts, M., Van, I.G., De, C.R., Wang, J.Y., Meuli, N., Vanneste, S., Friml, J., Hilson, P., Jurgens, G., Ingram, G.C., Inze, D., Benfey, P.N., and Beeckman, T. (2008). Receptor-like kinase ACR4 restricts formative cell divisions in the *Arabidopsis* root. Science *322*, 594-597.

Dello Ioio, R., Linhares, F.S., and Sabatini, S. (2008). Emerging role of cytokinin as a regulator of cellular differentiation. Curr. Opin. Plant Biol. *11*, 23-27.

Dello Ioio, R., Linhares, F.S., Scacchi, E., Casamitjana-Martinez, E., Heidstra, R., Costantino, P., and Sabatini, S. (2007). Cytokinins determine *Arabidopsis* root-meristem size by controlling cell differentiation. Curr. Biol. *17*, 678-682.

Deyoung, B.J., Bickle, K.L., Schrage, K.J., Muskett, P., Patel, K., and Clark, S.E. (2006). The CLAVATA1-related BAM1, BAM2 and BAM3 receptor kinase-like proteins are required for meristem function in *Arabidopsis*. Plant J. *45*, 1-16.

Deyoung, B.J. and Clark, S.E. (2008). BAM receptors regulate stem cell specification and organ development through complex interactions with CLAVATA signaling. Genetics *180*, 895-904.

Dharmasiri, N., Dharmasiri, S., Weijers, D., Lechner, E., Yamada, M., Hobbie, L., Ehrismann, J.S., Jurgens, G., and Estelle, M. (2005). Plant development is regulated by a family of auxin receptor F box proteins. Dev. Cell *9*, 109-119.

Dievart, A. and Clark, S.E. (2004). LRR-containing receptors regulating plant development and defense. Development *131*, 251-261.

Dievart, A. and Clark, S.E. (2003). Using mutant alleles to determine the structure and function of leucine-rich repeat receptor-like kinases. Current Opinion in Plant Biology *6*, 507-516.

Dievart, A., Dalal, M., Tax, F.E., Lacey, A.D., Huttly, A., Li, J., and Clark, S.E. (2003). CLAVATA1 Dominant-Negative Alleles Reveal Functional Overlap between Multiple Receptor Kinases That Regulate Meristem and Organ Development. Plant Cell *15*, 1198-1211.

Fujita, H. and Syono, K. (1997). PIS1, a negative regulator of the action of auxin transport inhibitors in *Arabidopsis thaliana*. Plant J. *12*, 583-595.

Fujita, H., Takemura, M., Tani, E., Nemoto, K., Yokota, A., and Kohchi, T. (2003). An *Arabidopsis* MADS-box protein, AGL24, is specifically bound to and phosphorylated by meristematic receptor-like kinase (MRLK). Plant Cell Physiol *44*, 735-742.

Gao, M., Wang, X., Wang, D., Xu, F., Ding, X., Zhang, Z., Bi, D., Cheng, Y.T., Chen, S., Li, X., and Zhang, Y. (2009). Regulation of cell death and innate immunity by two receptor-like kinases in *Arabidopsis*. Cell Host. Microbe *6*, 34-44.

Gross-Hardt, R. and Laux, T. (2003). Stem cell regulation in the shoot meristem. J. Cell Sci. *116*, 1659-1666.

Hall, T.A. (1999). BioEdit: a user-friendly biological sequence alignment editor and analysis program for Windows 95/98/NT. Nucleic Acids Symp. Ser. *41*, 95-98.

Hara, K., Kajita, R., Torii, K.U., Bergmann, D.C., and Kakimoto, T. (2007). The secretory peptide gene EPF1 enforces the stomatal one-cell-spacing rule. Genes Dev. *21*, 1720-1725.

Hasegawa, P.M., Bressan, R.A., Zhu, J.K., and Bohnert, H.J. (2000). PLANT CELLULAR AND MOLECULAR RESPONSES TO HIGH SALINITY. Annual Review of Plant Physiology and Plant Molecular Biology *51*, 463-499.

Hattan, J., Kanamoto, H., Takemura, M., Yokota, A., and Kohchi, T. (2004). Molecular characterization of the cytoplasmic interacting protein of the receptor kinase IRK expressed in the inflorescence and root apices of *Arabidopsis*. Biosci. Biotechnol. Biochem. *68*, 2598-2606.

Heese, A., Hann, D.R., Gimenez-Ibanez, S., Jones, A.M., He, K., Li, J., Schroeder, J.I., Peck, S.C., and Rathjen, J.P. (2007). The receptor-like kinase SERK3/BAK1 is a central regulator of innate immunity in plants. Proc. Natl. Acad. Sci. U. S. A *104*, 12217-12222.

Hord, C.L., Chen, C., Deyoung, B.J., Clark, S.E., and Ma, H. (2006). The BAM1/BAM2 receptor-like kinases are important regulators of *Arabidopsis* early anther development. Plant Cell *18*, 1667-1680.

Ito, Y., Nakanomyo, I., Motose, H., Iwamoto, K., Sawa, S., Dohmae, N., and Fukuda, H. (2006). Dodeca-CLE peptides as suppressors of plant stem cell differentiation. Science *313*, 842-845.

Iyer-Pascuzzi, A., Simpson, J., Herrera-Estrella, L., and Benfey, P.N. (2009). Functional genomics of root growth and development in *Arabidopsis*. Current Opinion in Plant Biology *12*, 165-171.

Johnson, K.L. and Ingram, G.C. (2005). Sending the right signals: regulating receptor kinase activity. Current Opinion in Plant Biology *8*, 648-656.

Kanamoto, H., Hattan, J., Takemura, M., Yokota, A., and Kohchi, T. (2002). Molecular cloning and characterization of a gene coding for a putative receptor-like protein kinase with a Leucine-rich repeat expressed in inflorescence and root apices from *Arabidopsis*. Plant Biotech *19*, 113-120.

Kinoshita, A., Nakamura, Y., Sasaki, E., Kyozuka, J., Fukuda, H., and Sawa, S. (2007). Gain-of-function phenotypes of chemically synthetic CLAVATA3/ESR-related (CLE) peptides in *Arabidopsis thaliana* and Oryza sativa. Plant Cell Physiol *48*, 1821-1825.

Li, J., Wen, J., Lease, K.A., Doke, J.T., Tax, F.E., and Walker, J.C. (2002). BAK1, an *Arabidopsis* LRR receptor-like protein kinase, interacts with BRI1 and modulates brassinosteroid signaling. Cell *110*, 213-222.

Matsubayashi, Y., Ogawa, M., Kihara, H., Niwa, M., and Sakagami, Y. (2006). Disruption and overexpression of *Arabidopsis* phytosulfokine receptor gene affects cellular longevity and potential for growth. Plant Physiol *142*, 45-53.

Miwa, H., Betsuyaku, S., Iwamoto, K., Kinoshita, A., Fukuda, H., and Sawa, S. (2008). The receptor-like kinase SOL2 mediates CLE signaling in *Arabidopsis*. Plant Cell Physiol *49*, 1752-1757.

Morillo, S.A. and Tax, F.E. (2006). Functional analysis of receptor-like kinases in monocots and dicots. Current Opinion in Plant Biology *9*, 460-469.

Muller, R., Bleckmann, A., and Simon, R. (2008). The receptor kinase CORYNE of *Arabidopsis* transmits the stem cell-limiting signal CLAVATA3 independently of CLAVATA1. Plant Cell *20*, 934-946.

Nam, K.H. and Li, J. (2002). BRI1/BAK1, a receptor kinase pair mediating brassinosteroid signaling. Cell *110*, 203-212.

Nemhauser, J.L., Mockler, T.C., and Chory, J. (2004). Interdependency of Brassinosteroid and Auxin Signaling in *Arabidopsis*. PLoS Biol *2*, e258.

Ogawa, M., Shinohara, H., Sakagami, Y., and Matsubayashi, Y. (2008). *Arabidopsis* CLV3 peptide directly binds CLV1 ectodomain. Science *319*, 294.

Ohtake, Y., Takahashi, T., and Komeda, Y. (2000). Salicylic acid induces the expression of a number of receptor-like kinase genes in *Arabidopsis thaliana*. Plant Cell Physiol *41*, 1038-1044.

Penfield, S. and King, J. (2009). Towards a systems biology approach to understanding seed dormancy and germination. Proceedings of the Royal Society B: Biological Sciences *276*, 3561-3569.

Petrášek, J. and Friml, J. (2009). Auxin transport routes in plant development. Development *136*, 2675-2688.

Pillitteri, L.J., Bemis, S.M., Shpak, E.D., and Torii, K.U. (2007). Haploinsufficiency after successive loss of signaling reveals a role for ERECTA-family genes in *Arabidopsis* ovule development. Development *134*, 3099-3109.

Rieu, I. and Laux, T. (2009). Signaling pathways maintaining stem cells at the plant shoot apex. Seminars in Cell & Developmental Biology *20*, 1083-1088.

Rosso, M.G., Li, Y., Strizhov, N., Reiss, B., Dekker, K., and Weisshaar, B. (2003). An *Arabidopsis thaliana* T-DNA mutagenized population (GABI-Kat) for flanking sequence tag-based reverse genetics. Plant Mol Biol *53*, 247-259.

Sablowski, R. (2007). Flowering and determinacy in *Arabidopsis*. J. Exp. Bot. *58*, 899-907.

Saeed, A.I., Sharov, V., White, J., Li, J., Liang, W., Bhagabati, N., Braisted, J., Klapa, M., Currier, T., Thiagarajan, M., Sturn, A., Snuffin, M., Rezantsev, A., Popov, D., Ryltsov, A., Kostukovich, E., Borisovsky, I., Liu, Z., Vinsavich, A., Trush, V., and Quackenbush, J. (2003). TM4: a free, open-source system for microarray data management and analysis. Biotechniques *34*, 374-378.

Sarkar, A.K., Luijten, M., Miyashima, S., Lenhard, M., Hashimoto, T., Nakajima, K., Scheres, B., Heidstra, R., and Laux, T. (2007). Conserved factors regulate signalling in *Arabidopsis thaliana* shoot and root stem cell organizers. Nature *446*, 811-814.

Scheres, B. (2007). Stem-cell niches: nursery rhymes across kingdoms. Nat. Rev. Mol. Cell Biol. *8*, 345-354.

Sessions, A., Burke, E., Presting, G., Aux, G., McElver, J., Patton, D., Dietrich, B., Ho, P., Bacwaden, J., Ko, C., Clarke, J.D., Cotton, D., Bullis, D., Snell, J., Miguel, T., Hutchison, D., Kimmerly, B., Mitzel, T., Katagiri, F., Glazebrook, J., Law, M., and Goff, S.A. (2002). A high-throughput *Arabidopsis* reverse genetics system. Plant Cell *14*, 2985-2994.

Shiu, S.H. and Bleecker, A.B. (2001b). Plant receptor-like kinase gene family: diversity, function, and signaling. Sci. STKE. *2001*, RE22.

Shiu, S.H. and Bleecker, A.B. (2001a). Receptor-like kinases from *Arabidopsis* form a monophyletic gene family related to animal receptor kinases. Proc. Natl. Acad. Sci. U. S. A *98*, 10763-10768.

Shiu, S.H. and Bleecker, A.B. (2003). Expansion of the receptor-like kinase/Pelle gene family and receptor-like proteins in *Arabidopsis*. Plant Physiol *132*, 530-543.

Shpak, E.D., Berthiaume, C.T., Hill, E.J., and Torii, K.U. (2004a). Synergistic interaction of three ERECTA-family receptor-like kinases controls *Arabidopsis* organ growth and flower development by promoting cell proliferation. Development *131*, 1491-1501.

Shpak, E.D., McAbee, J.M., Pillitteri, L.J., and Torii, K.U. (2005). Stomatal patterning and differentiation by synergistic interactions of receptor kinases. Science *309*, 290-293.

Shpak, E.D., Berthiaume, C.T., Hill, E.J., and Torii, K.U. (2004b). Synergistic interaction of three ERECTA-family receptor-like kinases controls *Arabidopsis* organ growth and flower development by promoting cell proliferation. Development *131*, 1491-1501.

Shpak, E.D., Berthiaume, C.T., Hill, E.J., and Torii, K.U. (2004c). Synergistic interaction of three ERECTA-family receptor-like kinases controls *Arabidopsis* organ growth and flower development by promoting cell proliferation. Development *131*, 1491-1501.

Stahl, Y. and Simon, R. (2009). Is the *Arabidopsis* root niche protected by sequestration of the CLE40 signal by its putative receptor ACR4? Plant Signal. Behav. *4*, 634-635.

Stahl, Y., Wink, R.H., Ingram, G.C., and Simon, R. (2009). A signaling module controlling the stem cell niche in *Arabidopsis* root meristems. Curr. Biol. *19*, 909-914.

Stenvik, G.E., Butenko, M.A., and Aalen, R.B. (2008a). Identification of a putative ligand-receptor pair controlling cell separation in plants. Plant Signal. Behav. *3*, 1109-1110.

Stenvik, G.E., Tandstad, N.M., Guo, Y., Shi, C.L., Kristiansen, W., Holmgren, A., Clark, S.E., Aalen, R.B., and Butenko, M.A. (2008b). The EPIP peptide of INFLORESCENCE DEFICIENT IN ABSCISSION is sufficient to induce abscission in *arabidopsis* through the receptor-like kinases HAESA and HAESA-LIKE2. Plant Cell *20*, 1805-1817.

Tamura, K., Dudley, J., Nei, M., and Kumar, S. (2007). MEGA4: Molecular Evolutionary Genetics Analysis (MEGA) software version 4.0. Mol. Biol Evol. *24*, 1596-1599.

Tarutani, Y., Morimoto, T., Sasaki, A., Yasuda, M., Nakashita, H., Yoshida, S., Yamaguchi, I., and Suzuki, Y. (2004). Molecular characterization of two highly homologous receptor-like kinase genes, RLK902 and RKL1, in *Arabidopsis thaliana*. Biosci. Biotechnol. Biochem. *68*, 1935-1941.

ten Hove, C.A. and Heidstra, R. (2008). Who begets whom? Plant cell fate determination by asymmetric cell division. Curr Opin Plant Biol *11*, 34-41.

Torii, K.U., Mitsukawa, N., Oosumi, T., Matsuura, Y., Yokoyama, R., Whittier, R.F., and Komeda, Y. (1996). The *Arabidopsis* ERECTA gene encodes a putative receptor protein kinase with extracellular leucine-rich repeats. Plant Cell *8*, 735-746.

Tromas, A., Braun, N., Muller, P., Khodus, T., Paponov, I.A., Palme, K., Ljung, K., Lee, J.Y., Benfey, P., Murray, J.A., Scheres, B., and Perrot-Rechenmann, C. (2009). The AUXIN BINDING PROTEIN 1 is required for differential auxin responses mediating root growth. PLoS One. *4*, e6648.

Tsuwamoto, R., Fukuoka, H., and Takahata, Y. (2008). GASSHO1 and GASSHO2 encoding a putative leucine-rich repeat transmembrane-type receptor kinase are essential for the normal development of the epidermal surface in *Arabidopsis* embryos. Plant J. *54*, 30-42.

Valon, C., Smalle, J., Goodman, H.M., and Giraudat, J. (1993). Characterization of an *Arabidopsis thaliana* gene (TMKL1) encoding a putative transmembrane protein with an unusual kinase-like domain. Plant Mol. Biol *23*, 415-421.

van Zanten, M., Snoek, L.B., Proveniers, M.C.G., and Peeters, A.J.M. (2009). The many functions of ERECTA. Trends in Plant Science *14*, 214-218.

Vert, G.g., Nemhauser, J.L., Geldner, N., Hong, F., and Chory, J. (2005). MOLECULAR MECHANISMS OF STEROID HORMONE SIGNALING IN PLANTS. Annual Review of Cell and Developmental Biology *21*, 177-201.

Wang, H., Chevalier, D., Larue, C., Ki, C.S., and Walker, J.C. (2007). The Protein Phosphatases and Protein Kinases of *Arabidopsis thaliana*. In The *Arabidopsis* Book, The American Society of Plant Biologists), pp. 1-38.

Whippo, C.W. and Hangarter, R.P. (2005). A Brassinosteroid-Hypersensitive Mutant of BAK1 Indicates That a Convergence of Photomorphogenic and Hormonal Signaling Modulates Phototropism. Plant Physiol. *139*, 448-457.

Whitford, R., Fernandez, A., De, G.R., Ortega, E., and Hilson, P. (2008). Plant CLE peptides from two distinct functional classes synergistically induce division of vascular cells. Proc. Natl. Acad. Sci. U. S. A *105*, 18625-18630.

Willemsen, V., Wolkenfelt, H., de Vrieze G., Weisbeek, P., and Scheres, B. (1998). The HOBBIT gene is required for formation of the root meristem in the *Arabidopsis* embryo. Development *125*, 521-531.

Wolters, H. and Jurgens, G. (2009). Survival of the flexible: hormonal growth control and adaptation in plant development. Nat. Rev. Genet. *10*, 305-317.

Xiong, L. and Zhu, J.K. (2001). Abiotic stress signal transduction in plants: Molecular and genetic perspectives. Physiol Plant *112*, 152-166.

Xiong, L. and Zhu, J. (2002). Salt Tolerance. In The *Arabidopsis* Book, The American Society of Plant Biologists), pp. 1-22.

Xu, S.L., Rahman, A., Baskin, T.I., and Kieber, J.J. (2008). Two leucine-rich repeat receptor kinases mediate signaling, linking cell wall biosynthesis and ACC synthase in *Arabidopsis*. Plant Cell *20*, 3065-3079.

Yamaguchi, Y., Pearce, G., and Ryan, C.A. (2006). The cell surface leucine-rich repeat receptor for AtPep1, an endogenous peptide elicitor in *Arabidopsis*, is functional in transgenic tobacco cells. Proc. Natl. Acad. Sci. U. S. A *103*, 10104-10109.

Chapter 6

Activation tagged *RLK902* links *Arabidopsis* root growth inhibition and downy mildew resistance by *trans*-repression of gene activity

Colette A. ten Hove[1]*, Mark de Jong[2]*, Annemiek Andel[2], Gabino F. Sanchez-Perez[3], Yoshiaki Tarutani[4], Yoshihito Suzuki[4], Guido Van den Ackerveken[2]** and Renze Heidstra[1]**†

[1]Faculty of Science, Department of Biology, section Molecular Genetics, Utrecht University, Padualaan 8, 3584 CH Utrecht, the Netherlands. [2]Faculty of Science, Department of Biology, section Plant-Microbe Interactions, Utrecht University, Padualaan 8, 3584 CH Utrecht, the Netherlands. [3]Faculty of Science, Department of Biology, section Theoretical Biology and Bioinformatics, Utrecht University, Padualaan 8, 3584 CH Utrecht, the Netherlands. [4]Department of Applied Biological Chemistry, the University of Tokyo, 1-1-1 Yayoi, Bunkyo-ku, Tokyo, 113-8657, Japan.

*/***These authors contributed equally to this work. † Corresponding author*

Summary

Receptor-like kinases (RLKs) constitute a large family of signal perception molecules in *Arabidopsis*. The largest group of RLKs is of the leucine-rich repeat (LRR) class that has been described to function in development and defense. Of these, *CLAVATA1 (CLV1)* and *ERECTA (ER)* receptors function in maintaining shoot meristem homeostasis and organ growth, but LRR RLKs with similar function in the root remain unknown. For the interaction of *Arabidopsis* with the oomycete pathogen *Hyaloperonospora arabidopsidis* the involvement of LRR RLKs has not been demonstrated. A set of homozygous T-DNA insertion lines mutated in LRR RLKs was investigated to assess the potential role of these receptors in root meristem maintenance and compatibility. One mutant line, *rlk902*, was discovered that showed both reduced root growth and resistance to downy mildew in a recessive manner. The phenotypes of this mutated line could not be rescued by complementation, but are nevertheless linked to the T-DNA insertion. Microarray studies showed that gene expression spanning a region of approximately 84 kb upstream of the mutated gene was downregulated. The results suggest that T-DNA mediated *trans*-repression of multiple genes upstream of the *RLK902* locus links both phenotypes.

Introduction

Plants continuously form new organs during their entire lifecycle. These organs are derived from two main populations of stem cells located in the meristems in the shoot and root apices. The shoot apical meristem produces all the aboveground organs and tissues of the plant, i.e. the stems, leaves and flowers, whereas the root meristem gives rise to the entire root system. The radial organization of the *Arabidopsis* root is derived from stereotyped asymmetric cell divisions of different stem cells and their daughters (Figure 1a). To achieve indeterminate growth, meristems must maintain a strict regulation of stem cell maintenance, cell division and cell differentiation. In the heart of the shoot meristem a feedback loop involving LRR RLK signaling ensures the integrity and size of the stem cell pool (reviewed by Laux, 2003). However, LRR RLK members involved in root meristem maintenance remain elusive.

During their lifetime, plants are exposed to a wide range of potential pathogens. Many pathogen derived cell surface components have been described that function as pathogen associated molecular patterns (PAMPs), triggering innate immunity in various plant species. For their survival plants depend on either *R*-gene mediated resistance and/or an efficient detection system for PAMPs that may include (LRR) RLKs (reviewed by Zipfel and Felix, 2005). The involvement of LRR RLKs in the *Arabidopsis-H. arabidopsidis* (downy mildew) interaction remains to be established. Oomycetes like downy mildew form specialized feeding structures called haustoria that play an important role in host-pathogen signaling and nutrient retrieval. Indications for compatible downy mildew recognition via PAMPs are given by studies that show that compatible isolates also trigger plant immune responses (Maleck et al., 2000), although to a lesser extent than incompatible isolates. Important is the observation that LRR RLKs like *NORK* and *SYMRK* are involved in nodulation, i.e. these proteins trigger development of a new organ by actively contributing to the compatible interaction (Endre et al., 2002; Stracke et al., 2002). LRR RLKs could also function as cues, e.g. docking factors, for compatible downy mildew. Absence of these cues would ideally lead to resistance whereas reduced PAMP perception could render a plant more susceptible.

Phylogenetic studies revealed over 400 transmembrane RLKs in the *Arabidopsis* genome (Shiu and Bleecker, 2001) and for an increasing number of RLKs the function has been elucidated over the years (Morillo and Tax, 2006). LRR RLKs represent the largest group of RLKs with approximately 235 members and this clade has functions in development and pathogen detection (Dievart and Clark, 2004; Tor et al., 2009). LRR RLKs involved in plant development include *CLV1* in controlling shoot and floral meristem size (Clark et al., 1993; Clark et al., 1997) and *SCRAMBLED* (*SCM*)

involved in root epidermis cell fate (Kwak et al., 2005). Around 50 LRR RLK genes have been demonstrated to be upregulated when plants are treated with various PAMPs (Nurnberger and Kemmerling, 2006). Members involved in biotic stress signaling include *Xa21* from *Oryza sativa* in resistance towards *Xanthomonas oryzae* pv *oryzae* (Song et al., 1995) and bacterial PAMP perception like flagellin by *FLAGELLIN SENSITIVE2* (*FLS2*) (Gomez-Gomez and Boller, 2000). Some LRR RLKs regulate both biological processes; *ER* and *BAK1* (*BRI1-associtated kinase1*) control both organ growth and pathogen resistance (Torii et al., 1996; van Zanten et al., 2009; Nam and Li, 2002; Tor et al., 2009).

To study the involvement of LRR RLKs in root development and in the *Arabidopsis-H. arabidopsidis* compatible interaction, we screened a set of homozygous LRR RLK T-DNA insertion lines. Here, we report on the characterization of a line mutated in *RLK902* that is linked with the observed root growth defect and resistance phenotypes. Surprisingly, the gene itself is not required for root meristem maintenance and susceptibility to downy mildew. Instead, it appears that the T-DNA insertion in *RLK902* leads to downregulation of gene expression within a flanking 84 kb genomic region.

Results

A T-DNA insertion in *RLK902* affects root growth and meristem size

To investigate the function of LRR RLKs in root development we screened a collection of homozygous LRR RLK T-DNA insertion mutants (described in Chapter 5). One mutant line, harboring an insertion in the *RLK902* gene (Figure 1b) (Tarutani et al., 2004), displayed an obvious reduction in root length. Root growth was quantified by measuring the root length of wild type (Col-7) and *rlk902* seedlings at different time points and revealed that despite a reduction in length *rlk902* roots generally continued to grow (Figure 1i). Correspondingly, *rlk902* seedling roots displayed a reduced meristem size compared to wild type (Figure 1c,d). Occasionally, the root meristem completely differentiated within 16 days post germination (Figure 1f).

RLK902 is a member of subfamily LRR III of plant RLKs (Shiu and Bleecker, 2001). *RKL1* (Ohtake et al., 2000) is the closest family member of *RLK902* showing 75% amino acid sequence identity over the entire protein and 82% in the kinase domain (Tarutani et al., 2004). To investigate possible redundancy within this subclade we constructed double mutant combinations. We obtained two T-DNA insertion lines for *RKL1*, identified homozygous mutant plants by polymerase chain reaction (PCR) based genotyping and named these alleles *rkl1-1* and *rkl1-2* (Figure 1b). Analysis of the single mutants at different developmental stages did not reveal any obvi-

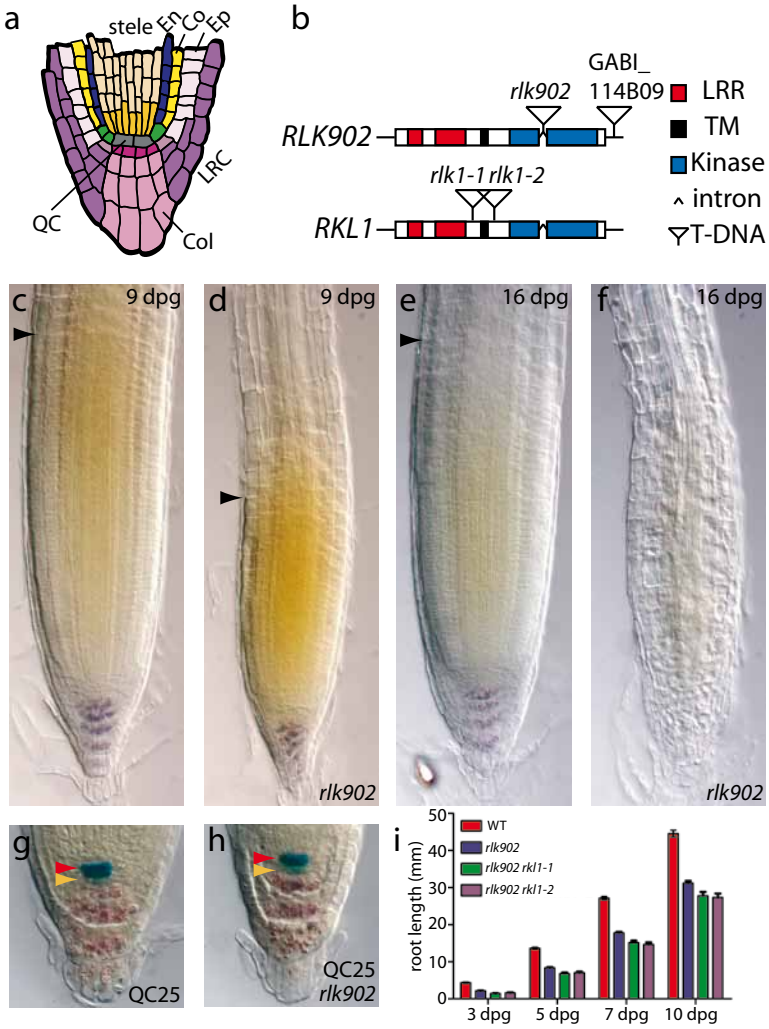

Figure 1. ***rlk902* mutants are affected in root length and meristem size.** (a) Schematic view of the *Arabidopsis* root meristem. (En) endodermis; (Co) cortex; (Ep) epidermis; (LRC) lateral root cap; (Col) columella; (QC) quiescent center. (b) Schematic representation of *RLK902* (*At3g17840*) and *RKL1* (*At1g48480*) genes and T-DNA insertion sites. Boxes indicate coding sequence. (c-f) Nomarski images of nine-day-old and sixteen-day-old wild type (c,e) and *rlk902* (d,f) roots. In some *rlk902* seedlings the root completely differentiated within 16 days post germination (f). Root meristem boundary (black arrowhead); starch granules (purple). (g,h) Nomarski images showing QC25 expression (blue) in 9-day-old wild type (g) and *rlk902* (h) roots. Starch granules are present in differentiated columella cells but absent from columella stem cells in both wild type and *rlk902*. QC (red arrowhead), columella stem cells (yellow arrowhead). (i) Root length measurements (in mm) of wild type, *rlk902*, *rlk902 rkl1-1* and *rlk902 rkl1-2* seedlings. A minimum of 24 seedlings were measured for each time point. Error bars represent standard error of the mean. Root length is significantly reduced in *rlk902* compared to wild type seedlings. Root length is further reduced in *rlk902 rkl1* double mutants.

ous phenotypic differences from wild type plants (data not shown). However, root length measurements of *rlk902 rkl1-1* and *rlk902 rkl1-2* double mutant seedlings revealed a slight but significant enhanced reduction in root length compared to *rlk902* mutant seedlings (Figure 1i).

rlk902 does not primarily affect the stem cell niche

Reduction in root length and failure of root meristem maintenance can be caused by the loss of stem cells, due to lack of QC activity or specification (van den Berg et al., 1997; Sabatini et al., 2003). Alternatively, loss of division potential and/or more rapid differentiation of stem cell daughters interfere with root growth. In the first scenario, primary defects in the QC region are expected, while in the second scenario, a decrease in meristem size would be observed before QC and stem cell defects appear.

We introduced the QC25, QC46 and QC184 markers in *rlk902* to investigate whether QC specification is affected in these plants. Expression of these markers is similar to wild type even when the root meristem is already significantly reduced in 9-day-old *rlk902* roots (Figure 1g,h, data not shown). Stem cell presence in *rlk902* roots was analyzed by starch granule accumulation that marks differentiated columella cell layers but are absent from columella stem cells. Columella stem cells could be detected at 9 days after germination, suggesting that stem cell status is maintained for a prolonged period at a stage when meristem size is significantly reduced (Figure 1d,h). Only upon occasional complete differentiation of the root meristem are QC marker expression and columella stem cells lost (data not shown). These results indicate that the observed reduction in root growth and meristem size in *rlk902* is not primarily caused by interference of QC specification and/or stem cell maintenance.

rlk902 is resistant to downy mildew

Surprisingly, screening for resistance to the compatible downy mildew isolate Waco9 also positively identified the *rlk902* mutant (Figure 2c). In contrast, wild type seedlings showed severe disease symptoms and supported sporulation of the pathogen (Figure 2a). Microscopic analysis showed that the wild type was fully colonized by downy mildew (Figure 2b), whereas *rlk902* was resistant at early infection stages. Almost no haustoria were formed (Figure 2d) or they were encased by pappilae (Figure 2d, insert).

To test whether the resistance is caused by constitutive activation of plant defense associated with broad range resistance the *rlk902* mutant was analyzed for resistance to *Pseudomonas syringae* pv *tomato* DC3000 and for defense associated gene expression. Growth of the bacterial pathogen was similar at 3 days post inoculation (dpi) with 5.0 $\log_{10}$ CFUs for wild type and 5.1 $\log_{10}$ CFUs for *rlk902*, indicating

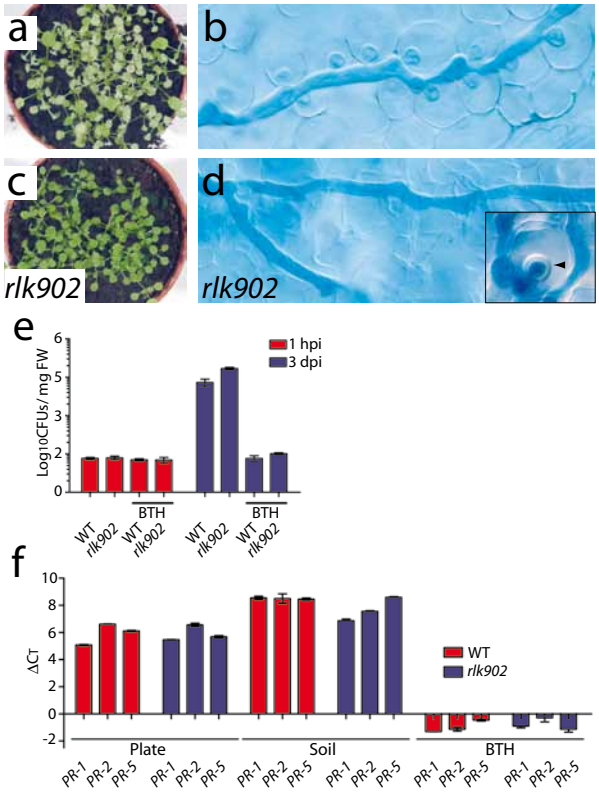

Figure 2. ***rlk902* shows resistance to *H. arabidopsidis*.** (a,c) Two-week-old wild type (a) and *rlk902* (c) seedlings were inoculated with *H. arabidopsidis* isolate Waco9 and analyzed at 7 dpi. Severe disease symptoms are visible in wild type (a) as discoloration of the leaves and the presence of a white down, which are the conidia bearing conidiophores. In contrast, *rlk902* (c) shows healthy green leaves and no conidiophores indicating that growth of the pathogen is halted, giving fully resistant plants. (b,d) Trypan blue staining of wild type (b) and *rlk902* (d) inoculated with Waco9 at 7 dpi. The wild type shows downy mildew hyphal growth and haustoria formation in encountered cells (b). Haustoria formation in *rlk902* is impaired (d) and are often encased (d, inset, black arrowhead). (e) *rlk902* does not show alterations in susceptibility towards *Pseudomonas*. Colony forming units (CFUs) of *Pseudomonas* were counted per mg fresh weight (FW) after 1 hpi and 3 dpi of wild type and *rlk902* with or without BTH. The error bars represent the standard error of mean. (f) Transcripts levels of *PR-1*, *PR-2* and *PR-5* were measured by qRT-PCR in wild type and *rlk902*. Transcript levels were normalized with and compared to *Arabidopsis ACTIN-2* levels to determine ΔC_T values. A slight induction for *PR-1* and *PR-2* was observed in *rlk902* grown on soil (Note that lower bars represent higher transcripts abundance). Error bars represent the standard error of mean.

that *rlk902* is not resistant to *Pseudomonas* (Figure 2e). Pretreating plants with benzothiadiazole (BTH, a chemical inducer of systemic acquired resistance) 2 days prior to *Pseudomonas* inoculation prevented bacterial growth in both wild type and *rlk902* (Figure 2e).

To analyze the possibility that resistance is caused by constitutive defense gene expression, transcript levels of *PR-1*, *PR-2* and *PR-5* were measured by quantitative real time reverse transcriptase PCR (qRT-PCR) in wild type and *rlk902* lines grown on MS agar plates and soil. A small increase was observed for *PR-1* and *PR-2* in *rlk902* when grown on soil, but their upregulation was small compared to the accumulation of *PR* transcripts in plants pretreated with BTH (Figure 2f). These results show that expression of *PR-1*, *PR-2* and *PR-5* is not upregulated in *rlk902*, indicating that the defense machinery of the host is not constitutively activated.

***RLK902* and *RKL1* expression studies**

To examine the expression profile of *RLK902* in detail, *in situ* hybridization analysis was performed and promoter and protein fusions were constructed. mRNA *in situ* hybridizations on 2-day-old seedlings indicate that *RLK902* is highly expressed in the root stem cell niche (Figure 3a). Expression is maintained at reduced levels in the vascular domain and fades in the ground tissue. For the *RLK902* promoter fusion, a 1411 base pair (bp) genomic DNA fragment upstream of the coding region of *RLK902* was fused to β-glucuronidase (GUS). GUS activity was detected in the root tip, comparable to the mRNA localization data (Figure 3b). The primary root expression is reiterated in lateral roots (data not shown). In the arial parts, promoter GUS activity was observed in the vascular tissue in the leaf (Figure 3d) and in the stomata (Figure 3d, arrowhead). To assess the subcellular localization of the RLK902 protein, a translational fusion was made in which the genomic *RLK902* coding fragment was fused in frame to GFP under the control of the *RLK902* promoter. RLK902:GFP was expressed in what appears to be the cell membrane, consistent with its supposed receptor function (Figure 3f).

Double mutant combinations of *rlk902* with two knockout alleles of its closest homolog *RKL1* showed a further reduction of root length compared to the *rlk902* single mutant. To examine the expression profile of *RKL1* we constructed the *RKL1::GUS* reporter by fusing a 2548 bp genomic DNA fragment upstream of the coding region to GUS. *RKL1::GUS* is expressed in the vascular tissue of the entire root with weaker expression in a subset of provascular tissues of the root tip (Figure 3c). In the arial parts, promoter GUS activity was observed in the vascular tissue in the leaf (Figure 3e) and in the stomata (Figure 3e, arrowhead). The observed root expression shows some overlap with that of *RLK902* in agreement with the enhanced effect of *rkl1* on *rlk902* root growth.

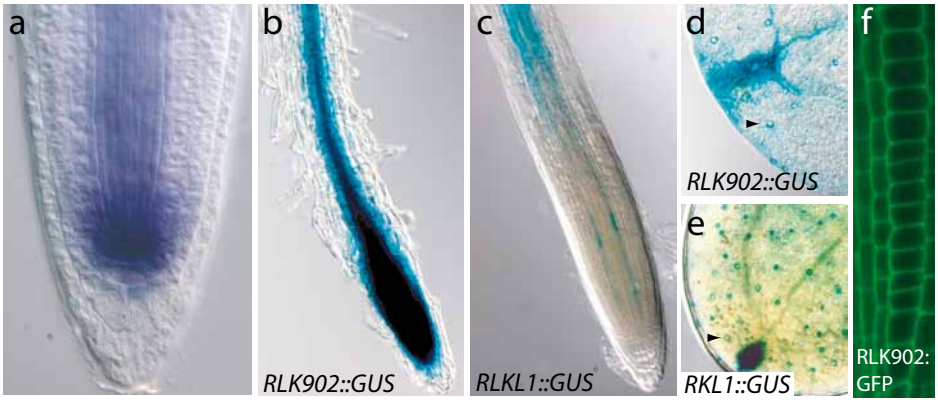

Figure 3. Expression analysis of *RLK902* and *RKL1*. (a) Whole mount *in situ* hybridization with *RLK902* antisense probe in a two-day-old wild type seedling. mRNA accumulates highly in the root stem cell niche, is maintained at reduced levels in the vascular domain, and fades in the ground tissue. (b-e) Nomarski images showing *RLK902::GUS* (b,d) and *RKL1::GUS* (c,e) activity. *RLK902::GUS* is expressed in the root tip and vasculature (b). Expression in the leaf (d) is observed in and around the vascular tissue, at the leaf tips and in stomata (arrowhead). *RKL1::GUS* is expressed in root vascular tissue (c). *RKL1::GUS* expression in the leaf is similar to *RLK902::GUS* in and around the vascular tissue, at the leaf tips and in stomata (arrowhead) (e). (f) Longitudinal confocal section of root expressing *RLK902::RLK902:GFP* shows RLK902:GFP localization to the cell membrane.

To test for pathogen induced expression of *RLK902::GUS*, transgenic plants were inoculated with the downy mildew isolate Waco9. Surprisingly, no change in GUS expression at 4 dpi was observed compared to mock treated plants (data not shown). No GUS activity was detected in cells that were in contact with the pathogen or in which haustoria were formed. This suggests that *RLK902* expression is not associated with downy mildew infection.

Defects observed in *rlk902* are not caused by inactivation of *RLK902*

The *rlk902* mutant contains an activation tag T-DNA insertion (Weigel et al., 2000) at the end of the single intron of the *RLK902* gene (Figure 1b). To test if the *RLK902* gene is disrupted, accumulation of *RLK902* transcript was analyzed in *rlk902* by Northern blot analysis using probes against exon 1 and 2. A single transcript was detected in wild type with either probe, whereas both probes were unable to detect a transcript in *rlk902* (Figure 4a). The *ACTIN-2* control probe detected its corresponding transcript in both wild type and *rlk902*. In addition, RT-PCRs on RNA of wild type plants succeeded to amplify part of the coding region of *RLK902* spanning the single intron, whereas no amplicons were obtained for *rlk902* (Figure 4c). These results show that the activation tag T-DNA in *rlk902* causes complete inactivation of the *RLK902* gene.

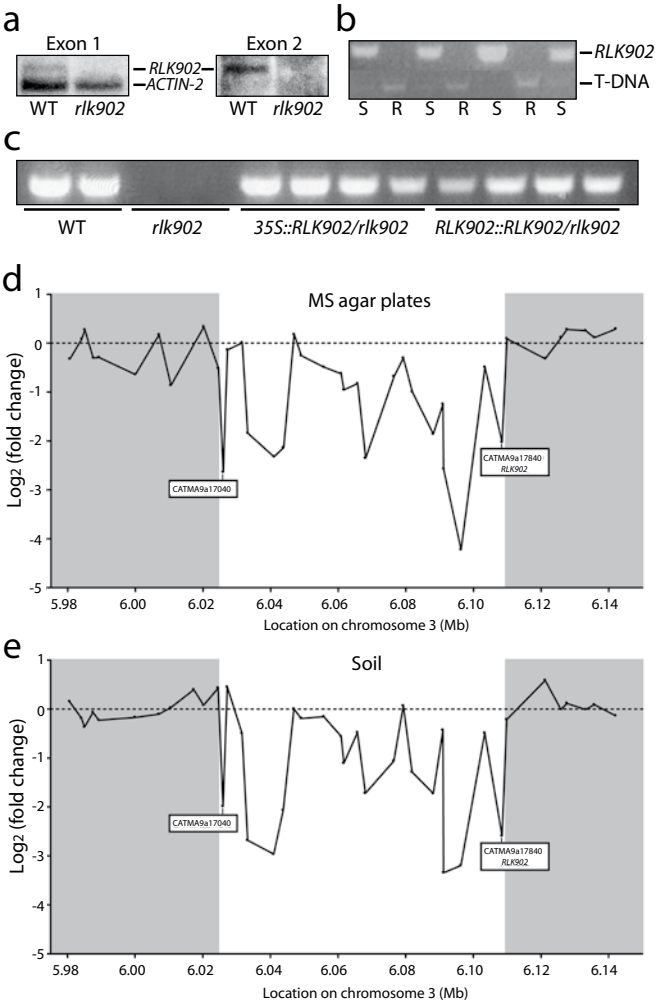

Figure 4. Analysis of gene expression in *rlk902*. (a) Northern blots of wild type (WT) and *rlk902* RNA hybridized with probes derived from exon 1 and 2 of the *RLK902* gene. *RLK902* transcripts are not detected in *rlk902*. The *ACTIN-2* probe was used as a loading control. (b) Representation of genotypes of F2 plants, from a *rlk902* to wild type cross, segregating for susceptibility (S) or resistance (R) to downy mildew. Resistant plants gave only a genomic amplicon including part of the T-DNA in *RLK902* indicating homozygosity. Susceptible plants always contained a wild type *RLK902* copy. (c) RT-PCR expression analysis of *RLK902* in biological replicates of wild type, *rlk902* and *35S::RLK902 rlk902* and *RLK902::RLK902 rlk902* complementing lines. Wild type and complemented lines show expression of *RLK902*. (d,e) Microarray expression ratios ($\log_2$ [*rlk902*/wild type]) of CATMA-IDs were plotted against their position on chromosome 3 for plants grown on MS agar plates (d) and soil (e). The downregulated region which is shown in white starts at CATMA3a17040 (*At3g17611*) and ends at CATMA3a17340 (*At3g17840* = *RLK902*). Gene expression flanking this region (shown in grey) appears unaffected.

To investigate whether disruption of *RLK902* is responsible for the observed root growth defect and resistance to downy mildew two constructs were made for complementation analysis. *35S::RLK902* harbored *RLK902* cDNA under control of the constitutive Cauliflower Mosaic Virus (CaMV) 35S promoter and *RLK902::RLK902* contained the *RLK902* genomic region starting at 1441 bp upstream of the predicted start codon and ending at 1274 bp downstream of the stop codon. RT-PCR analyses showed that both complementation constructs in the *rlk902* background were able to restore *RLK902* expression approaching wild type levels (Figure 4c). Surprisingly, root length and meristem size of the *rlk902* complementation lines were comparable to the *rlk902* mutant (data not shown). In addition, at 7 dpi with downy mildew isolate Waco9 no sporulation was observed in the complementation lines and *rlk902*, in contrast to the susceptible wild type plants (data not shown).

To investigate *rlk902* specific effects, two additional putative T-DNA insertion lines were obtained for *RLK902*. PCR based genotyping indicated that only one of these (GABI_114B09) contained a T-DNA insertion located in the 3' UTR (Figure 1b). No phenotypic difference with respect to root length defects and resistance to downy mildew isolate Waco9 was observed between the homozygous T-DNA insertion line and wild type (data not shown). In addition, we constructed lines with reduced *RLK902* levels using (i) RNA interference (RNAi) (Wesley et al., 2001) and (ii) artificial micoRNAs (amiRNAs) (Schwab et al., 2006). None of the resulting transgenic lines displayed reduced root length or conferred resistance to Waco9 (data not shown).

The possibility remained that an additional mutation in the *rlk902* lines causes the observed root growth defect and resistance. Therefore, *rlk902* was backcrossed to wild type (Col-7) and the F2 population was analyzed for segregation of resistance to downy mildew and the root growth defect. Analysis of 216 plants for segregation of resistance gave 169 susceptible and 47 resistant plants (~22%) corresponding to a single-locus recessive phenotype. PCR based genotyping of a subset of 18 susceptible and 18 resistant plants showed that all resistant plants were homozygous for the T-DNA insertion in *RLK902* (Figure 4b). Progeny of these plants all showed the characteristic *rlk902* root growth defect. Susceptible plants were heterozygous or carried two functional *RLK902* copies and their progeny segregated for the short and wild type root phenotype, respectively. Together, these studies indicate that both resistance to downy mildew and the root growth defect are recessive traits and genetically linked to *rlk902* but are not caused by the disruption of *RLK902*.

What causes the *rlk902* phenotype?

The fact that *rlk902* could not be complemented and that downregulation of *RLK902* did not result in reduced root growth or resistance to downy mildew raises the question what molecular mechanism is underlying the root growth defect and

resistance to downy mildew observed in *rlk902*. To address this question, microarray studies were performed to analyze the gene expression profile of this mutant line. Two different growth conditions were chosen as biological replicates, seedlings grown (i) on soil and (ii) on MS agar plates. Materials from (i) and (ii) were hybridized on 4 CATMA microarrays per growth condition. Data analysis confirmed that in the mutant under both conditions *RLK902* is downregulated, with $\log_2$-ratios (*rlk902*/ wild type) of -2.6 for soil and -2.0 for MS agar plates. 39 genes were differentially expressed in both individual microarray experiments, based on at least two-fold up or downregulation (Table 1). Interestingly, 31,6% of the genes that were downregulated more than 2-fold in one or both CATMA microarray experiments cluster in a genomic region of approximately 84 kb upstream of *RLK902* (Table 1). The CATMA probes in this region and their corresponding expression levels were plotted against their position on chromosome III for both growth conditions (Figure 4d,e). Although the level of downregulation is not equally strong for all genes in this region, the downregulation patterns observed in *rlk902* grown on soil or MS agar plate are very similar. 19 of the 25 genes in the 84 kb region are present on the Affymetrix ATH1 chip which allowed us to search for their predicted root expression profiles (Birnbaum et al., 2003; Brady et al., 2007). A small cluster of 6 genes immediately upstream of *RLK902* shows high expression levels in the different tissues of the developing root (Figure 5).

Since the root growth defect and downy mildew resistance are linked to the activation tag insertion, we analyzed whether any of the 25 genes in the downregulated region was responsible for the *rlk902* phenotypes. When available, at least three different T-DNA insertion lines per gene were investigated for root growth and resistance to Waco9 (Table 1). Surprisingly, none of the mutant lines showed a short root phenotype or downy mildew resistance.

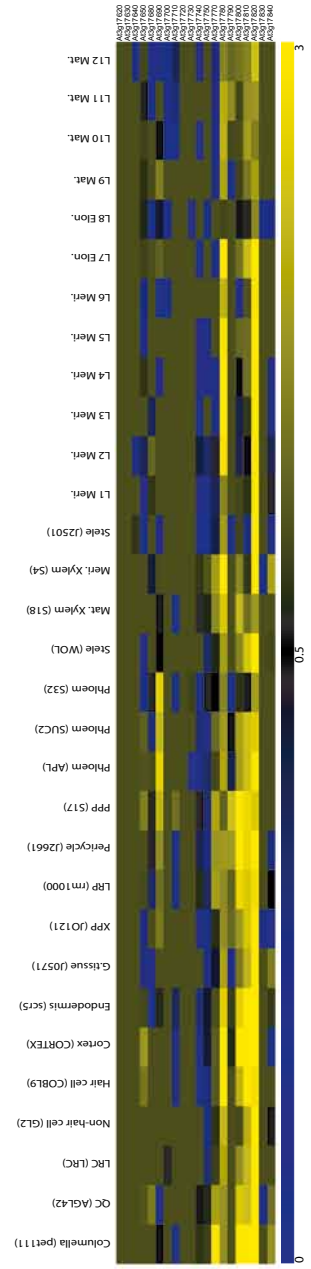

Figure 5. Root expression profiles of genes in the downregulated region of 84 kb in *rlk902*. Heat map of expression profiles in different subzones of the root of genes in the downregulated region of 84 kb, including *RLK902* that are present on the Affymetrix ATH1 GeneChip. The expression indices for each marker/section were obtained from (Brady et al., 2007) and were visualized in MultiExperiment Viewer (MeV) v4.5.0 (Saeed et al., 2003). Colors indicate lowered (blue) or increased (yellow) transcript accumulation relative to the respective controls within a 0 to +3 range. A small cluster of 6 genes upstream of *RLK902* is highly expressed in the different tissues of the developing root.

Table 1. Differentially expressed genes in *rlk902* and investigated T-DNA insertion lines of genes flanking *rlk902*. Genes (AGI-ID) that are differentially expressed in wild type and *rlk902* in both individual microarray experiments, based on at least two-fold up- or downregulation (ratio = >1 or <-1, respectively) and genes in the downregulated region of 84 kb are listed with their corresponding CATMA-ID and AFFY-ID (if present, otherwise marked "x") and expression ratios (soil and MS plates; $\log_2$ [*rlk902*/wild type]). Indicated T-DNA insertion lines for the genes in the 84 kb region were investigated for root length and/or resistance to downy mildew.

AFFY-ID	CATMA-ID	AGI-ID	MS agar plates Ratio	Soil Ratio	Description	T-DNA lines
263209_at	CATMA1a09360	*At1g10522*	1.03	1.28	Similar to unknown protein	x
262456_at	CATMA1a10175	*At1g11260*	-1.56	-1.04	STP1 - sugar transporter 1	x
256186_at	CATMA1a42785	*At1g51680*	-1.07	-1.03	4CL1 - 4-coumarate-CoA ligase	x
259717_at	CATMA1a50030	*At1g61010*	-1.19	-1.11	CPSF73-I - cleavage and polyadenylation specificity factor 73-I	x
259990_s_at	CATMA1a57435	*At1g68050*	-1.46	-1.87	FKF1 - flavin-binding kelch repeat F box 1	x
260267_at	CATMA1a57905	*At1g68530*	-1.27	-1.37	KCS6 - 3-ketoacyl-coa synthase 6	x
259058_at	CATMA3a02400	*At3g03470*	-1.66	-1.23	CYP89A9	x
257280_at	CATMA3a13720	*At3g14440*	-1.20	-1.54	NCED3 - 9-cis-epoxycarotenoid dioxygenase 3	x
258117_at	CATMA3a14050	*At3g14700*	-2.34	-2.66	Molecular function unknown	x
257207_at	CATMA3a14260	*At3g14900*	1.03	1.15	Similar to unknown protein	x
x	CATMA3a17040	*At3g17611*	-2.64	-1.99	Rhomboid family protein	N857350 (E,a), N606187 (E,a), N606188 (5,a), N500152 (3,b), N856063 (E,b), N652415 (E,b)
258407_at	CATMA3a17050	*At3g17620*	-0.14	0.45	F-box family protein	N508035 (E,a), N606415 (E,a), N568161 (E,b), N568164 (E,b)
258408_at	CATMA3a17070	*At3g17630*	0.01	-0.50	Putative Na+/H+ antiporter family	N605601 (E,a), N600047 (E,a), N655778 (E,h,b), N870235 (E,b)
258409_at	CATMA3a17080	*At3g17640*	-1.84	-2.68	Leucine-rich repeat family protein	N829071 (5,a), N808284 (5,a), N170225 (5,a), N828246 (E,b), N802812 (5,b)
258353_s_at	x	*At3g17650*	x	x	YSL5 - Metal-nicotianamine transporter	N558656 (E,a), N562030 (E,a), N662603 (E,h,b), N668383 (E,h,b)
x	x	*At3g17660*	x	x	AGD15 - Member of ARF GAP domain (AGD)	N815874 (5,a), FLAG_424G12 (5,a), N631749 (3,b), N650224 (3,b)
x	CATMA3a17110	*At3g17668*	-3.13	-2.23	ENA - Enhancer of ATNSI activity	N539429 (E,a), N160933 (I,a), N620826 (5,a), N539430 (5,a)

x	CATMA3a17120	*At3g17670*	-2.32	-2.97	Similar to stress-inducible protein	N521028 (E,b), N538448 (3,b)
258376_at	CATMA3a17130	*At3g17680*	-2.13	-2.07	Similar to putative kinase interacting protein	N630159 (5,a), N576870 (E,b), N657296 (5,h,b)
258377_at	CATMA3a17140	*At3g17690*	0.18	0.00	Member of cyclic nucleotide gated channel family	N629200 (E,a), N507105 (I,a), N655942 (E,h,b), N527306 (E,b)
258351_at	CATMA3a17145	*At3g17700*	-0.26	-0.19	Cyclic nucleotide-binding transporter 1	N643671 (5,a), N629133 (E,b), N574919 (E,b)
258348_at	CATMA3a17150	*At3g17710*	-0.49	-0.15	F-box family protein	N538051 (5,a), N854212 (5,a), N668097 (5,h,b), N321361 (E,h,b)
x	CATMA3a17170	*At3g17715*	-0.62	-0.56	Similar to SAM decarboxylase proenzyme 3	N855134 (E,a), N643604 (5,a)
257862_s_at	x	*At3g17720*	x	x	Pyridoxal-dependent decarboxylase family protein	N568885 (E,b), N550626 (I,b), N643604 (5,b)
257863_at	CATMA3a17210	*At3g17730*	-0.82	-0.47	ANAC057	FLAG_519F08 (I,a), FLAG_389D07 (I,a), N735859 (I,h,b), N103459 (I,b)
257864_at	CATMA3a17220	*At3g17740*	-2.35	-1.72	Protein of unknown function DUF1740	N559902 (E,a), N558499 (E,a), N566309 (E,a), N595212 (E,a), N555926 (E,a), N501657 (5,a), N599476 (5,a), N666095 (E,h,b), N670422 (E,h,b)
257865_at	CATMA3a17230	*At3g17750*	-0.68	-1.06	Protein kinase family protein	N564507 (E,a), N665043 (E,h,b), N850588 (I,b)
x	CATMA3a17240	*At3g17760*	-0.30	0.07	Putative glutamate decarboxylase	FLAG_460F07 (E,a), N567408 (3,a), N381133 (5,h,b), N398853 (3,h,b)
257866_at	CATMA3a17250	*At3g17770*	-1.00	-1.29	Dihydroxyacetone kinase family protein	FLAG_119A06 (5,a), N528386 (I,b)
257867_at	CATMA3a17280	*At3g17780*	-1.86	-1.73	Similar to unknown protein	N514002 (E,a), N502741 (I,a), N517811 (5,a)
258158_at	CATMA3a17290	*At3g17790*	-1.25	-3.34	ATACP5 - Acid phosphatase 5	N597940 (E,a), N597938 (E,a), N546977 (E,a), N547922 (5,a), N658665 (5,h,b), N546785 (E,b)
258188_at	CATMA3a17290	*At3g17800*	-2.57	-3.34	MEB5.2	N570769 (E,a), N573038 (E,a), N629803 (E,a), N545784 (P,a), N545827 (P,a), N660956 (E,h,b), N666385 (E,h,b)
258162_at	CATMA3a17310	*At3g17810*	-4.22	-3.20	Dihydroorotate dehydrogenase family protein	N583897 (E,a), N573490 (I,a), N623318 (I,a), N424069 (I,a), N663150 (E,h,b), N573489 (I,b), N873523 (E,b)

258160_at	x	*At3g17820*	x	x	Cytosolic glutamine synthetase	N572283 (E,a), N572275 (I,a), N538156 (I,a), N502524 (I,a), N651573 (5,a)
258220_at	CATMA3a17330	*At3g17830*	-0.49	-0.49	DNAJ heat shock family protein	N642169 (I,a), N519829 (I,a), N658951 (I,h,b), N626111 (E,b), N669232 (E,h,b)
258159_at	CATMA3a17340	*At3g17840*	-2.03	-2.59	RLK902 - Receptor-like kinase 902	FLAG_286C06 (E,b), GABI_114B09 (E,b), N586401 (P,b), N556722 (P,b), N826365 (P,b)
258021_at	CATMA3a18990	*At3g19380*	-1.13	-1.11	PUB25 - plant U-box 25	x
252079_at	CATMA3a44615	*At3g51630*	-1.27	-1.30	WNK5 - with no lysine (K) kinase 5	x
x	CATMA3a44615	*At3g51632*	-1.27	-1.30	CPuORF44 - Conserved peptide upstream open reading frame 44	x
251225_at	CATMA3a55830	*At3g62660*	-1.05	-1.55	GATL7 - Galacturonosyltransferase-like 7	x
253421_at	CATMA4a34070	*At4g32340*	-1.28	-1.56	Expressed	x
250253_at	CATMA5a11870	*At5g13640*	-1.05	-1.19	ATPDAT - phosphatidylcholine-sterol O-acyltransferase	x
250196_at	CATMA5a12805	*At5g14580*	1.07	1.03	Polyribonucleotide nucleotidyltransferase, putative	x
246595_at	CATMA5a13000	*At5g14780*	-1.17	-1.19	FDH - formate dehydrogenase	x
246476_at	CATMA5a15060	*At5g16730*	-1.13	-1.40	Expressed	x
246432_at	CATMA5a15770	*At5g17490*	-1.02	-1.22	RGL3 - RGA-like protein 3	x
x	CATMA5a20730	*At5g23235*	-1.06	-1.45	Pseudogene	x
249850_at	CATMA5a20730	*At5g23240*	-1.06	-1.45	DNAJ heat shock N-terminal domain-containing protein	x
x	CATMA5a21090	*At5g23575*	-1.00	-1.19	Transmembrane protein, putative	x
x	CATMA5a22220	*At5g24593*	-2.17	-2.45	Similar to unknown protein	x
246651_at	CATMA5a30270	*At5g35170*	-1.19	-1.02	Adenylate kinase family protein	x
249042_at	CATMA5a40120	*At5g44350*	-1.37	-1.09	Ethylene-responsive nuclear protein -related	x
248756_at	CATMA5a43535	*At5g47560*	-1.10	-1.12	TDT - tonoplast dicarboxylate transporter	x
247095_at	CATMA5a61730	*At5g66400*	-1.58	-1.53	RAB18 - responsive to ABA 18	x

*Abbreviations: E: Exon; I: Intron; P: 1000-Promoter; 5: 300-UTR5; 3: 300-UTR3; h: ordered as homozygous from stock center, a: screened for resistance; b: screened for root length and resistance.

Discussion

Here, we characterize the *Arabidopsis* mutant *rlk902* that combines two diverse phenotypes: reduced root growth and resistance to the downy mildew pathogen *H. arabidopsidis*.

The activation tag T-DNA in *rlk902* is inserted at the end of the single intron of *RLK902* disrupting its expression. *RLK902* is expressed in the root meristem, which correlates with a role for *RLK902* in cell proliferation. However, *RLK902* promoter driven GUS activity did not correlate with downy mildew Waco9 infection as inoculated plants did not show alterations in expression. Complementation of the *rlk902* mutant with the intact *RLK902* gene could not rescue the root growth and resistance phenotypes. In addition, *RLK902* RNAi and amiRNA approaches did not mimic the *rlk902* mutant phenotypes. We conclude that the *rlk902* root growth defect and downy mildew resistance are not caused by the disruption of *RLK902*.

Backcrosses to wild type revealed that only plants homozygous for the *rlk902* T-DNA insertion showed a reduction in root length and resistance to downy mildew arguing for linkage between the T-DNA insertion and the observed phenotypes. Microarray studies revealed that genes within a region of approximately 84 kb upstream of *RLK902* are downregulated in *rlk902*. However, neither root length reduction nor resistance to downy mildew was observed in T-DNA insertion lines for any of the 25 genes tested within this 84 kb region. There are several possibilities to explain this observation: (1) the affected gene responsible for the phenotypes may not be annotated and therefore not present on the CATMA array. The use of tiling arrays may give a more complete picture of gene expression in the *RLK902* region; (2) the tested T-DNA insertion did not cause disruption of the responsible gene; (3) downregulation of a combination of genes in the 84 kb region is causing the observed phenotypes. This combination may be identified adopting an RNAi strategy, constructing multiple gene knockdown combinations in this area. Alternatively, large and overlapping DNA fragments in the form of TAC clones (http://www.getcid.co.uk) may be tested for complementation in the *rlk902* background.

How can a T-DNA insertion cause such a detrimental effect on the expression of neighboring genes? It has been described that activation tags, containing for example 35S enhancer elements, are able to alter the expression of genes in the vicinity of the T-DNA insertion (Yoo et al., 2005). Ren et al., (2004) report on a gene that showed *trans*-activation 78 kb away from the insertion site in *Arabidopsis* and there are many examples of long distance activation of promoters by distant enhancers in a variety of other species (Merli et al., 1996; Calhoun and Levine, 2003; Nobrega et al., 2003). For *rlk902*, no *trans*-activation was observed but *trans*-repression and this phenomenon can be added to the effects caused by activation tags. Down-

regulation of a genomic region could be explained by induction of changes in the chromatin structure through e.g. DNA methylation and/or histone modifications. Our results underline the caution of Yoo et al., (2005) in the interpretation of phenotypes/results when 35S enhancer elements are used (Weigel et al., 2000).

Whatever the cause, it is interesting to note that the susceptibility to *Pseudomonas syringae* pv *tomato* DC3000 and absence of *PR-1*, *PR-2* and *PR-5* gene induction in *rlk902* demonstrate that the downy mildew incompatibility is not caused by constitutive defense gene expression. With respect to the root phenotype, double mutant combinations of *rlk902* with two knockout alleles of its closest homolog *RKL1* showed a further reduction of root length compared to the *rlk902* single mutant. As the root growth defect cannot be linked to *RLK902* disruption this suggests *RKL1* has an overlapping biological function with gene(s) in the downregulated region upstream of *RLK902*.

Identifying the gene(s) involved in root growth and/or downy mildew compatibility by any of the means discussed above will be the challenge for future studies involving *rlk902*.

Experimental procedures

Plant materials, growth conditions and *H. arabidopsidis* conditions

Origins and backgrounds of mutant and transgenic lines: *rlk902* (Col-7) (Tarutani et al., 2004); QC25 (WS) (Sabatini et al., 2003). *rkl1-1* (sail_772_B09) and *rkl1-2* (sail_525_D09) (both Col-0) were obtained from the *Arabidopsis* Biological Resource Center (ABRC) (Sessions et al., 2002). Col-7 (N3731) was obtained from the Nottingham *Arabidopsis* Stock Centre (NASC) (Scholl et al., 2000). FLAG_286C06 (WS-4) was obtained from Génétique et amélioration des plantes (INRA, FLAG-lines) (Bechtold and Pelletier, 1998). GABI_114B09 (Col-0) was obtained from the German plant genomics research program (GABI) (Rosso et al., 2003). T-DNA lines for genes in the downregulated region as described in Table 2 were obtained from NASC (Alonso et al., 2003), INRA or GABI, respectively.

For analysis of root development, seedlings were sterilized, plated and grown as described in (Sabatini et al., 2003). To test for *H. arabidopsidis* compatibility, plants were grown as described (de Jong et al., 2006). Plants were subsequently mock-inoculated or treated with a 50 sporangia per µl suspension of Cala2 or Waco9 *H. arabidopsidis* isolates, respectively, using a spray gun. After inoculation plants were allowed to dry for 2 hours and subsequently incubated under a sealed lid with 100% relative humidity in a growth chamber at 16 °C with 9 h of light (~100 µmol photons m^{-2} sec^{-1}).

Table 2. Primers used for cloning, Northern probe synthesis, (q)RT-PCR, *in situ* probe synthesis and genotyping.

Gateway cloning fragment	**Primer**	**Primer sequences ('5 - '3)**
RLK902 promoter (1411 bp)	RLK902attB1-Fw	aaaaagcaggcttcgttttatcatttatatatggttaaga
	RLK902prom-attB2-Rv	agaaagctgggtatgtaagaaacaaagagagaaac
RLK902 promoter (1588 bp)	pRLK902FattB4	ggggacaactttgtatagaaaagttgcatttcgtcaaaaaccctgaaacccca
	pRLK902RattB1	ggggactgctttttttgtacaaacttgttgtaagaaacaaagagagaaaccct
RLK902 cDNA / gene	RLK902cDNAattB1-Fw	aaaaagcaggcttcatgcgactcttcttcacaccgt
	RLK902cDNAattB2-Rv	agaaagctgggtaccccacccgatctgcacc
RLK902 complementation	RLK902attB1-Fw	aaaaagcaggcttcgttttatcatttatatatggttaaga
	RLK902attB2-Rv	agaaagctgggtaacagtgacaacctgtgtttta
RKL1 promoter (2548 bp)	pRKL1FattB4	ggggacaactttgtatagaaaagttgcagctttagacttttcttcgttttgg
	pRKL1RattB1	ggggactgctttttttgtacaaacttgttgtgactattcagagaagaagacg
	attB1	ggggacaagtttgtacaaaaaagcaggct
	attB2	ggggaccactttgtacaagaaagctgggt
Northern analysis	**Primer**	**Primer sequences ('5 - '3)**
RLK902 (At3G17840) Exon1	RLK902 exon1-Fw	ggacgcttagtctccgtctc
	RLK902 exon1-Rv	tccaccagaaagcttcttcc
RLK902 (At3G17840) Exon2	RLK902 exon2-Fw	cctccattgaactgggaagt
	RLK902 exon2-Rv	cttgtctgggtgctgctct
ACTIN-2 (At3g18780)	ACTIN2-Fw	tcagattttgtttcgaattctctt
	ACTIN2-Rv	aaaagaaactttgatcccattca
Quantitative PCR primers	**Primer**	**Primer sequences ('5 - '3)**
ACTIN-2	ACT2-Fw	aatcacagcacttgcacca
	ACT2-Rv	gagggaagcaagaatggaac
PR-1 (*At2g14610*)	PR1-Fw	gaacacgtgcaatggagttt
	PR1-Rv	ggttccaccattgttacacct

PR-2 (*At3g57260*)	PR2-Fw	cccgtagcatactccgattt
	PR2-Rv	aaggagcttagcctcaccac
PR-5 (*At1g75040*)	PR5-Fw	ggcaaatatctccagtattcaca
	PR5-Rv	ggtagggcaattgttccttaga

***In situ* analysis**	**Primer**	**Primer sequences ('5 - '3)**
RLK902 cDNA (433 bp)	rch3probeF	gggaagtcagatcaggcatcgcccttgg
	rch3probeR	tcttcttccaccgagacaactgtctcg

***RLK902* amplification**	**Primer**	**Primer sequences ('5 - '3)**
from (c)DNA or genomic DNA	RLK902-Fw	ctcttccgtcaatcggagat
	RLK902-Rv	caccacctccaccataactg
T-DNA specific primer	RB-Fw	gttttcccagtcacgacgtt

Microscopy

Light microscopy, starch granule staining and β-glucuronidase activity, measurement of root length or number of meristematic cells was performed as described in (Willemsen et al., 1998) and (Welch et al., 2007). For confocal microscopy, roots were mounted in propidium iodide (PI; 20 µg/mL in distilled water). Whole mount RNA *in situ* hybridization was performed manually as described (Hejatko et al., 2006). A gene specific 433 bp fragment riboprobe for *RLK902* was made from cDNA using primers listed in Table 2. Infections of *H. arabidopsidis* in *Arabidopsis* leaves were visualized by trypan blue staining as described (van Damme et al., 2009). For β-glucuronidase activity in green tissues, *RLK902::GUS* dissected leaves were collected in microcentrifuge tubes on ice and incubated for 20 min in cold 90% acetone. Samples were washed in staining buffer (50 mM sodium phosphate buffer (pH 7.2), 0.2% Triton X-100, 2 mM potassium ferrocyanide and 2 mM potassium ferricyanide) on ice. Staining buffer was removed and replaced with staining buffer supplemented with 5-bromo-4-chloro-3-indolyl-beta-D-glucuronic acid (X-Gluc) to a final concentration of 2 mM. Samples were infiltrated under vacuum on ice for 15 min and incubated overnight. Samples were subjected to ethanol series of 20%, 35% and 50% (v/v) for 30 min each and incubated in fixative containing 50% ethanol (v/v), 10% glacial acetic acid (v/v) and 5% formaldehyde (v/v) for at least 30 min. Fixative was removed and 70% ethanol (v/v) was added.

Constructs and plant transformation

The pGreenII (Hellens et al., 2000) and pMDC vectors (Curtis and Grossniklaus, 2003) were used for plant transformation. *RLK902::GUS*, *35S::RLK902:GFP* and *RLK902::RLK902* were made using a two-step PCR protocol, in which the respective fragments were made full length with AttB1 and AttB2 extension primers (Table 2). For *RLK902* promoter fusions, a 1411 bp genomic DNA fragment upstream of the coding region of *RLK902* was fused into the *pMDC162* vector. For overexpression analysis, whole *RLK902* cDNA was fused in the *pMDC32* vector. For complementation analysis, the genomic region of *RLK902* starting at 1441 bp upstream of the ATG and ending at 1274 bp downstream of the stop codon was fused into the *pMDC99* vector. RKL902:GFP was generated by fusing a 1588 bp *RLK902* promoter fragment to the genomic sequence of *RLK902* in turn fused in frame to GFP and the NOS terminator and transferred to a pGreenII-vector carrying the norflurazon resistance cassette (Heidstra et al., 2004). For the *RKL1* promoter fusion, a 2548 bp genomic DNA fragment upstream of the coding region of *RKL1* was placed before *GUS* and the NOS terminator and transferred to a pGreenII-vector carrying the kanamycin resistance cassette. Plants were transformed using the floral dip method (Clough and Bent, 1998) and analyzed in next generations.

Pseudomonas growth assay

Pseudomonas syringae pv *tomato* DC3000 was grown in KB medium to an OD_{600} of 1 at 28°C and pelleted at 2500xg for 10 minutes. The bacterial cells were resuspended in 10 mM $MgSO_4$ with 0.02% (v/v) Silwet L-77 to an OD_{600} of 0.05. Plants were dipped in the bacterial suspension for a few seconds and placed immediately in a covered tray to prevent evaporation. After one hour 5 seedlings were taken, their weight was determined and processed as described below. Plants were incubated for 3 days at high humidity (80-90%) at 22°C in a short-day room. Again, 5 seedlings were taken and their weight determined. Tissue samples were ground in 500 µl 10 mM $MgSO_4$ and 5 tenfold dilutions were made in a 96-well microtiter plate. 50 µl samples were spotted onto KB agar plates containing 25 µg/ml rifampicin. The whole procedure was performed in triplicate for each measurement. The plates were incubated for 2 days at 28°C and the bacterial colonies were counted.

Nothern analysis and quantitative PCR

Northern blots were performed according to (Ausubel et al., 2003). For quantitative PCR analysis, RNA was extracted from the parental line and *rlk902* grown on soil and MS agar plates using the RNeasy kit (Qiagen). cDNA was subsequently synthesized with SuperScript III reverse transcriptase (Invitrogen) and oligo(dT)15 (Promega, Madison, WI, USA). Cycle thresholds (C_T) were determined in triplicate per transcript

by the ABI PRISM 7700 sequence detection system (Applied Biosystems, Foster City, CA, USA) using SYBR Green I (Applied Biosystems) as reporter dye. Primersets used for Northern probe amplification and C_T determinations are listed in Table 2.

CATMA arrays, labelling, hybridization, scanning and statistics

Microarray analysis was performed with CATMA version 2 arrays (complete *Arabidopsis* transcriptome microarray) (Hilson et al., 2004; Allemeersch et al., 2005). Information about CATMA and database access can be found at http://www.catma.org/ (Crowe et al., 2003). The complete microarray procedure used, analysis of spot intensities from the CATMA arrays and applied statistics were performed as described (de Jong et al., 2006).

Acknowledgements

This research was funded by the Centre for BioSystems Genomics (CBSG), which is part of the Netherlands Genomics Initiative/Netherlands Organization for Scientific Research (NGI/NWO) (CAtH and RH) and by a VIDI innovational grant from NWO (GVdA).

References

Allemeersch, J., Durinck, S., Vanderhaeghen, R., Alard, P., Maes, R., Seeuws, K., Bogaert, T., Coddens, K., Deschouwer, K., Van, H.P., Vuylsteke, M., Moreau, Y., Kwekkeboom, J., Wijfjes, A.H., May, S., Beynon, J., Hilson, P., and Kuiper, M.T. (2005). Benchmarking the CATMA microarray. A novel tool for *Arabidopsis* transcriptome analysis. Plant Physiol *137*, 588-601.

Alonso, J.M., Stepanova, A.N., Leisse, T.J., Kim, C.J., Chen, H., Shinn, P., Stevenson, D.K., Zimmerman, J., Barajas, P., Cheuk, R., Gadrinab, C., Heller, C., Jeske, A., Koesema, E., Meyers, C.C., Parker, H., Prednis, L., Ansari, Y., Choy, N., Deen, H., Geralt, M., Hazari, N., Hom, E., Karnes, M., Mulholland, C., Ndubaku, R., Schmidt, I., Guzman, P., guilar-Henonin, L., Schmid, M., Weigel, D., Carter, D.E., Marchand, T., Risseeuw, E., Brogden, D., Zeko, A., Crosby, W.L., Berry, C.C., and Ecker, J.R. (2003). Genome-wide insertional mutagenesis of *Arabidopsis thaliana*. Science *301*, 653-657.

Ausubel, F.M., Brent, R., Kingston, R.E., Moore, D.D., Seidman, J.F., Smith, J.A., and Struhl, K. (2003). Current protocols in molecular biology - Analysis of RNA by Northern and slot blot hybridization. John Wiley & Sons, Inc., N.Y.).

Bechtold, N. and Pelletier, G. (1998). In planta Agrobacterium-mediated transformation of adult *Arabidopsis thaliana* plants by vacuum infiltration. Methods Mol. Biol. *82*, 259-266.

Birnbaum, K., Shasha, D.E., Wang, J.Y., Jung, J.W., Lambert, G.M., Galbraith, D.W., and Benfey, P.N. (2003). A gene expression map of the *Arabidopsis* root. Science *302*, 1956-1960.

Brady, S.M., Orlando, D.A., Lee, J.Y., Wang, J.Y., Koch, J., Dinneny, J.R., Mace, D., Ohler, U., and Benfey, P.N. (2007). A high-resolution root spatiotemporal map reveals dominant expression patterns. Science *318*, 801-806.

Calhoun, V.C. and Levine, M. (2003). Long-range enhancerGÇôpromoter interactions in the Scr-Antp interval of the Drosophila Antennapedia complex. Proceedings of the National Academy of Sciences of the United States of America *100*, 9878-9883.

Clark, S.E., Running, M.P., and Meyerowitz, E.M. (1993). CLAVATA1, a regulator of meristem and flower development in *Arabidopsis*. Development *119*, 397-418.

Clark, S.E., Williams, R.W., and Meyerowitz, E.M. (1997). The CLAVATA1 gene encodes a putative receptor kinase that controls shoot and floral meristem size in *Arabidopsis*. Cell *89*, 575-585.

Clough, S.J. and Bent, A.F. (1998). Floral dip: a simplified method for Agrobacterium-mediated transformation of *Arabidopsis thaliana*. Plant J. *16*, 735-743.

Crowe, M.L., Serizet, C., Thareau, V., Aubourg, S., Rouze, P., Hilson, P., Beynon, J., Weisbeek, P., Van, H.P., Reymond, P., Paz-Ares, J., Nietfeld, W., and Trick, M. (2003). CATMA: a complete *Arabidopsis* GST database. Nucleic Acids Res. *31*, 156-158.

Curtis, M.D. and Grossniklaus, U. (2003). A gateway cloning vector set for high-throughput functional analysis of genes in planta. Plant Physiol *133*, 462-469.

de Jong, M., van, B.B., Wittink, F.R., Menke, F.L., Weisbeek, P.J., and Van den, A.G. (2006). Membrane-associated transcripts in *Arabidopsis*; their isolation and characterization by DNA microarray analysis and bioinformatics. Plant J. *46*, 708-721.

Dievart, A. and Clark, S.E. (2004). LRR-containing receptors regulating plant development and defense. Development *131*, 251-261.

Endre, G., Kereszt, A., Kevei, Z., Mihacea, S., Kalo, P., and Kiss, G.B. (2002). A receptor kinase gene regulating symbiotic nodule development. Nature *417*, 962-966.

Gomez-Gomez, L. and Boller, T. (2000). FLS2: an LRR receptor-like kinase involved in the perception of the bacterial elicitor flagellin in *Arabidopsis*. Mol. Cell *5*, 1003-1011.

Heidstra, R., Welch, D., and Scheres, B. (2004). Mosaic analyses using marked activation and deletion clones dissect *Arabidopsis* SCARECROW action in asymmetric cell division. Genes Dev. *18*, 1964-1969.

Hejatko, J., Blilou, I., Brewer, P.B., Friml, J., Scheres, B., and Benkova, E. (2006). In situ hybridization technique for mRNA detection in whole mount *Arabidopsis* samples. Nat Protoc. *1*, 1939-1946.

Hellens, R.P., Edwards, E.A., Leyland, N.R., Bean, S., and Mullineaux, P.M. (2000). pGreen: a versatile and flexible binary Ti vector for Agrobacterium-mediated plant transformation. Plant Mol Biol *42*, 819-832.

Hilson, P., Allemeersch, J., Altmann, T., Aubourg, S., Avon, A., Beynon, J., Bhalerao, R.P., Bitton, F., Caboche, M., Cannoot, B., Chardakov, V., Cognet-Holliger, C., Colot, V., Crowe, M., Darimont, C., Durinck, S., Eickhoff, H., de Longevialle, A.F., Farmer, E.E., Grant, M., Kuiper, M.T., Lehrach, H., Leon, C., Leyva, A., Lundeberg, J., Lurin, C., Moreau, Y., Nietfeld, W., Paz-Ares, J., Reymond, P., Rouze, P., Sandberg, G., Segura, M.D., Serizet, C., Tabrett, A., Taconnat, L., Thareau, V., Van, H.P., Vercruysse, S., Vuylsteke, M., Weingartner, M., Weisbeek, P.J., Wirta, V., Wittink, F.R., Zabeau, M., and Small, I. (2004). Versatile gene-specific sequence tags for *Arabidopsis* functional genomics: transcript profiling and reverse genetics applications. Genome Res. *14*, 2176-2189.

Kwak, S.H., Shen, R., and Schiefelbein, J. (2005). Positional Signaling Mediated by a Receptor-like Kinase in *Arabidopsis*. Science *307*, 1111-1113.

Laux, T. (2003). The stem cell concept in plants: a matter of debate. Cell *113*, 281-283.

Maleck, K., Levine, A., Eulgem, T., Morgan, A., Schmid, J., Lawton, K.A., Dangl, J.L., and Dietrich, R.A. (2000). The transcriptome of *Arabidopsis thaliana* during systemic acquired resistance. Nat. Genet. *26*, 403-410.

Merli, C., Bergstrom, D.E., Cygan, J.A., and Blackman, R.K. (1996). Promoter specificity mediates the independent regulation of neighboring genes. Genes & Development *10*, 1260-1270.

Morillo, S.A. and Tax, F.E. (2006). Functional analysis of receptor-like kinases in monocots and dicots. Current Opinion in Plant Biology *9*, 460-469.

Nam, K.H. and Li, J. (2002). BRI1/BAK1, a Receptor Kinase Pair Mediating Brassinosteroid Signaling. Cell *110*, 203-212.

Nobrega, M.A., Ovcharenko, I., Afzal, V., and Rubin, E.M. (2003). Scanning Human Gene Deserts for Long-Range Enhancers. Science *302*, 413.

Nurnberger, T. and Kemmerling, B. (2006). Receptor protein kinases--pattern recognition receptors in plant immunity. Trends Plant Sci. *11*, 519-522.

Ohtake, Y., Takahashi, T., and Komeda, Y. (2000). Salicylic acid induces the expression of a number of receptor-like kinase genes in *Arabidopsis thaliana*. Plant Cell Physiol *41*, 1038-1044.

Ren, S., Johnston, J.S., Shippen, D.E., and McKnight, T.D. (2004). TELOMERASE ACTIVATOR1 Induces Telomerase Activity and Potentiates Responses to Auxin in *Arabidopsis*. Plant Cell *16*, 2910-2922.

Rosso, M.G., Li, Y., Strizhov, N., Reiss, B., Dekker, K., and Weisshaar, B. (2003). An *Arabidopsis thaliana* T-DNA mutagenized population (GABI-Kat) for flanking sequence tag-based reverse genetics. Plant Mol. Biol. *53*, 247-259.

Sabatini, S., Heidstra, R., Wildwater, M., and Scheres, B. (2003). SCARECROW is involved in positioning the stem cell niche in the *Arabidopsis* root meristem. Genes Dev. *17*, 354-358.

Saeed, A.I., Sharov, V., White, J., Li, J., Liang, W., Bhagabati, N., Braisted, J., Klapa, M., Currier, T., Thiagarajan, M., Sturn, A., Snuffin, M., Rezantsev, A., Popov, D., Ryltsov, A., Kostukovich, E., Borisovsky, I., Liu, Z., Vinsavich, A., Trush, V., and Quackenbush, J. (2003). TM4: a free, open-source system for microarray data management and analysis. Biotechniques *34*, 374-378.

Scholl, R.L., May, S.T., and Ware, D.H. (2000). Seed and molecular resources for *Arabidopsis*. Plant Physiol *124*, 1477-1480.

Schwab, R., Ossowski, S., Riester, M., Warthmann, N., and Weigel, D. (2006). Highly specific gene silencing by artificial microRNAs in *Arabidopsis*. Plant Cell *18*, 1121-1133.

Sessions, A., Burke, E., Presting, G., Aux, G., McElver, J., Patton, D., Dietrich, B., Ho, P., Bacwaden, J., Ko, C., Clarke, J.D., Cotton, D., Bullis, D., Snell, J., Miguel, T., Hutchison, D., Kimmerly, B., Mitzel, T., Katagiri, F., Glazebrook, J., Law, M., and Goff, S.A. (2002). A high-throughput *Arabidopsis* reverse genetics system. Plant Cell *14*, 2985-2994.

Shiu, S.H. and Bleecker, A.B. (2001). Receptor-like kinases from *Arabidopsis* form a monophyletic gene family related to animal receptor kinases. Proc. Natl. Acad. Sci. U. S. A *98*, 10763-10768.

Song, W.Y., Wang, G.L., Chen, L.L., Kim, H.S., Pi, L.Y., Holsten, T., Gardner, J., Wang, B., Zhai, W.X., Zhu, L.H., Fauquet, C., and Ronald, P. (1995). A receptor kinase-like protein encoded by the rice disease resistance gene, Xa21. Science *270*, 1804-1806.

Stracke, S., Kistner, C., Yoshida, S., Mulder, L., Sato, S., Kaneko, T., Tabata, S., Sandal, N., Stougaard, J., Szczyglowski, K., and Parniske, M. (2002). A plant receptor-like kinase required for both bacterial and fungal symbiosis. Nature *417*, 959-962.

Tarutani, Y., Morimoto, T., Sasaki, A., Yasuda, M., Nakashita, H., Yoshida, S., Yamaguchi, I., and Suzuki, Y. (2004). Molecular characterization of two highly homologous receptor-like kinase genes, RLK902 and RKL1, in *Arabidopsis thaliana*. Biosci. Biotechnol. Biochem. *68*, 1935-1941.

Tor, M., Lotze, M.T., and Holton, N. (2009). Receptor-mediated signalling in plants: molecular patterns and programmes. J. Exp. Bot. *60*, 3645-3654.

Torii, K.U., Mitsukawa, N., Oosumi, T., Matsuura, Y., Yokoyama, R., Whittier, R.F., and Komeda, Y. (1996). The *Arabidopsis* ERECTA gene encodes a putative receptor protein kinase with extracellular leucine-rich repeats. Plant Cell *8*, 735-746.

van Damme, M., Zeilmaker, T., Elberse, J., Andel, A., de Sain-van der Velden, and Van den, A.G. (2009). Downy mildew resistance in *Arabidopsis* by mutation of HOMOSERINE KINASE. Plant Cell *21*, 2179-2189.

van den Berg, C., Willemsen, V., Hendriks, G., Weisbeek, P., and Scheres, B. (1997). Short-range control of cell differentiation in the *Arabidopsis* root meristem. Nature *390*, 287-289.

van Zanten, M., Snoek, L.B., Proveniers, M.C.G., and Peeters, A.J.M. (2009). The many functions of ERECTA. Trends in Plant Science *14*, 214-218.

Weigel, D., Ahn, J.H., Blazquez, M.A., Borevitz, J.O., Christensen, S.K., Fankhauser, C., Ferrandiz, C., Kardailsky, I., Malancharuvil, E.J., Neff, M.M., Nguyen, J.T., Sato, S., Wang, Z.Y., Xia, Y., Dixon, R.A., Harrison, M.J., Lamb, C.J., Yanofsky, M.F., and Chory, J. (2000). Activation tagging in *Arabidopsis*. Plant Physiol *122*, 1003-1013.

Welch, D., Hassan, H., Blilou, I., Immink, R., Heidstra, R., and Scheres, B. (2007). *Arabidopsis* JACKDAW and MAGPIE zinc finger proteins delimit asymmetric cell division and stabilize tissue boundaries by restricting SHORT-ROOT action. Genes Dev. *21*, 2196-2204.

Wesley, S.V., Helliwell, C.A., Smith, N.A., Wang, M.B., Rouse, D.T., Liu, Q., Gooding, P.S., Singh, S.P., Abbott, D., Stoutjesdijk, P.A., Robinson, S.P., Gleave, A.P., Green, A.G., and Waterhouse, P.M. (2001). Construct design for efficient, effective and high-throughput gene silencing in plants. Plant J. *27*, 581-590.

Willemsen, V., Wolkenfelt, H., de Vrieze G., Weisbeek, P., and Scheres, B. (1998). The HOBBIT gene is required for formation of the root meristem in the *Arabidopsis* embryo. Development *125*, 521-531.

Yoo, S.Y., Bomblies, K., Yoo, S.K., Yang, J.W., Choi, M.S., Lee, J.S., Weigel, D., and Ahn, J.H. (2005). The 35S promoter used in a selectable marker gene of a plant transformation vector affects the expression of the transgene. Planta *221*, 523-530.

Zipfel, C. and Felix, G. (2005). Plants and animals: a different taste for microbes? Current Opinion in Plant Biology *8*, 353-360.

Summary and concluding remarks

We have investigated asymmetric cell division, root patterning and meristem maintenance using forward and reverse genetics approaches. In this summarizing chapter I will discuss the results in light of recent insights and give directions for future research.

Chapter 2 describes the identification of the *schizoriza* (*scz*) mutant from a QC-marker based mutagenesis screen aimed to isolate plants with QC/stem cell defective roots. A previous study implicated *SCZ* as a suppressor of epidermal fate and mediator of periclinal ground tissue divisons (Mylona et al., 2002). We went on to provide a detailed description of the *scz* mutant phenotype and show that it is involved in fate segregation during asymmetric divisions in the stem cell region. The *SCZ* gene was cloned based on map position and shown to encode a member of the family of heat shock transcription factors, albeit one that appears to be recruited for development instead of stress signaling. The pleiotropic effects of the *scz* mutation define the existence of a novel mechanism for patterning cell identity in the *Arabidopsis* root. The proposed activity of *SCZ* is that it acts in the ground tissue to determine its fate from embryogenesis onward and suppresses epidermis and lateral root cap fate in the ground tissue. Non-cell autonomous *SCZ* action maintains QC fate and suppresses columella fate in the QC and in addition segregates epidermis and lateral root cap fate, presumably through a ground tissue derived unknown factor. The next challenge will be to provide a mechanistic understanding of how *SCZ* exerts its function during asymmetric division. From the complementation studies it appears that cortical expression of SCZ is sufficient to restore the mutant phenotype to wild type. The non-cell autonomous activity of SCZ on neighboring tissue fate segregation implies signaling from the cortex. Complementation analysis also shows that it is not SCZ itself that is moving. Instead, a target of SCZ is likely traveling between tissues, possibly a transcription factor, moving in a way similar to what has been described for the action of SHR in ground tissue patterning. Using an inducible SCZ protein that can completely rescue the mutant phenotype upon induction allows identification of such downstream targets by microarray analysis. In addition, expression of SCZ in the ground tissue domain by way of N9094 enhancer transactivation rescues the *scz-2* mutant defect. This allows the specific selection of the immediate SCZ responsive cells from the N9094 expression domain whilst driving inducible SCZ protein by way of fluorescence activated cell sorting in combination with microarray analysis. These experiments can be elaborated on by sorting cells from those tissues affected by SCZ induction to identify links to the process of fate segregation. Another application of the inducible SCZ is to follow the fate segregation upon induction, which provides a tool to study the components of the cell machinery, e.g. cytoskeleton components and vesicle transport that are recruited for this process. Given that

SCZ contains a recently identified repressor domain it is possible that the protein acts as a transcriptional repressor. Alleviated expression of SCZ targets would then be responsible for the phenotypic defects in the mutant. Currently, a mutagenesis screen for suppressors of *SCZ* is being undertaken, which may lead to the identification of such components. Yeast two hybrid studies showed protein interaction between SCZ and another Hsf protein amongst others (CAtH, unpublished data), indicating that SCZ may act together with other factors in the control of cell division asymmetry. Indeed, several close paralogs of *SCZ* are highly expressed in the root stem cell niche (Derbyshire et al., 2008). However, analysis of the single knockouts did not reveal root developmental phenotypes (CAtH, unpublished data). Possibly, the double mutant may reveal additional or enhanced phenotypes compared to the *scz* single mutant. Taken together, these diverse approaches should shed more light on SCZ action.

In **Chapter 3** we report on the *SCZ* interaction with the well characterized root patterning transcription factor genes *SHR*, *SCR*, *PLT1* and *PLT2*, all of which show expression overlap in the root QC and stem cell niche progenitors (Di Laurenzio et al., 1996; Helariutta et al., 2000; Wysocka-Diller et al., 2000; Nakajima et al., 2001; Sabatini et al., 2003; Aida et al., 2004; Galinha et al., 2007). *scz-2 plt1-4 plt2-2* triple mutants resembled *plt1-4 plt2-2* double mutants whereas *scz-2 shr-2* and *scz-2 scr-4* double mutants showed severely enhanced phenotypes compared to the *scz-2*, *shr-2* and *scr-4* single mutants. Given the results we suggested that *SCZ* acts in a parallel pathway with *SHR/SCR* to specify the stem cell niche in the early embryo. How *SCZ*, *SHR* and *SCR* genes act together remains unclear. Interaction studies revealed no binding in yeast. In addition, *SCZ* was not identified as a target of SHR (Levesque et al., 2006), nor was *SCZ* promoter activity hampered in *shr-2* or *scr-4* mutants. However, we cannot rule out the possibility that local activity of SHR/SCR initiates *SCZ* expression in the embryo. A puzzling result in the *scz-2 shr-2* double mutant mature embryo is the apparent presence of two ground tissue layers that extend from the hypocotyl all the way down in the embryonic root tip compared to a single layer in the *shr-2* mutant mature embryo. Future studies introducing markers should determine the tissue identities in the *scz-2 shr-2* double mutant to support the interaction proposed here. Downstream *SCZ* effectors should reveal the putative overlap with SHR targets.

Chapters 4, 5 and **6** of this thesis probe the conservation of shoot and root meristem maintenance pathways in light of paralogous ligands and receptors identified in shoots, in particular CLE type ligands and CLV1 type receptor-like kinases (RLKs). Two different approaches have been used in these chapters to investigate this link: a ligand based approach based on meristem consumption upon CLE overexpression

(Chapter 4), and a phenotype screen using a custom collection of root expressed LRR RLK T-DNA insertion lines (Chapters 5 and 6).

Chapter 4 describes the identification of *sol3* from an activation tagging screen aimed to find suppressors of RCH1>>CLE19 induced root meristem consumption. This implicates *SOL3* as a putative new component of the CLE signaling pathway. Phenotypic characterization revealed that *SOL3* has a dual role in the root, controlling both growth and formative cell divisions. *sol3* roots grow faster than wild type reminiscent of cytokinin synthesis or signaling mutants. Indeed, *sol3* appears largely unaffected to cytokinin treatment. Whether the enhanced root growth phenotype is due to lower levels of cytokinin or signaling awaits further characterization, e.g. measuring cytokinin levels or determining expression of cytokinin biogenesis and signaling related genes. The long root phenotype is combined with a delay in ground tissue formative division, particularly in the embryo. In addition, root columella layers are consistently reduced throughout development. CLE signaling by means of the CLE40 peptide and its putative receptor ACR4 has recently been implicated in controling columella formative divisions in the root apex (De Smet et al., 2008; Stahl et al., 2009; Stahl and Simon, 2009). Whether SOL3 is involved in this signaling awaits further characterization and double mutant analysis. The identity of the *SOL3* gene is bound to shed more light on its function. So far, the complex T-DNA insertions and unsequenced Columbia Utrecht ecotype background have hampered its cloning. However, with the aid of new generation sequencing it is now feasible to elucidate the insertion sites. CLE peptides are one of many peptides that have recently been described with functions in various aspects of growth and development. Peptide signaling turns out to play a greater than anticipated role in intercellular and extracellular signaling in plants, e.g. controlling defense responses, callus growth, meristem organization, self-incompatibility, root growth, leaf-shape regulation and organ abscision. A further characterization of these peptides together with the identification of their ligand-receptor interactions should improve the understanding of peptide signaling in plants.

With the complete *Arabidopsis* genome available it is possible to do large scale reverse genetic studies. In **Chapter 5**, we describe such a reverse genetics approach where we surveyed the roles of LRR RLK genes in roots using a custom T-DNA insertion set concentrating on receptors that are expressed in the root meristem. Our objectives were to analyze CLV1 paralogs for involvement in root meristem maintenance and to gain a broader understanding of the function of LRR RLKs in root growth in general. We established a collection of 134 homozygous T-DNA insertion lines for 69 LRR RLKs. No root developmental phenotypes were observed for single receptor mutants that were not already described. This result indicates a high level of redundancy among these receptors or the unlikely situation that none of these

are involved in root development. In addition, we analyzed this collection for altered root growth responsiveness to various external stimuli, including hormonal, chemical and abiotic stress. We showed the involvement of many LRR RLKs in several of the conditionally induced phenotypes. The observation that many T-DNA insertion lines respond to more than one treatment supports the existence of extensive cross talk and signal integration among different signaling pathways. With respect to hormones, for which receptors are identified, resistance or sensitivity may indicate a function of receptor signaling in secondary signaling events. We could not detect a clear relationship between conditional phenotypes and phylogeny, suggesting that these transmembrane LRR RLKs, despite a fairly similar domain organization, can easily acquire different functions compared to their closest paralogs during evolution. A large scale analysis of the transcriptional response of the 604-member RLK gene family to a range of known environmental and developmental stimuli demonstrated a broad response of these kinases to multiple treatments (Chae et al., 2009). With our functional data at hand we took it one step further and analyzed whether there was overlap between LRR RLK behavior at the transcriptome level and the functional characterization of corresponding mutants. Although we could distinguish LRR RLK gene clusters with similar behavior at the transcriptome level upon different stress treatments, there was no indication for functional overlap among the LRR RLKs tested and their clustered expression patterns.

Chapter 6 dealt with the characterization of one of the tested mutant LRR RLKs, *rlk902*, which combined two diverse phenotypes: reduced root growth and resistance to the downy mildew pathogen *H. arabidopsidis*. The resistance phenotype appears to be pathogen specific as defense genes are not constitutively overexpressed and no resistance to *Pseudomonas syringae pv. tomato* 3000 is observed in *rlk902*. An activation tag T-DNA in *rlk902* was inserted at the end of the single intron of *RLK902* disrupting its expression. *RLK902* is expressed in the root meristem, which correlates with a role for *RLK902* in cell proliferation. However, *RLK902* promoter driven GUS activity did not correlate with downy mildew Waco9 infection. Complementation of the *rlk902* mutant with the intact *RLK902* gene failed to rescue and *RLK902* RNAi and amiRNA approaches did not mimic the *rlk902* mutant phenotypes. We concluded that the *rlk902* root growth defect and downy mildew resistance are not caused by the disruption of *RLK902*. Nevertheless, backcross analysis argued for linkage between the T-DNA insertion and the observed phenotypes in *rlk902*. Subsequent microarray studies revealed gene expression was downregulated within a region of approximately 84 kb upstream of the *rlk902* mutation. However, no phenotypes were observed in T-DNA insertion lines for any of the 25 genes tested within this region. There are several possibilities to explain this observation: the affected gene responsible for the phenotypes may not be annotated and therefore not present

on the CATMA array, the tested T-DNA insertion did not cause disruption of the responsible gene or downregulation of a combination of genes in the 84 kb region is perhaps causing the observed phenotypes. Identifying the gene(s) involved will be the challenge for future studies involving *rlk902*. Currently, large and overlapping DNA fragments in the form of TAC clones are tested for complementation in the *rlk902* background to identify the gene(s) causing the mutant phenotype.

The identification of *SCZ* as factor involved in tissue specification and cell fate segregation provides a basis for future research into mechanisms of asymmetric division. Work on CLE ligand signaling identified *SOL3* as a factor controlling root growth and formative divisions and the LRR RLK reverse genetics indicated the existence of extensive cross talk and signal integration among different RLK signaling pathways in the *Arabidopsis* root. A challenge for the future will be to integrate these results with signaling networks for root patterning and growth.

References

Aida, M., Beis, D., Heidstra, R., Willemsen, V., Blilou, I., Galinha, C., Nussaume, L., Noh, Y.S., Amasino, R., and Scheres, B. (2004). The PLETHORA genes mediate patterning of the *Arabidopsis* root stem cell niche. Cell *119*, 109-120.

Chae, L., Sudat, S., Dudoit, S., Zhu, T., and Luan, S. (2009). Diverse transcriptional programs associated with environmental stress and hormones in the *Arabidopsis* receptor-like kinase gene family. Mol. Plant *2*, 84-107.

De Smet, I., Vassileva, V., De, R.B., Levesque, M.P., Grunewald, W., Van, D.D., Van, N.G., Naudts, M., Van, I.G., De, C.R., Wang, J.Y., Meuli, N., Vanneste, S., Friml, J., Hilson, P., Jurgens, G., Ingram, G.C., Inze, D., Benfey, P.N., and Beeckman, T. (2008). Receptor-like kinase ACR4 restricts formative cell divisions in the *Arabidopsis* root. Science *322*, 594-597.

Derbyshire, P., Drea, S., Shaw, P.J., Doonan, J.H., and Dolan, L. (2008). Proximal-distal patterns of transcription factor gene expression during *Arabidopsis* root development. J. Exp. Bot. *59*, 235-245.

Di Laurenzio, L., Wysocka-Diller, J., Malamy, J.E., Pysh, L., Helariutta, Y., Freshour, G., Hahn, M.G., Feldmann, K.A., and Benfey, P.N. (1996). The SCARECROW gene regulates an asymmetric cell division that is essential for generating the radial organization of the *Arabidopsis* root. Cell *86*, 423-433.

Galinha, C., Hofhuis, H., Luijten, M., Willemsen, V., Blilou, I., Heidstra, R., and Scheres, B. (2007). PLETHORA proteins as dose-dependent master regulators of *Arabidopsis* root development. Nature *449*, 1053-1057.

Helariutta, Y., Fukaki, H., Wysocka-Diller, J., Nakajima, K., Jung, J., Sena, G., Hauser, M.T., and Benfey, P.N. (2000). The SHORT-ROOT gene controls radial patterning of the *Arabidopsis* root through radial signaling. Cell *101*, 555-567.

Levesque, M.P., Vernoux, T., Busch, W., Cui, H., Wang, J.Y., Blilou, I., Hassan, H., Nakajima, K., Matsumoto, N., Lohmann, J.U., Scheres, B., and Benfey, P.N. (2006). Whole-genome analysis of the SHORT-ROOT developmental pathway in *Arabidopsis*. PLoS. Biol. *4*, e143.

Mylona, P., Linstead, P., Martienssen, R., and Dolan, L. (2002). SCHIZORIZA controls an asymmetric cell division and restricts epidermal identity in the *Arabidopsis* root. Development *129*, 4327-4334.

Nakajima, K., Sena, G., Nawy, T., and Benfey, P.N. (2001). Intercellular movement of the putative transcription factor SHR in root patterning. Nature *413*, 307-311.

Sabatini, S., Heidstra, R., Wildwater, M., and Scheres, B. (2003). SCARECROW is involved in positioning the stem cell niche in the *Arabidopsis* root meristem. Genes Dev. *17*, 354-358.

Stahl, Y. and Simon, R. (2009). Is the *Arabidopsis* root niche protected by sequestration of the CLE40 signal by its putative receptor ACR4? Plant Signal. Behav. *4*, 634-635.

Stahl, Y., Wink, R.H., Ingram, G.C., and Simon, R. (2009). A signaling module controlling the stem cell niche in *Arabidopsis* root meristems. Curr. Biol. *19*, 909-914.

Wysocka-Diller, J.W., Helariutta, Y., Fukaki, H., Malamy, J.E., and Benfey, P.N. (2000). Molecular analysis of SCARECROW function reveals a radial patterning mechanism common to root and shoot. Development *127*, 595-603.

Nederlandse samenvatting

Meercellige organismen zoals plant en dier ontwikkelen zich uit een enkele cel, de zygote. Gedurende ontwikkeling wordt er een bouwplan aangelegd; de zygote deelt en creëert zo vele miljoenen cellen, die complexe weefsels vormen. Een essentieel en universeel mechanisme om deze diversiteit te genereren is asymmetrische celdeling waarbij twee verschillende dochtercellen ontstaan uit een oudercel. Tijdens de ontwikkeling van plant en dier spelen stamcellen een grote rol. Deze relatief ongedifferentieerde cellen handhaven zich door zichzelf te vernieuwen en leveren continu cellen aan om de verschillende weefsels te kunnen vormen. In tegenstelling tot dieren blijven planten gedurende hun hele levenscyclus nieuwe organen ontwikkelen. Ook hier zijn de stamcellen voor verantwoordelijk. Deze oorspronkelijke set stamcellen zijn tijdens de embryogenese aangelegd in het scheut apicale meristeem en het wortelmeristeem. Het scheut apicale meristem vormt alle bovengrondse delen en het wortelmeristeem vormt het wortelstelsel. Cellen in het meristeem ondergaan een gedefinieerd aantal delingen voordat ze het meristeem verlaten en gaan strekken en differentiëren. Door een juiste balans tussen celdeling en celdifferentiatie te handhaven behoudt het meristeem een bepaalde omvang en wordt de groei van organen op de juiste manier gereguleerd. In het wortelmeristeem omringen de stamcellen het quiescent center (QC); samen worden ze vaak aangeduid als de stamcel niche. De huidige hypothese is dat gedurende de evolutie het wortelmeristeem zich ontwikkeld heeft uit het scheutmeristeem. Dit is vermoedelijk het resultaat van de veranderende condities over het verloop van tijd waaraan de plant zich heeft moeten aanpassen voor het succesvol kunnen blijven verkrijgen van voedingstoffen en water opname en om zichzelf te kunnen verankeren. Dit doet vermoeden dat er gen-netwerken, vergelijkbaar aan degene die belangrijk zijn in de ontwikkeling en handhaving van de scheut, een rol kunnen spelen in de regulatie van het wortelmeristeem. Verschillende studies die gebruik maken van de model plant *Arabidopsis thaliana* (de zandraket) duiden hierop wat betreft fytohormonen, transcriptiefactoren alsook peptide liganden en hun receptoren.

Het doel van dit proefschrift was om een beter begrip te krijgen van de mechanismen betrokken bij patroonvorming in de *Arabidopsis* wortelpunt en de handhaving van het wortelmeristeem tijdens de ontwikkeling. Hierbij is gebruik gemaakt van "forward genetics" en "reverse genetics" technieken. Waar **Hoofdstukken 1, 2** en **3** van dit proefschrift zich bezig houden met het verkrijgen van cel identiteit door asymmetrische celdeling in de wortel, wordt in **Hoofdstukken 4, 5** en **6** gekeken naar ligand-receptor signalering en conservering van signaaltransductieketens in scheut en wortel.

Hoofdstuk 1 geeft een overzicht van de huidige kennis van celspecificatie via asymmetrische celdeling in *Arabidopsis*. Specifieke voorbeelden waarop wordt ingegaan zijn stamceldelingen, patroonvorming van een subset van weefsels in de wortel en van de huidmondjes (stomata).

In **Hoofdstuk 2** wordt de *schizoriza* (*scz*) mutant gekarakteriseerd. *scz* werd opgepikt als een mutant met een QC -en stamceldefect in de wortel uit een mutagenese screen op planten die QC-specifieke markers dragen. *SCZ* codeert voor een nucleaire factor die gelijkenissen vertoont met de familie van heat shock transcriptiefactoren. Het gen blijkt verantwoordelijk voor het scheiden van cel identiteit gedurende asymmetrische deling in de stamcel niche van de wortel en voor de specificatie van de cortex laag. De resultaten duiden erop dat *SCZ* een nieuw mechanisme voor asymmetrische celdeling definieert in de plant.

De functie van *SCZ* is verder onderzocht in **Hoofdstuk 3** door te kijken naar interacties met de bekende wortel patroonvormingsgenen: *PLETHORA1* (*PLT1*), *PLT2*, *SHORT-ROOT* (*SHR*) en *SCARECROW* (*SCR*). Uit de resultaten blijkt dat *SCZ* samen met *SHR* en *SCR* werkt om de stamcel niche in de wortel aan te leggen gedurende embryogenese.

Het CLV3-CLV1 ligand-receptor paar is verantwoordelijk voor handhaving van het scheutmeristeem. Overexpressie van A-klasse CLE peptiden, zoals CLV3 en CLE19, leidt tot differentiatie van het scheutmeristeem alsook het wortelmeristeem. Dit doet vermoeden dat ook in de wortel een CLV-type signaaltransductieketen actief is die de handhaving van dit meristeem reguleert. Deze hypothese wordt verder uitgewerkt in **Hoofdstukken 4, 5** en **6**.

Hoofdstuk 4 beschrijft de isolatie en karakterisatie van de *sol3* mutant. Om nieuwe factoren te vinden die betrokken zijn bij de CLE signalering is een "suppressor mutagenese screen" uitgevoerd. De mutant *sol3* herstelt het door CLE19 veroorzaakte wortelmeristeemdifferentiatie defect en laat tegelijkertijd een toename van wortelgroei zien. Versterkte wortelgroei wordt vaak waargenomen in cytokinine biosynthese -en signaleringsmutanten en de verminderde wortelrespons van *sol3* na toediening van dit hormoon doet vermoeden dat een cytokinine defect verantwoordelijk is voor defecten in *sol3*. Daarnaast blijkt dat *SOL3* ook een rol speelt bij het controleren van weefselvormende delingen in de wortel.

In **Hoofdstuk 5** beschrijf ik een "reverse genetics" strategie om te onderzoeken of CLV1 paraloge leucine-rijke repeat (LRR) receptor kinases betrokken zijn bij wortelontwikkeling. Hiervoor is een homozygote set van T-DNA insertielijnen samengesteld van LRR receptor kinases die in het wortelmeristeem tot expressie komen. Deze set is vervolgens gescreend op veranderingen in wortelontwikkeling en veranderde respons na het toedienen van verschillende soorten van stress. Het feit dat er naast eerder beschreven genen slechts één mutant met fenotypes onder

normale groeiomstandigheden is gevonden duidt op een hoge mate van redundantie. De resultaten uit de conditionele screen, echter, geven blijk van het bestaan van een omvangrijke samenspraak en signaal integratie van de verschillende LRR receptor kinases in de wortel.

In **Hoofdstuk 6** wordt de mutant *rlk902*, in Hoofdstuk 5 opgepikt als een mutant met een kortere wortel, verder gekarakteriseerd. Naast een korter wortelmeristeem blijkt *rlk902* ook resistent te zijn tegen valse meeldauw. De gevonden fenotypes lijken echter niet veroorzaakt door mutatie van het *RLK902* gen. Desondanks is het fenotype wel gelinkt aan de T-DNA insertie en microarray studies laten zien dat een in gebied van 84 kilobase expressie van genen verlaagd is in deze lijn. Naar alle waarschijnlijkheid is downregulatie van een of meerdere genen in dit gebied de oorzaak van de fenotypes.

Aan het eind van dit proefschrift worden de behaalde resultaten samengevat en mogelijkheden voor vervolgonderzoek aangedragen.

Dankwoord

Graag wil ik op deze plaats iedereen bedanken die mij op welke manier dan ook gesteund heeft in het welslagen van mijn promotieonderzoek gedurende de tijd die ik bij de vakgroep Moleculaire Genetica heb doorgebracht.
Allereerst wil ik mijn ouders, mijn zus, zwager en nichtjes bedanken voor de nimmer aflatende steun en liefde. Ik prijs me zeer gelukkig met jullie in mijn leven.
Zoltán, ook al is het niet in woorden uit te drukken wat ik aan je heb, ik zal toch een poging wagen. Brain, looks and personality, je hebt het alle drie. Het spijt me dat alle extra tijd die in deze promotie ging zitten ten koste ging van de tijd die ik met jou doorbracht. Iets dat zo veel belangrijker is. Vanaf nu beter ik mijn leven. Je bent een ontzettend eigenwijs, koppig en irritant, maar bovenal een ontzettend lief, mooi, knap en bijzonder mens. Ik ben blij dat ik mijn leven met je door mag brengen en ik hou van je.
Mijn schoonouders bedank ik graag voor hun belangstelling en voor het geven van de vele etenswaren om ons zo wat werk uit handen te kunnen nemen. Natuurlijk bedank ik hier ook mijn twee favoriete poezen voor hun eigen, unieke bijdrage aan het afschrijven van dit boekje.
Alle vriendjes bedankt voor de broodnodige afleiding. Sylvia, Renske, Luc, Pauline, Fleur, Tine (en aanhang), al vele jaren zorgen jullie voor ontspanning en gezelligheid. Ik hoop dat we nog lang door mogen gaan met de vele etentjes en weekendjes weg. Dennis, Sylvia, Jochem, Joost, Rinse, Daan, het heeft even geduurd, maar zo meteen is echt iedereen gepromoveerd. Jessica, dank je voor alle aangeboden hulp. Marije, graag pak ik vanaf nu het squashen weer op. Iedereen van het veld -en zaalvoetbal, die er voor zorgde dat ik niet hoefde na te denken en alleen maar tegen een balletje hoefde te trappen, gevolgd door een gezellige derde helft.
Tijdens mijn studie raakte ik gefascineerd door ontwikkelingsbiologie door de colleges van Wim Dictus en André van Loon, gevolgd door een eerste onderszoeksstage bij de vakgroep Ontwikkelingsbiologie, waar ik het genoegen had om met mensen zoals Adri, Willem, Peter, Lex, Pascal en Rosanna te mogen werken. Bedankt voor het aanwakkeren van mijn interesse.
Graag bedank ik de mensen die dagelijks betrokken waren bij het werk hier beschreven; de vele collega's die er voor zorgden dat ik elke dag met plezier naar het werk ging. Om er een aantal uit te lichten: Anja, mijn kamer –en Lunetten fietsgenoot, bedankt voor de gezelligheid en sterkte met al het labregelwerk. Viola, jammer dat ik je een jaar heb moeten missen. Vera en Fenne, bedankt voor het vele pipetteerwerk dat jullie verricht hebben voor de conditionele RLK screen. Vera, veel succes met het SCZ vervolgproject en Inez met het afmaken van het SCZ-SHR verhaal. Wouter, bedankt voor je bijdrage aan SCZ. Het bleek een interessanter project te zijn dan je zelf

wilde inzien. Mark, bedankt voor de leuke samenwerking aan de *rlk902* mutant. Mijn kamergenoten: Carla, Jeroen, José, Cristina, Marta, Bea, labgenoten: Marijn, Hala, Noor, Ana, Akie, Pankaj, Maartje en de vele collega's die nog in het lab rondlopen of naar andere oorden vertrokken zijn: Marion, Alexis, Smita, AaPee, Jose, David, Jian, Prem, Frank, Hugo, Klaartje, Guy, Violaine, Kalika, Albert, Tom, Herman, Hongtao, René (pardon, dr. Benjamins), Sara, Gabino, Verônica, Alfredo, Sharon, Maaike en alle studenten bedank ik voor alle gezelligheid op de werkvloer, de waardevolle discussies, gezellige borrels, filmavonden, Sinterklaas -en kerstvieringen. Ook de mensen van Guido's en Sjefs groep bedank ik voor de gezelligheid, de vele taart en de gezamenlijke kerstdiners. Frits en Ronald wil ik graag bedanken voor alle hulp. Ik ben de tel kwijtgeraakt hoe vaak ik bij jullie heb aangeklopt, maar het was altijd een feest. Pieter, bedankt voor het maken van prijswinnende posters. Miriam, Maartje, Ton, Cor, Jan, Nebal, Mohammed, Tony, Ria en Fred, bedankt voor alle ondersteuning en belangstelling.

Ikram en Marjolein, mijn paranimfen, bedankt dat jullie tijdens de verdediging aan mijn zijde zullen staan. Ikram, altijd stond je voor me klaar, op welke dag en/of tijdstip dan ook. Niet meer met jou op het lab staan is iets dat ik erg zal missen. Marjolein, meer dan eens heb ik je het schaamrood op de kaken laten krijgen.. Ik heb de laatste jaren steeds meer bewondering voor je gekregen.

Renze, bedankt voor de vruchtbare samenwerking. Je gaf me alle ruimte om zelf een richting te geven aan het onderzoek, maar was altijd bereikbaar om, waar nodig, hulp te bieden. Ik denk dat we de verschillende, lastige projecten tot een goed einde gebracht hebben. Ben, bedankt voor het achter de schermen aanwezig zijn, voor het evalueren van de resultaten en voor het overzien van het grote geheel.

Iedereen bedankt.

Colette

Curriculum vitae

Colette Alexandra ten Hove was born on March 20th, 1979 in Zeist, the Netherlands. After finishing high school (gymnasium) at "Het Christelijk Lyceum" in Zeist in 1997, she started her study Biology at Utrecht University in 1997. She performed her first research project in 2000 at the Developmental Biology group of prof. dr. Rolf Zeller at Utrecht University, where she studied the role of FGF2 in spinal cord development under the supervision of dr. Rosanna Dono. After completion of this project she worked part-time as a technician at the Hubrecht Institute in the group of prof. dr. Ronald Plasterk in 2001 on sequencing the *Danio rerio* (zebrafish) genome before starting her second research project in the same year at the Harvard Medical School in Boston, Massachusetts, USA, in the department of Cell Biology in the group of prof. dr. Fred Goldberg, where she studied the function of the muscle specific ubiquitin ligase Atrogin-1 (muscle atrophy F box1 [MAFbx1]) under the supervision of dr. Marcelo Gomez and dr. Adri Thomas of Utrecht University. She received her M.sc. degree in 2003 and started working as a Ph.D. student in the Molecular Genetics group of prof. dr. Ben Scheres at Utrecht University under the supervision of dr. Renze Heidstra in the same year. Her research on the regulation of cell fate and meristem maintenance in *Arabidopsis* root development resulted in the publication of this thesis in 2010. Starting from February 2010, she works as a post-doctoral researcher at the Cell Microscopy Center, Department of Cell Biology of dr. Catherine Rabouille at the University Medical Center Utrecht.

Publications

ten Hove, C.A. and Heidstra, R. (2008). Who begets whom? Plant cell fate determination by asymmetric cell division. Curr Opin Plant Biol *11*, 34-41.

Laskowski*, M., Grieneisen*, V.A., Hofhuis*, H., **ten Hove, C.A.**, Hogeweg, P., Maree, A.F.M., and Scheres, B. (2008). Root system architecture from coupling cell shape to auxin transport. PLoS Biology *6*, e307.
* These authors contributed equally

ten Hove, C.A., Willemsen, V., de Vries, W.J., van Dijken, A., Scheres, B., and Heidstra, R. (2010). *SCHIZORIZA* encodes a nuclear factor regulating asymmetry of stem cell divisions in the *Arabidopsis* root. Curr Biol, doi:10.1016/j.cub.2010.01.018.